

**Wyoming Water Research Program  
Annual Technical Report  
FY 2011**

# Introduction

The NIWR/State of Wyoming Water Research Program (WRP) coordinates participation in the NIWR program through the University of Wyoming Office of Water Programs (OWP). The primary purposes of the WRP are to support and coordinate research relative to important water resources problems of the State and Region, support the training of scientists in relevant water resource fields, and promote the dissemination and application of the results of water-related research. In addition to administrating the WRP, the Director of the OWP serves as the University of Wyoming advisor to the Wyoming Water Development Commission (WWDC).

State support for the WRP includes direct funding through the WWDC and active State participation in identifying research needs and project selection and oversight. Primary participants in the WRP are the USGS, the WWDC, and the University of Wyoming. A Priority and Selection Committee (P&S Committee), consisting of representatives from agencies involved in water related activities in the State, solicits and identifies research needs, selects projects, and reviews and monitors project progress. The Director of the OWP serves as a point of coordination for all activities and serves to encourage research by the University of Wyoming addressing the needs identified by the P&S Committee. The State provides direct WWDC funding for the OWP, which was approved by the 2002 Wyoming Legislature, to identify water related research needs, coordinate research activities, coordinate the Wyoming WRP, and serve as the University advisor to the WWDC.

The WRP supports faculty and students in University of Wyoming academic departments. Faculty acquire their funding through competitive, peer reviewed grants, submitted to the WRP. Since its inception in the year 2000, the WRP has funded a wide array of water related projects across several academic departments.

## Research Program Introduction

Since inception of the NIWR program in 1965, the Wyoming designated program participant has been the University of Wyoming. Until 1998, the Wyoming NIWR program was housed in the Wyoming Water Resources Center (WWRC). However, in 1998 the WWRC was closed. In late 1999, the Wyoming Water Research Program (WRP) was initiated to oversee the coordination of the Wyoming participation in the NIWR program. The primary purpose of the Wyoming Institute beginning with FY00 has been to identify and support water-related research and education. The WRP supports research and education by existing academic departments rather than performing research in-house. Faculty acquire funding through competitive, peer reviewed proposals. A goal of the WRP is to minimize administrative overhead while maximizing the funding allocated toward water-related research and training. Another goal of the program is to promote coordination between the University, State, and Federal agency personnel. The WRP provides interaction from all groups involved rather than being solely a University of Wyoming research program.

In conjunction with the WRP, an Office of Water Programs (OWP) was established by State Legislative action beginning July 2002. The duties of the Office are specified by the legislation as: (1) to work directly with the director of the Wyoming Water Development Office to identify research needs of state and federal agencies regarding Wyoming water resources, including funding under the National Institutes of Water Resources (NIWR), (2) to serve as a point of coordination for and to encourage research activities by the University of Wyoming to address research needs, and (3) to submit a report annually prior to each legislative session to the Select Water Committee and the Wyoming Water Development Commission on the activities of the office.

The WRP, which is coordinated through the OWP, is a cooperative Federal, State, and University effort. All activities reported herein are in response to the NIWR program, with additional funding provided by the Wyoming Water Development Commission and the University of Wyoming. The OWP Director reports to the University of Wyoming Vice President of Research and Economic Development. A State Advisory Committee (entitled the Priority and Selection Committee) serves to identify research priorities and select projects for funding. The Director coordinates all activities.

Reports for the following eight FY11 WRP research projects are given herein in the order listed below:

Project 2009WY46B, Final Report: Detecting the Signature of Glaciogenic Cloud Seeding in Orographic Snowstorms in Wyoming II: Further Airborne Cloud Radar and Lidar Measurements, Bart Geerts, Dept of Atmospheric Science, UW, Mar 2009 thru Feb 2012.

Project 2010WY57B, Annual Report (Project extended): Development of a Contaminant Leaching Model for Aquifer Storage and Recovery Technology, Maohong Fan, SER Associate Professor, Dept. of Chemical & Petroleum Engineering, UW, Mar 2010 thru Feb 2012.

Project 2010WY58B, Final Report: Development of GIS-based Tools and High-Resolution Mapping for Consumptive Water Use for the State of Wyoming, Gi-Hyeon Park, Assistant Prof. and Mohan Reddy Junna, Prof., Dept. of Civil and Architectural Engineering, UW, Mar 2010 thru Feb 2012.

Project 2010WY59B, Final Report: Treatment of High-Sulfate Water used for Livestock Production Systems, Kristi M. Cammack, Ph.D., Assistant Professor, and Kathy J. Austin, M.S., Senior Research Scientist, Dept. of Animal Science, UW, and Ken C. Olson, Associate Professor, West River Ag Center, South Dakota State University, Rapid City, SD, and Cody L. Wright, Associate Prof., Dept. of Animal and Range Sciences, South Dakota State University, Brookings, SD, Mar 2010 thru Feb 2012.

## Research Program Introduction

Project 2010WY60B, Annual Report: Multi-Century Droughts in Wyoming Headwaters: Evidence from Lake Sediments, Bryan N. Shuman, Associate Prof., Dept. of Geology & Geophysics, Jacqueline J. Shinker, Assistant Prof., Dept. of Geography, Thomas A. Minckley, Assistant Prof., Dept. of Botany, UW, Mar 2010 thru Feb 2013.

Project 2010WY61B, Annual Report: Impact of Bark Beetle Outbreaks on Forest Water Yield in Southern Wyoming, Brent E. Ewers, Assoc. Prof., Dept. of Botany, Elise Pendall, Assoc. Prof., Dept. of Botany, and David G. Williams, Prof., Dept. of Renewable Resources, UW, Mar 2010 thru Feb 2013.

Project 2011WY74B, Annual Report: Fate of Coalbed Methane Produced Water in Disposal Ponds in the Powder River Basin, T.J. Kelleners, Assist. Prof. and K.J. Reddy, Professor, Dept. of Renewable Resources, UW, Mar 2011 thru Feb 2013.

Project 2011WY75B, Annual Report: Instrumentation for Improved Precipitation Measurement in Wintertime Snowstorms, Jefferson Snider, Professor, Dept. of Atmospheric Science, UW, Mar 2011 thru Feb 2013.

# Detecting the Signature of Glaciogenic Cloud Seeding in Orographic Snowstorms in Wyoming II: Further Airborne Cloud Radar and Lidar Measurements

## Basic Information

<b>Title:</b>	Detecting the Signature of Glaciogenic Cloud Seeding in Orographic Snowstorms in Wyoming II: Further Airborne Cloud Radar and Lidar Measurements
<b>Project Number:</b>	2009WY46B
<b>Start Date:</b>	3/1/2010
<b>End Date:</b>	2/29/2012
<b>Funding Source:</b>	104B
<b>Congressional District:</b>	1
<b>Research Category:</b>	Climate and Hydrologic Processes
<b>Focus Category:</b>	Water Quantity, Climatological Processes, Hydrology
<b>Descriptors:</b>	Weather modification, cloud radar, aircraft measurements
<b>Principal Investigators:</b>	Bart Geerts

## Publications

1. Geerts, B. and Q. Miao, 2010. Vertically-pointing airborne Doppler radar observations of Kelvin-Helmholtz billows, *Monthly Weather Review*, 138, 982-986.
2. Geerts, B., Q. Miao, Y. Yang, R. Rasmussen, and D. Breed, 2010. An airborne profiling radar study of the impact of glaciogenic cloud seeding on snowfall from winter orographic clouds. *J. Atmos. Sci.*, 67, 3286-3302.
3. Geerts, B., Q. Miao, Y. Yang, R. Rasmussen, and D. Breed, 2010. The impact of glaciogenic seeding on orographic cloud processes: preliminary results from the Wyoming Weather Modification Pilot Project. *J. Weather Mod.*, 42, 105-107.
4. Geerts, B., Q. Miao, and Y. Yang, 2011. Boundary-layer turbulence and orographic precipitation growth in cold clouds: evidence from profiling airborne radar data. *J. Atmos. Sci.*, 68, 2344-2365.

**Detecting the signature of glaciogenic cloud seeding in orographic snowstorms in Wyoming II:  
Further airborne cloud radar and lidar measurements**

**Final Report**

for a three-year (Mar 2009 - Feb 2012)

UW Office of Water Programs

U. S. Geological Survey and the Wyoming Water Development Commission grant

Dr. Bart Geerts, PI

5/1/2012

**1. Abstract**

This proposal (referred to as Cloud Seeding II) called for two research flights of the University of Wyoming King Air (UWKA) over the Medicine Bow mountains (aka the Snowy Range) in Wyoming during the time of glaciogenic cloud seeding conducted as part of the multi-year Wyoming Weather Modification Pilot Project (WWMPP). This pilot project, administered by WWDC and contracted to the National Center for Atmospheric research (NCAR) and Weather Modification Inc (WMI), involves seeding from a series of silver iodide (AgI) generators located in the Snowy Range. The flights were conducted on 3/25 and 3/30 2009. A previous grant from the UW Office of Water programs, referred to as Cloud Seeding I, supported five UWKA flights, flown in Feb 2008 and in Feb-Mar 2009. All seven flights were a remarkable success in terms of both the target weather conditions and instrument performance. The key findings from these seven flights led to a remarkable paper in the *J. Atmos. Sci.* (Geerts et al. 2010), and apparently national recognition in the form of a National Institutes of Water Resources (NIWR) "IMPACT" Award.

**2. Summary of the field work**

All seven flights followed the general flight pattern shown in **Fig. 1**. We targeted west- to northwesterly wind, because in such flow the Snowy Range forms the first obstacle following a long fetch over relatively flat terrain (the Red Desert), because three generators (Barret Ridge, Mullison Park, and Turpin Reservoir) are aligned with the cross-wind flight legs (Fig. 1), and because this flow pattern does not interfere with NCAR's randomized experiment. This is because under such flow the seed generators are upwind of both the target and the control snow gauges. Aside from the along-wind leg (whose orientation depends on the prevailing wind, pivoting around GLEES), there are five fixed tracks roughly aligned across the wind. The NW-most of these five tracks is upwind of the three generators, and the 2<sup>nd</sup>, 3<sup>rd</sup>, 4<sup>th</sup>, and 5<sup>th</sup> tracks are about 2, 6, 9, and 13 km downwind of the generators. The first four legs are on the upwind side, while the 5<sup>th</sup> one (tracking over GLEES) is mostly on the downwind side.

The pattern shown in Fig. 1 was repeated four times on several flights: the first two patterns had the seed generators off, and the last two patterns were flown with the seed generators on. On other flights we concentrated on the three most-downwind legs, and the number of patterns with seeding was increased at the expense of flight time without seeding.

On all flights the Wyoming Cloud Radar (WCR) operated flawlessly, with three antennas (up, down, and forward-of-nadir). We recently discovered a small ( $0.60 \text{ m s}^{-1}$ ) downward bias in the Doppler vertical velocity from the up-looking antenna, on all flights. This correction was found after

extensive comparisons with the down-looking antenna and with flight-level vertical wind data. On all flights we also had the up-looking lidar (Wyoming Cloud Lidar, WCL). On the last four flights, we also collected data from the recently-purchased down-looking lidar.

No less than 4 graduate students participated in the field campaign, although only one graduate student (Yang Yang) is focusing her MSc research on the data from these five flights.

The seven cases have been used to construct composites of radar data and flight-level data, in order to tease out the effect of AgI seeding on cloud processes and snowfall. In all cases the static stability was rather low, and the wind speed strong, such that (a) boundary-layer turbulence effectively mixed tracers over a depth of at least 1 km, and sometimes above flight level (2,000 ft above the Med Bow Peak) up to cloud top, and (b) the Froude number exceeded one and thus the flow went over (rather than around) the mountain range.

## 2008-09 Wyoming King Air flight pattern

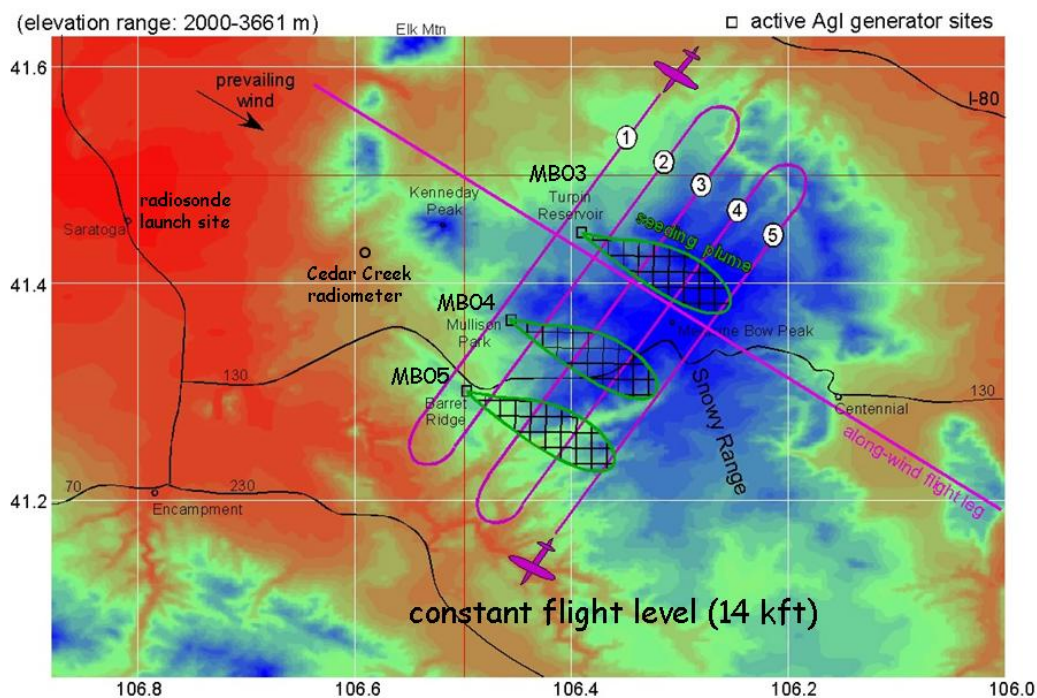


**Fig. 1.** A schematic of the UWKA flight legs in the Snowy Range, over the AgI plumes (shown schematically with a green outline) released from three generators on the ground. The color background field shows the terrain. On all flights the flight level was set at 4,276 m (14,000 ft) MSL. The prevailing wind was from the NW. One flight leg was across the terrain (along the wind), the other 5 flight legs were roughly across the winds at various distances downstream of the three active AgI sources.

### 3. Objectives and methodology

The key objective is to examine the impact of cloud seeding on radar reflectivity between the AgI generators and the slopes of the target mountain. To do this, a composite of reflectivity for seed and no-seed conditions for all downstream flight legs along the wind needs to be built. And

it needs to be ascertained that the observed differences in composites is both statistically significant and not attributable to differences in vertical air velocity.

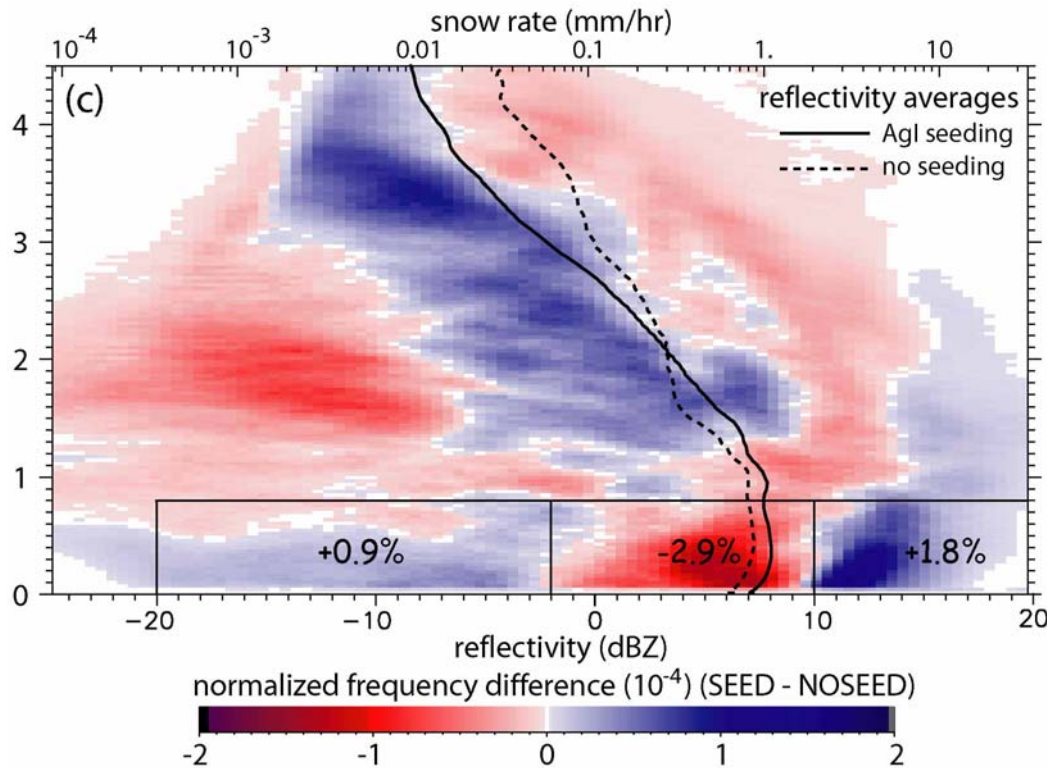


**Fig. 2:** Normalized frequency by altitude (FAD) of the difference in WCR reflectivity during seed and no-seed conditions. Also shown are cumulative normalized frequency differences (seed minus no-seed) in three boxes near the ground, expressed as a percentage, and the mean reflectivity profile during seed and no-seed conditions. The snow rate ( $S$ ) shown in the upper abscissa is inferred from  $S=0.11 Z^{1.25}$  (Matrosov 2007).

#### 4. Principal findings

In Feb 2010 a paper was submitted to *J. Atmos. Sci.* (Geerts et al. 2010), the most prestigious journal in its field. In April 2010, Geerts was an invited keynote speaker at the Annual Weather Modification Association meeting in Santa Fe NM. In that talk, he presented the main findings of the *J. Atmos. Sci.* paper.

Our ongoing study provides experimental evidence from vertically-pointing airborne radar data, collected on seven flights (Table 1), that ground-based AgI seeding can significantly increase radar reflectivity within the PBL in shallow orographic snow storms. Theory and a comparison between flight-level snow rate and near-flight-level radar reflectivity indicate a ~25% increase in surface snow rate during seeding (Fig. 2), notwithstanding slightly stronger updrafts found on average during no-seeding periods. The partitioning of the dataset based on atmospheric stability and proximity to the generators yields physically meaningful patterns and strengthens the evidence.

Firstly, the AgI seeding signature is stronger and occurs over a greater depth on the less stable days than on the three more stable days. Secondly, it is stronger for the two legs close to the generators than for the two distant legs. A random resampling of all flight passes irrespective of seeding action indicates that the observed enhancement of high reflectivity values (>10 dBZ) in the PBL during AgI seeding has a mere 2.2% probability of being entirely by chance (Fig. 3).

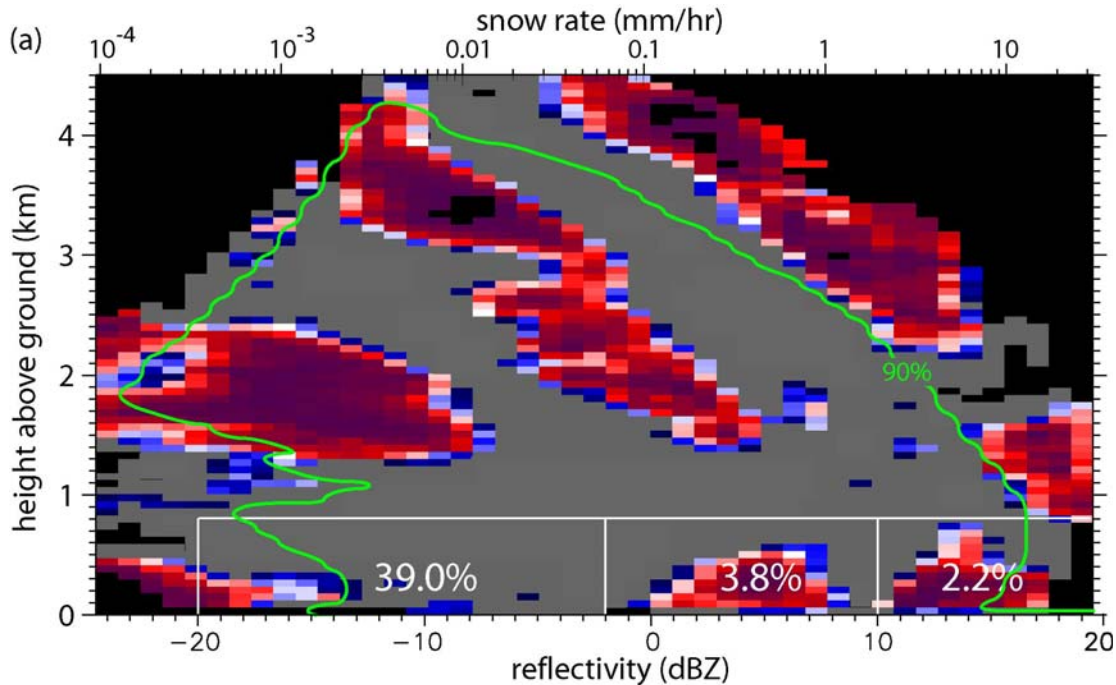


**Fig. 3:** Percentage of differences between randomly selected subgroups that exceeds the observed seed minus no-seed difference in WCR reflectivity (shown in Fig. 2). The white numbers show the same, not at the bin level but within the same boxes as in Fig. 2. In the grey areas there is a more than 10% probability that the seed minus no-seed difference is by chance. The green contour comprises 90% of the cumulative data frequency.

The results presented have limitations, mainly because just seven storms were sampled and these storms represent a rather narrow region in the spectrum of precipitation systems in terms of stability, wind speed, storm depth and cloud base temperature. While the analysis yields strong evidence for an increase in reflectivity near the surface, the quoted change in snowfall rate (25%) is unlikely to be broadly representative. It appears that PBL turbulence over elevated terrain is important in precipitation growth, both in natural and in seeded conditions, and thus the same results may not be obtained if the precipitation growth primarily occurs in the free troposphere. This work needs to be followed up with a longer field campaign under similar as well as more diverse weather conditions. Such campaign should include ground-based instruments, such as vertically pointing or scanning radars and particle sizing and imaging probes.

## 5. Further plans

So far we conducted seven flights over the Snowy Range, five funded under Cloud Seeding I and two under this grant (Cloud Seeding II). Following the review of the *J. Atmos Sci.* paper

(Geerts et al. 2010), we wrote a paper dealing with the importance of PBL turbulence on orographic precipitation (Geerts et al. 2011), and another paper further exploring seeded cloud properties with flight-level data (Miao et al. 2012).

The seven flights and follow-up publications, esp. Geerts et al. (2010), have served as a pilot effort for a much larger research project, known as ASCII (AgI Seeding Cloud Impact Investigation), funded by the National Science Foundation. This grant is a collaboration between Dr. Geerts' team and several NCAR scientists (Rasmussen, Breed, Xue). The USGS/WWDC-funded field work and data analysis (esp. Geerts et al. 2010, in *J. Atmos. Sci.*) were instrumental in the success of this \$569,097 grant entitled "The cloud microphysical effects of ground-based glaciogenic seeding of orographic clouds: new observational and modeling tools to study an old problem" (Aug 2011 - Jul 2014; reference: AGS-1058426). The emphasis of ASCII is on the cloud microphysical effects of glaciogenic seeding in cold orographic clouds, but ASCII examines glaciogenic seeding in the context of natural snow growth processes. The ASCII research grant is the first time in nearly three decades that NSF (or any federal agency) has supported weather modification research.

The first ASCII field phase was conducted in the Sierra Madre (Fig. 4) between 4 Jan and 4 March 2012, and it deployed the UWKA, a MGAUS sounding system, an automated weather station, and a Doppler on Wheels (DOW) radar, all funded directly by NSF at an additional cost of about \$500K. The DOW was positioned on Battle Pass, and often encountered hostile conditions during ASCII. Hidden in the trees about 600 m downwind of the pass, a scaffold was erected to make measurements with an array of instruments characterizing snow at the surface and overhead (Fig. 4b). ASCII-phase 1 involved 17 intensive observation periods, and is regarded a success, notwithstanding several technical challenges and a relatively warm, dry winter.

The second ASCII field phase will be conducted in Jan-Feb 2013, and will again be focused on the Medicine Bow Range. The NSF funding supports 10 UWKA research flights. We may also be able to deploy a series of snow probes at GLEES. Both ASCII campaigns are conducted in the context of the WWMPP, which conducts the ground-based glaciogenic seeding.

## 6. Significance

Our findings are believed to be very significant. Geerts was an invited keynote speaker at the Annual Weather Modification Association meeting in Santa Fe NM in April 2010. At that meeting, Arlen Huggins, a veteran researcher in weather modification, mentioned our work as one of the most significant achievements in glaciogenic seeding efficacy research in the past decade.

Dr. Geerts has been informed that this project was selected along with the Wyoming Institute, for the 2012 National Institutes of Water Resources (NIWR) "IMPACT" Award. At the time of writing, this NIWR Impact Award was not officially presented, but if confirmed, this award confirms the significance of the present work in terms of the greatest potential impact on water supply enhancement. Three equally-weighted criteria have been used to select the winner of this award, i.e. magnitude, timing, and confidence. The award is national, following a regional selection process, and then a selection amongst the 8 NIWR regions nationwide. It will officially be presented at the NIWR annual conference held in Santa Fe, NM in July 2012, where Dr. Geerts will deliver a presentation.

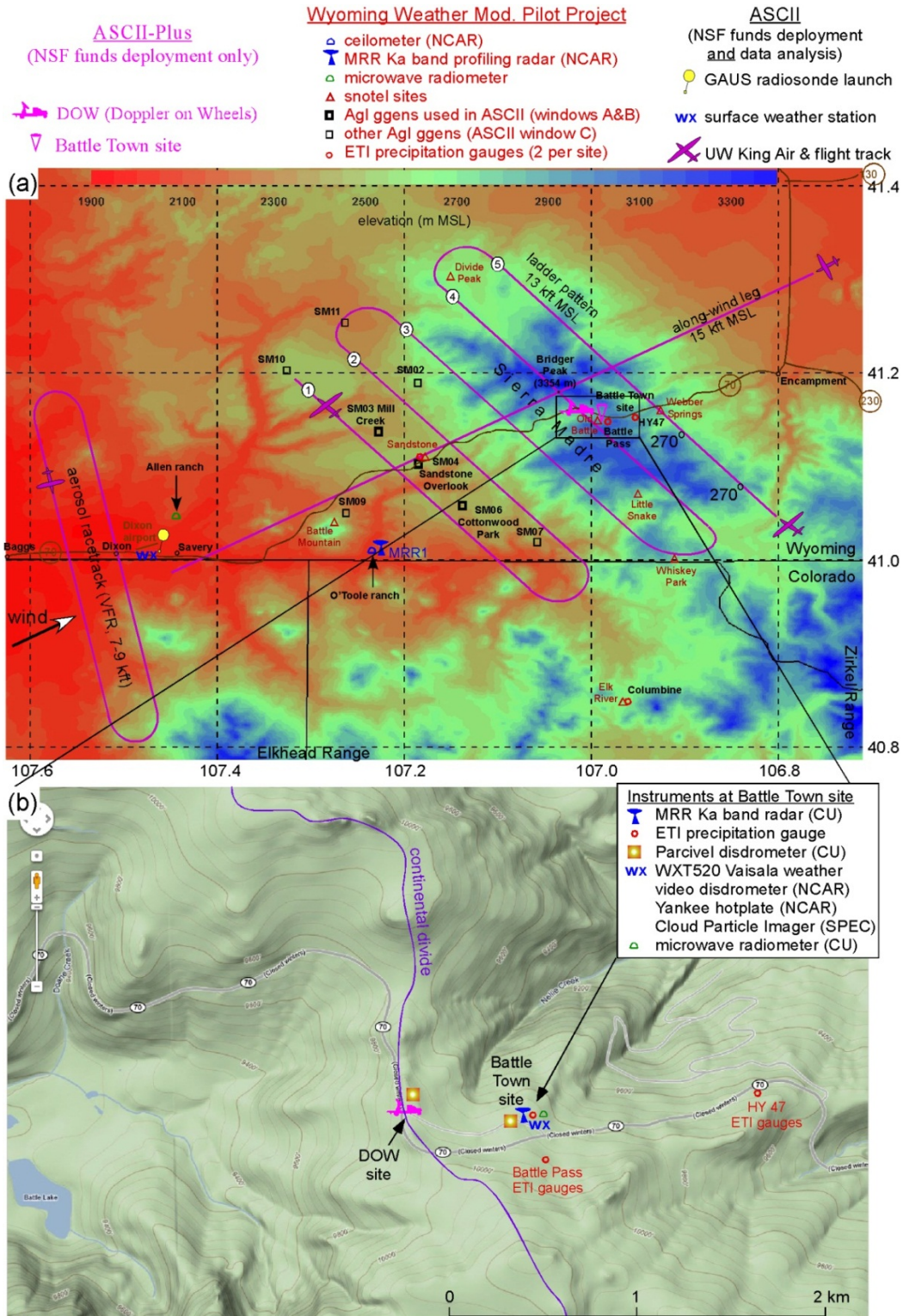


**Fig. 4:** ASCII/WWMPP experimental design map, showing UWKA flight tracks and ground-based instruments. The terrain is shown in the background, in color in (a) and using contours in (b). The highways are shown as well. Panel (b) is a zoom-in of (a) around Battle Pass. The scale in (a) can be derived from the latitude/longitude values.

## 7. Peer-reviewed publications

The following papers directly resulted from the research in this grant and (where possible) were paid for by this grant:

Geerts, B. and Q. Miao, 2010: Vertically-pointing airborne Doppler radar observations of Kelvin-Helmholtz billows. *Mon. Wea. Rev.*, **138**, 982-986.

Geerts, B., Q. Miao, Y. Yang, R. Rasmussen, and D. Breed, 2010: An airborne profiling radar study of the impact of glaciogenic cloud seeding on snowfall from winter orographic clouds. *J. Atmos. Sci.*, **67**, 3286-3302.

Geerts, B., Q. Miao, Y. Yang, R. Rasmussen, and D. Breed, 2010: The impact of glaciogenic seeding on orographic cloud processes: preliminary results from the Wyoming Weather Modification Pilot Project. *J. Weather Mod.*, **42**, 105-107.

Geerts, B., Q. Miao, and Y. Yang, 2011: Boundary-layer turbulence and orographic precipitation growth in cold clouds: evidence from profiling airborne radar data. *J. Atmos. Sci.*, **68**, 2344-2365.

Miao, Q., B. Geerts, and Y. Yang 2011: The impact of ground-based glaciogenic cloud seeding on orographic precipitation: new insights from an airborne down-looking radar. *Advances in Atmospheric Science*, accepted.

Yang, Y. and B. Geerts, 2012: Observations of hydrometeor trajectories in winter orographic clouds. *Mon. Wea. Rev.*, in review.

## 8. Presentations supported by the Grant

Cloud seeding: Dr. Geerts gave oral presentations at the following meetings:

- 2010 Annual Meeting of the Weather Modification Association and the North American Interstate Weather Modification Council, Santa Fe, NM, 21-23 April 2010;
- 18<sup>th</sup> AMS Conference on Planned and Inadvertent Weather Modification, Seattle, 23-27 January 2011;
- 2012 Annual Meeting of the Weather Modification Association, Las Vegas, 25-27 April 2012.

Dr. Geerts and/or his graduate students also gave regular research updates at the WWMPP Technical Advisory Team (TAT) meetings, in Lander (typically in July) and in Cheyenne (typically in January), at the WWMPP Ground School (typically in November), and in 2011 also at the WWMPP seasonal debriefing meeting in mid-April. And we have provided the WWMPP team with material for use in their presentations at meetings of the Select Water Committee, a group of Wyoming state senators and representatives, in the context of updates and further funding requests.

PBL turbulence, blowing snow, and orographic precipitation: Dr. Geerts gave talks on the importance of PBL turbulence on the growth of snow particles over mountains at the 19<sup>th</sup> AMS Conf. on Boundary Layer Processes and Turbulence, Keystone CO (2-6 August 2010), the 10<sup>th</sup> Annual Meeting of the European Meteorological Society, Zurich, Switzerland (13-17 Sept), and the UW Department of Atmospheric Science seminar on 11/23/2010. Dr. Miao presented updated work at the orographic precipitation workshop hosted by Dr. Roy Rasmussen in Boulder 17-19 March 2012.

## 9. Dissertations/theses

No graduate students funded by this grant have graduated yet, but we are close: Ms. Yang Yang (MSc) has been supported by this grant during its 3-year period, and she will defend her thesis in July 2012. Binod Pokharel (PhD), and Xia Chu (MSc), both supported by the follow-up NSF "ASCII" grant, are in their first year. A new PhD student is starting in summer 2012, to be funded by a follow-up grant from the UW Office of Water Programs. So while we have been slow graduating professional students supported by this grant, the prospect for graduate student participation and graduation is good.

One post-doctoral scientist, Dr. Qun Miao, has also been partly supported by this grant. He was essential in the data analysis leading to the *J. Atmos. Sci.* paper (Geerts et al. 2010). He left the group in Jan 2010 to assume a faculty position in Ningbo University in China. His research on this grant was essential to his success assuming a faculty position. Dr. Miao is now on his way to become a leading scientist on weather modification in China. He was back in summer 2010 and during the NSF-supported ASCII field campaign as a visiting research scientist, and he continues to work with us from China, as is evident in the list of publications (Section 7).

## Development of a Contaminant Leaching Model for Aquifer Storage and Recovery Technology

### Basic Information

<b>Title:</b>	Development of a Contaminant Leaching Model for Aquifer Storage and Recovery Technology
<b>Project Number:</b>	2010WY57B
<b>Start Date:</b>	3/1/2010
<b>End Date:</b>	2/29/2013
<b>Funding Source:</b>	104B
<b>Congressional District:</b>	1
<b>Research Category:</b>	Water Quality
<b>Focus Category:</b>	Water Quantity, Water Quality, Water Use
<b>Descriptors:</b>	Aquifer storage and recovery; Water injection; Contaminant leaching
<b>Principal Investigators:</b>	Maohong Fan

### Publications

There are no publications.

**Development of a Contaminant Leaching Model  
for Aquifer Storage and Recovery Technology**

Annual Report, Year 2 of 2 (Project Extended)

Abdulwahab M. Ali Tuwati and Maohong Fan

*Department of Chemical & Petroleum Engineering*  
**University of Wyoming**

Phone: (307) 766 5633    Email: mfan@uwyo.edu

May 8, 2012

## **ABSTRACT**

Aquifer storage and recovery (ASR) involves the storage of water in an aquifer, when water is available, and recovery of water from the well when it is needed. Accordingly, water injection could represent an important method for solving water shortages in semi-arid hydro-climatic regions such as Wyoming. However, water injection might also result in the contamination of ASRs due to the fractionation of heavy metals. In order to predict the potential mobility of those metals, is critically important to investigate and develop model ASR technologies for Wyoming and other states in the U.S. Part of this study focuses on factors that might contribute or enhance the mobility of metals, including pH, water injection flow rate, and temperature variation.

## **PROGRESS**

### **1. Objective**

The primary objective of this study is to design and provide a solution to the universal issue facing potential customers of ASR, a technology based on the physical and chemical properties of relevant rock formations and water resources analyzed through the kinetic theories of chemical engineering. Two models—batch and continuous—are used in this study. The purpose of developing the batching model is to obtain the kinetic parameters needed to develop a continuous-flow leaching model. The continuous models for multiple species will not be developed, but will be tested under various contaminant-leaching conditions.

## **2. Introduction**

### *2.1 Background*

The state of Wyoming is considered part of a semi-arid hydro-climatic region, with water levels varying throughout the year due to the warm temperatures and relatively little precipitations. Wyoming is ranked as the third driest state in US, and the drought is a constant threat in this region. According to the National Climatic Data Center (NCDC) [1], Wyoming is placed as the 48<sup>th</sup> wettest in the U.S with annual precipitation average of 12.97 inches. In general, the state has limited sustainable surface water available for use. Furthermore, Wyoming is one of the largest fossil fuel suppliers in the country [1], with large quantities of water generated during production released either onto land or into nearby lakes or rivers with no beneficial use. Worldwide, the oil and gas industry generates more than 70 billion barrels of produced water per year. Within the US alone, between 15 and 20 billion barrels of produced water are generated each year. This is equivalent to a volume of 1.7 to 2.3 billion gallons per day. Of the above total of produced water, state of Wyoming has shown a share of approximately 2 billion barrels per year as reported in the year 2007 [2]. Accordingly, an environmentally friendly and relatively inexpensive method could be used to store this large volume of the co-produced water after a necessary partial or comprehensive treatment. An aquifer storage and recovery (ASR) injection method could be a feasible technology for conserving natural and/or produced water that would otherwise be wasted. ASR technology provides a cost-effective solution to many of the world's water management needs, storing water during times of flood or when water quality is good, and recovering it later during emergencies or times of water shortage, or when water quality from the source may be poor. Large quantities of water are stored in deep underground, which reduces or eliminates the need for construction of large and

expensive surface reservoirs. This is the main driving forces of the implementation of ASR technology is water supply economics. The second driving force of development of ASR technology is to protect environment, aquatic and terrestrial ecosystems. Most ASR storage zones are ranged in depth from as shallow as about 200 feet (ft) to as deep as 2,700ft. Water is stored in different water-bearing geologic formations that may be in sand, clay sand, sandstone, gravel, limestone, dolomite, glacial drift, basalt and other types of geologic settings.

The types of aquifers in North America are generally classified into six groups: unconsolidated and semi-consolidated sand and gravel aquifers, sandstone aquifers, carbonate-rock aquifers, aquifers in interbedded sandstone and carbonate rocks, and aquifers in igneous and metamorphic rocks [3]. Sand and gravel, sandstone, carbonate-rock, and interbedded sandstone and carbonate rocks aquifers exist to some extent in the state of Wyoming. Regardless of the aquifer type, the injected “stored” water displaces the natural water that present in the aquifer and causes very large bubble around the well. This bubble is usually confined by overlying and underlying geologic formations that do not produce water. These bubbles have water storage capacities as small as about 13 million gallons in individual ASR wells to as much as 2.5 billion gallons or more in large ASR well fields [4]. However, in order for the ASR to be a successful technology for water storage, potential contamination should be addressed. The contamination might occur during water injection and storage as a result of the leaching of toxic metals.

The present project is designed to develop continuous and batch leaching [5] to predict the potential leaching of contaminants into aquifers. The effects of varying certain parameters on the mobility of heavy metals through rocks, including pH and temperature, will be studied using both leaching processes. Flow rate was also used a variable for continuous process studies. This work seeks to study mobility and investigate the leaching kinetics of several heavy metals that

may be present in “sandstone” rock types. Sandstones are arenaceous sedimentary rocks composed mainly of feldspar and quartz, and exhibit a wide color palette of grey, yellow, red and white. They are broadly divided into three groups: arkosic sandstones, which have a high (>25%) feldspar content, quartzose sandstones, such as quartzite, which have a high (>90%) quartz content; and argillaceous sandstones, such as greywacke, which have a significant fine-grained element.

The term “heavy metal” refers to any metallic element that has a relatively high density, and typically refers to the group of metals and metalloids with atomic densities greater than  $4\text{g/cm}^3$  [6]. Heavy metals are well known to be toxic to human beings and most other organisms when present in high concentrations in the environment [6]. Table 1 lists the standard levels of these elements considered safe in water, according to World Health Organization (WHO) [7] and the United States Environmental Protection Agency (EPA) [8].

Table 1: WHO/EU drinking water standards

Element	WHO standard (mg/L)	EPA standards (mg/L)
Arsenic (As)	0.01	0.01
Barium (Ba)	0.3	2
Beryllium (Be)	No guideline	0.004
Boron (B)	0.3	N/A
Cadmium (Cd)	0.003	0.005
Chromium (Cr)	0.05	0.1
Copper (Cu)	2	1.3
Iron (Fe)	No guideline	N/A
Lead (Pb)	0.01	0.015
Manganese (Mn)	0.5	N/A
Nickel (Ni)	0.02	N/A
Selenium (Se)	0.01	0.05
Silver (Ag)	No guideline	N/A
Zinc (Zn)	3	N/A

The leaching of heavy metals occurs naturally, as in the case of sulfide minerals in rocks that are oxidized upon contact with water and atmospheric oxygen, resulting in the formation of sulfates that generate so-called “acid rock drainage” and “metal leaching” (ARD-ML). ARD-ML is usually characterized by high concentrations of metals and sulfates in solution and lower pH values (2-4), which leads to the accelerated release of certain metals into aquifers [9-10]. The mobility of arsenic (As) as toxic element in the presence of pyrite in ASR has been reported in various studies as an example of such leaching, and geochemical modeling has examined the stability of pyrite in limestone during the injection into wells of surface water [11]. The goal of those modeling studies was to stabilize pyrite under certain conditions in order to alter the high leaching of As levels into ASRs. Another leaching model investigated interactions among immobilization reactions and transport mechanisms affecting the overall leaching of contaminants [12], and a characteristic leaching procedure for assessing the toxicity of soils contaminated with heavy metals has been reported elsewhere [13]. In addition, several reports have been cited for the release to groundwater of heavy metals from sources such as fly ash [14], water springs [15], soil [16], mine waste material (i.e., tailings) [17], acidic sandy soil amended with dolomite phosphate rock (DPR) fertilizers [18], and contaminated calcareous soil [19].

All of these reports indicate the mobility of heavy metals in soil to some extent under various amendment conditions. Further, it has been reported that the addition of organic material could result in the fixation of metals such as zinc (Zn) and lead (Pb) in soil, which in turn might help to reduce leaching of these metals into aquifers [19]. The study of metal leaching from various fly ash samples [14] showed different behavior patterns. The chemical partitioning of lead (Pb) and zinc (Zn) in soils, clays and rocks has been documented [20], with their migration

showing an increase under low pH conditions. In the present study, we found it both necessary and useful to design and develop leaching models to study the kinetics of each individual contaminant species; to investigate the potential leaching of some of these heavy metals from sandstone rocks using both continuous and batch leaching processes; and to measure the effects of varying parameters such as pH and temperature of the leachate on both leaching processes, as well as the effects of flow rate on the continuous leaching process.

## *2.2 Occurrence, physical, and chemical properties of heavy metals*

Heavy metals are naturally occurring elements that are found in various concentration levels in rocks, soils, water, and food. They can exist in different oxidation states and their chemical and physical properties are different. Their toxicities to humans and organisms depend on their concentration levels and their oxidation state they exist in. Their solubility's are governed by two major variables: pH and redox potential. Some of general geochemical, chemical and physical properties and occurrences of the metals under the present study are briefly outlined as follows.

Manganese (Mn): It is a naturally occurring element that can be found in several types of rocks, soil and water. It can exist in 11 oxidation states ranging from  $-3$  to  $+7$ , the most common ones are  $+2$  (e.g., manganese chloride,  $\text{MnCl}_2$ ),  $+4$  (e.g., manganese dioxide,  $\text{MnO}_2$ ) and  $+7$  (e.g., potassium permanganate,  $\text{KMnO}_4$ ). Mn and its compounds can exist as solids in the rocks and soil and as solutes or small particles in water. Most Mn salts are readily soluble in water, with the exception of the carbonate and phosphate which have low solubilities in water. The oxides compounds (manganese dioxide and manganese tetroxide) are poorly soluble in water. Mn does not occur naturally as a base metal but is a component of more than 100 minerals,

including various sulfides, oxides, carbonates, silicates, phosphates, and borates. The most commonly occurring manganese-bearing minerals are pyrolusite (manganese dioxide), rhodocrosite (manganese carbonate), rhodonite (manganese silicate), and hausmannite (manganese tetroxide) [Reference will be added later]. Ferromanganese minerals such as biotite and amphiboles (hydrous silicate minerals, containing calcium, magnesium, sodium, iron, and aluminum occurring as important constituents of many rocks) contain large amounts of Mn. An important source of dissolved Mn is anaerobic environments where particulate  $MnO_x$  are reduced, such as some soils and sediments, wetlands. Other possible sources include the direct reduction of particulate  $MnO_x$  in aerobic environments by organics, with or without ultraviolet light, the natural weathering of Mn(II)-containing minerals, and acid drainage and other acidic environments. Manganese exists in the aquatic systems as: Mn(II) and Mn(IV). The oxidation state of manganese is largely governed by pH and redox conditions; Mn(II) dominates at lower pH and redox potential, with an increasing proportion of colloidal manganese oxy hydroxides above pH 5.5 in non-dystrophic waters . A complex series of oxidation/precipitation and adsorption reactions occurs when Mn(II) is present in aerobic environments, which eventually renders the manganese biologically unavailable as insoluble manganese dioxide. Oxidation rates of Mn are directly proportional to pH. In groundwater with low oxygen levels, Mn (IV) can be reduced both chemically and bacterially to the Mn(II) oxidation state [Reference will be added]. There is little evidence for manganese–organic associations in natural waters, with manganese only weakly bound to dissolved organic carbon [Reference will be added]. Hence, organic complexation does not play a major role in controlling manganese speciation in natural waters. The presence of chlorides, nitrates, and sulfates in rocks or soil can increase manganese solubility.

Vanadium (V): It occurs naturally in about 65 different minerals at approximately 150ppm in the crust of the earth. During the weathering of some types of rocks, V is oxidized to vanadate ion which can penetrate through rocks and dissolves in water. However, its mobility through rocks and soils are known to be very slow. Vanadium is known to adsorb to iron (Fe) and aluminum oxides in the clay fraction. In the presence of Fe, vanadium may be precipitate as  $\text{Fe}(\text{VO}_3)_2$ , and some may be immobilized by anion exchange. Vanadium can also immobilize by binding to iron-manganese oxides. The oxide and some salts of vanadium are documented to have moderate toxicity. The common oxidation states of vanadium are +2, +3, +4 and +5. Vanadium (II) compounds are reducing agents, and vanadium (V) compounds are oxidizing agents. Vanadium (IV) compounds often exist as vanadyl derivatives which contain the  $\text{VO}_2^+$  center.

Boron (B): Boron is an inorganic compound, nonvolatile-metalloid, a relatively rare element in the Earth's crust, representing only 0.001%. It has an oxidation state (+3). It does not appear on Earth in elemental form but is found combined in borax, boric acid, colemanite ( $\text{CaB}_3\text{O}_4(\text{OH})_4 \cdot \text{H}_2\text{O}$ ), kernite ( $\text{Na}_2\text{B}_4\text{O}_6(\text{OH})_2 \cdot 3\text{H}_2\text{O}$ ), ulexite ( $\text{CaNaB}_5\text{O}_9 \cdot 8\text{H}_2\text{O}$ ) and borates. Borates are most predominantly found in nature in sedimentary rocks, coal, shale, and some soils. Boron is released from rocks and soils through weathering, and subsequently ends up in water [Reference will be added]. Under normal circumstances boron does not react with water. Boron salts are generally well water soluble. Boric acid has a water solubility of 57 g/L, borax of 25.2 g/L, and boron trioxide of 22 g/L. Boron trifluoride is the least water soluble boron compound, with a water solubility of 2.4 g/L. Some boron compounds, such as boron nitrite are completely water insoluble. Boron readily hydrolyzes in water. Adsorption to rock sediments is thought likely to be the most significant fate pathway for boron in water. The extent of

adsorption is determined by the pH of the water and the chemical composition of the sediment. The greatest adsorption takes place in a pH range of 7.5 to 9.0 [Reference will be included later on]. Boron compounds in water may also co-precipitate as hydroxyborate compounds with aluminum, iron, or silicon [Reference will be added later]. Boron is typically found in salt water at concentrations of about 4.6mg/L [Reference will be added].

Zinc (Zn): It is a metallic chemical element with one main oxidation state of (+2). It is the 24th most abundant element in the Earth's crust. It is a mineral that is usually not found by itself. It can be found in ores such as: sphalerite, franklinite, willemite, zincite, smithsonite, hemimorphite, and hydrozincite. Zinc is found in igneous and metamorphic rocks. It is a chalcophile metallic element and forms several minerals, such as: sphalerite (ZnS), smithsonite (ZnCO<sub>3</sub>) and zincite (ZnO), but is also widely dispersed as a trace element in pyroxene, amphibole, mica, garnet and magnetite. Zinc is readily partitioned into oxide and silicate minerals by substitution for Fe<sup>2+</sup> and Mg<sup>2+</sup>, both of which have similar ionic radii to Zn<sup>2+</sup>. The distribution of Zn in sedimentary rocks is primarily controlled by the abundance of ferromagnesian silicates and detrital oxides. Carbonate rocks and quartzo-feldspathic sand in general contain less Zn compared to reywacke and shale. Zinc is readily adsorbed onto ferric oxides, although when Fe is absent it is often associated with carbonate and silicate phases [Reference will be added]. It has a greater affinity for organic matter than Cd<sup>2+</sup>. The Zn content in soil depends on the nature of parent rocks, texture, organic matter and pH, and ranges from 10 to 300 mg/kg[Reference will be included]. Several soil profile studies have shown that extractable Zn generally decreases with depth, while total Zn is uniformly distributed throughout the profile. Extractable Zn usually correlates positively with total Zn, organic matter, clay content and cation exchange capacity. The concentration of Zn in weathering solutions is

controlled rather by adsorption (on clay minerals Fe, Mn and Al hydroxides and organic matter) than by solubility of Zn carbonates, hydroxides and phosphates. Zinc mobility in the environment is greatest under oxidising, acidic conditions and more restricted under reducing conditions. Weathering of sulphide minerals in oxidising conditions may give rise to high concentrations of dissolved Zn sulphates and carbonates. Below pH 7.5–8.0, Zn occurs predominantly in the  $Zn^{2+}$  form. At higher pH values, it forms low solubility complexes with carbonate and hydroxyl ions.

Barium (Ba): It is a metallic element with one oxidation state (+2). It is a lithophile element and is the 14th commonest element in the Earth's crust. The  $Ba^{2+}$  ion is large and has a high charge ratio (radius/valence) resulting in its concentration in more felsic components of magmas in the later stages of crystallisation. It occurs mostly in K-feldspar and mica through the substitution of  $K^+$  by  $Ba^{2+}$ , which have similar ionic radii. Barium concentrations tend to be higher in K-feldspars than in phyllosilicates. The  $Ba^{2+}$  ion also substitutes for  $Ca^{2+}$  in plagioclase, pyroxenes and amphibole, and in the non-silicate minerals apatite and calcite. The principal Ba mineral, barite  $BaSO_4$ , is frequently associated with metalliferous mineral deposits. Secondary Ba minerals may include authigenic barite and witherite  $BaCO_3$ . The Ba content of igneous rocks generally increases with increasing Si content from mafic to felsic, though some highly evolved granites contain very low levels. In sedimentary rocks the concentration of Ba is related to the abundance of K-feldspar, clay minerals and hydrous Fe and Mn oxides, on to which the element may be adsorbed. The highest Ba concentrations are found in shale, whilst carbonate rocks and sandstone contain small amounts. Elevated Ba values may indicate the presence of felsic rocks, especially kaolinised intrusives, in association with K, or calcareous rocks, in association with Ca, Mg and Sr. Ba released from weathered rocks is not very mobile

since it is easily precipitated as sulphate and carbonate, strongly adsorbed by clays, concentrated in Mn and P concretions, and specifically sorbed onto oxides and hydroxides [Reference will be added]. Barium easily displaces other sorbed alkaline earth metals from some oxides such as:  $\text{MnO}_2$  and  $\text{TiO}_2$  and it is displaced from  $\text{Al}_2\text{O}_3$  by alkaline earth metals such as Be and Sr. In soil of temperate humid climatic zones, Ba is likely to be fixed by Fe-oxides and becomes immobile. Barium in soil may be easily mobilised under different physico-chemical conditions. Its concentration in soil solutions shows considerable variation, from low concentrations in loamy soil to higher concentrations in sandy soil. The presence and concentration of Ba in surface water is strongly controlled by the abundance of Ba in the bedrock, as hydrogeochemical and biogeochemical processes show little variability from one environment to another. However, the behaviour of Ba in solution, particularly the insolubility of  $\text{BaSO}_4$ , tends to result in a smaller level range of Ba concentrations in solution than for many other elements. In natural water, Ba occurs as the  $\text{Ba}^{2+}$  ion. Its mobility is not controlled strongly by pH and Eh conditions, although oxic acidic conditions promote its release from biotite. Compared with the other alkaline earth metals, Ba carbonate and sulphate exhibit low solubilities.  $\text{BaCl}_2$  and  $\text{Ba}(\text{NO}_3)_2$  are more soluble, and the presence of high levels of Chloride ion may enable sulphate-rich water to retain more Ba in solution. The dispersal of Ba in water is also controlled by the presence or absence of hydrous Mn and Fe oxides, which adsorb  $\text{Ba}^{2+}$ . Adsorption on the surfaces of clay minerals and organic matter can also be significant at higher pH.

Iron (Fe): It is a metallic chemical element exists in abundance and it is the fourth most common element, comprising about 5.6% of the Earth's crust. It has a various oxidation states,  $-2$  to  $+6$ , although  $+2$  and  $+3$  are the most common. The main naturally occurring iron minerals are hematite ( $\text{Fe}_2\text{O}_3$ ) and magnetite ( $\text{Fe}_3\text{O}_4$ ). The minerals taconite, limonite ( $\text{FeO}(\text{OH}) \cdot n\text{H}_2\text{O}$ )

and siderite ( $\text{FeCO}_3$ ) are other important sources. Naturally occurring iron oxide, iron hydroxide, iron carbide and iron penta carbonyl are water insoluble. Weathering processes release the element into waters. Both mineral water and drinking water contain iron carbonate. The water solubility of some iron compounds increases at lower pH values. However, some other iron compounds such as: Iron carbonate, iron sulphide, and iron sulfate show some water solubility. Many iron chelation complexes are water soluble. Usually there is a difference between water soluble  $\text{Fe}^{2+}$  compounds and generally water insoluble  $\text{Fe}^{3+}$  compounds. Fe(III) compounds are only water soluble in strongly acidic solutions, but water solubility increases when these are reduced to  $\text{Fe}^{2+}$  under certain conditions.

**Arsenic (As):** Arsenic is odorless, tasteless, and highly toxic element. It can exist in four oxidation states: +5, +3, 0, -3. Inorganic and organic arsenic occur naturally in the environment, with inorganic forms being most abundant. Inorganic arsenic is associated with other metals in igneous and sedimentary rocks, and it also occurs in combination with many other elements, especially oxygen, chlorine, and sulfur. Native arsenic is usually found to have a trigonal symmetry but very rare orthorhombic arsenic is known from arsenolamprite. The two minerals are called polymorphs because they have the same chemistry, As, but different structures. Weathering of rock is the major natural source of inorganic arsenic. Its concentration in the earth's crust ranges from 2 to 5 (mg/kg). The mean natural soil concentration is 5 mg/kg, and it ranges from about 1 to 40 mg/kg. Water-soluble arsenites (As III) and arsenates (As V) are the most common forms. Arsenites especially can be relatively mobile, with a typical concentration associated with soil particles estimated to be 10 to 200 times higher than in the interstitial water.

**Selenium(Se):** Selenium is a naturally occurring substance that is widely but unevenly distributed in the earth's crust and is commonly found in sedimentary rock. It has four oxidation

states: selenates (Se, +6), selenites (Se, +4), selenides (Se, -2), and elemental selenium (Se, 0) which include compounds formed with oxygen, sulfur, metals, and/or halogens.

Selenium is not often found in its pure form but is usually combined with other substances. Much of the selenium in rocks is combined with sulfide minerals or with silver, copper, lead, and nickel minerals. When rocks change to soils, the selenium combines with oxygen to form several substances, the most common of which are sodium selenite and sodium selenate. Acid and reducing conditions reduce inorganic selenites to elemental selenium, whereas alkaline and oxidizing conditions favour the formation of selenates. Selenites and selenates are usually soluble in water. Elemental selenium is insoluble in water and not rapidly reduced or oxidized in nature. In alkaline soils, selenium is present as water-soluble selenate and is available to plants; in acid soils, it is usually found as selenite bound to iron and aluminium oxides in compounds of very low solubility [Reference will be added]. Its behavior in aquatic ecosystems, with respect to acidity, appears to be different than As. With As, the impact of acidification would appear to be mobilization from sediment (rock) to water, with Se, such a change has the effect of reducing water levels and increasing sediment Se content.

Lead (Pb): Lead is extremely rare as a mineral, though the element itself somewhat common. The element lead is found in the Earth's crust in concentration of about 13 ppb. It is sometimes found free in nature, but is usually obtained from the ores, galena (PbS), anglesite (PbSO<sub>4</sub>), cerussite (PbCO<sub>3</sub>) and minium (Pb<sub>3</sub>O<sub>4</sub>). It forms other compounds such as: lead monoxide (PbO), lead dioxide (PbO<sub>2</sub>), tri-lead tetraoxide (Pb<sub>3</sub>O<sub>4</sub>), lead arsenate (Pb<sub>3</sub>(AsO<sub>4</sub>)<sub>2</sub>), lead chromate (PbCrO<sub>4</sub>), lead nitrate (Pb(NO<sub>3</sub>)<sub>2</sub>) and lead silicate (PbSiO<sub>3</sub>). Elementary lead does not dissolve in water under normal conditions. However, it may occur dissolved in water as PbCO<sub>3</sub> or Pb(CO<sub>3</sub>)<sub>2</sub><sup>2-</sup>. Lead frequently binds to sulphur in sulphide form (S<sup>2-</sup>), or to phosphor in

phosphate form ( $\text{PO}_4^{3-}$ ). In these forms lead is extremely insoluble, and is present as immobile compounds in the environment. At low pH, Lead compounds are generally soluble in water.

**Beryllium (Be):** Beryllium is the lightest element of alkaline earth metals. It has two common oxidation states, Be(0) and Be(+2). It is relatively common and widely distributed in the Earth's crust. It is a naturally occurring element found in earth's surface rocks at levels of 1–15 mg/kg. It never occurs as a free element, but as a compound. There are approximately 45 mineralized forms of beryllium. The most common ore found of beryllium is  $\text{Be}_3(\text{Al}_2(\text{SiO}_3)_6)$  and  $(\text{Be}_4\text{Si}_2\text{O}_7(\text{OH})_2)$ . The small atomic radius of Be leads to significant covalent character in bonding. Solutions of beryllium salts such as beryllium sulfate and beryllium nitrate are acidic because of hydrolysis of the  $[\text{Be}(\text{H}_2\text{O})_4]^{2+}$  ion. Beryllium is located above aluminum in the electrochemical series which expected to show some significant chemical activity. However, its reactivity is rendered by the formation of an oxide layer when exposed to air and causes reduction of the reactivity with water even at high temperatures.[Reference will be added]. It dissolves in alkali solutions and forms  $\text{Be}(\text{OH})_4^{2-}$ . Beryllium hydroxide ( $\text{Be}(\text{OH})_2$ ), is insoluble even in acidic solutions with pH less than 6. It is amphoteric and dissolves in strongly alkaline solutions.

**Cobalt (Co):** Cobalt is a relatively abundant element at about 10 - 30 ppm. It is a silver-grey, hard metal, and can exist in six oxidation states, but in aquatic environment the +2 and +3 valence states predominate and form organic and inorganic salts. Although, the metallic form of cobalt is insoluble in water, the solubility of cobalt salts is highly variable and depends on its form. The basic cobaltous carbonate ( $2\text{CaCO}_3 \cdot \text{Co}(\text{OH})_2 \cdot \text{H}_2\text{O}$ ) is insoluble in water, whereas the water solubility of cobalt salts such as  $\text{CoCl}_2$ ,  $\text{CoSO}_4$ , and  $\text{CoS}$  show 450 000 mg/L, 362 000 mg/L, and 3.8 mg/L, respectively [Reference will be added]. It reacts with most acids and

produces hydrogen gas. It does not react with water at room temperatures. Common oxidation states of cobalt include +2 and +3, although compounds with oxidation states ranging from -3 to +4 are also known. In freshwater systems, the dominant species are  $\text{Co}^{+2}$ ,  $\text{CoCO}_3$ ,  $\text{Co(OH)}_3$ , and  $\text{CoS}$ . The concentration of cobalt in aquatic environments has been shown to correlate significantly with pH (inverse correlation) and suspended solids (positive correlation) in water [Reference will be added].

### 2.3 Kinetics of heavy metals desorption

To obtain the leaching rate of laws of chosen contaminants, which is the precondition to derive the contaminant leaching kinetic models of a flow system, a batch leaching is used to facilitate the derivation of rate laws. Both, leaching order and rate constant can be determined by experiments through trial and error method. If assumption can be made by letting the leaching of contaminant species,  $i$ , follows a first order kinetic model, then the leaching rate equation can be written as follows:

$$\frac{dC_i}{dt} = k_i[C_{e,i} - C_i] \quad \text{E1}$$

or

$$-\frac{d[C_{e,i} - C_i]}{dt} = k_i[C_{e,i} - C_i] \quad \text{(E2)}$$

Where  $k_i$  is the rate constant of species  $i$  during its leaching process,  $C_{e,i}$  is the leaching concentration of contaminant  $i$  at leaching equilibrium state, and  $C_i$  is the concentration of species  $i$  at any time  $t$  (min.).

After integrating and applying boundary condition  $C_{i,t=0} = 0$ , E1 becomes:

$$-\ln \frac{(C_{e,i} - C_i)}{C_{e,i}} = k_i t \quad \text{E3}$$

Rearranging E3, we have

$$-\ln[C_{e,i} - C_t] = k_i t - \ln C_{e,i} \quad \text{E4}$$

The left side,  $-\ln[C_{e,i} - C_t]$  in E4 can be plotted against time (t) and if the regression coefficient of the plot turn out to be high then the assumed leaching rate order is correct. Otherwise, an alternative leaching rate order needs to be assumed and checked until its regression coefficient is high.

### 3. Methods

#### 3.1 Sample collection and preparation

Sandstone rock samples were collected from an open pit (Figure 1) operated by Black Butte Coal and Mining Company, and located about 170 miles west of Laramie, Wyoming. The samples were obtained from an adjusted depth of about 169-214 feet, as shown in Table 2.

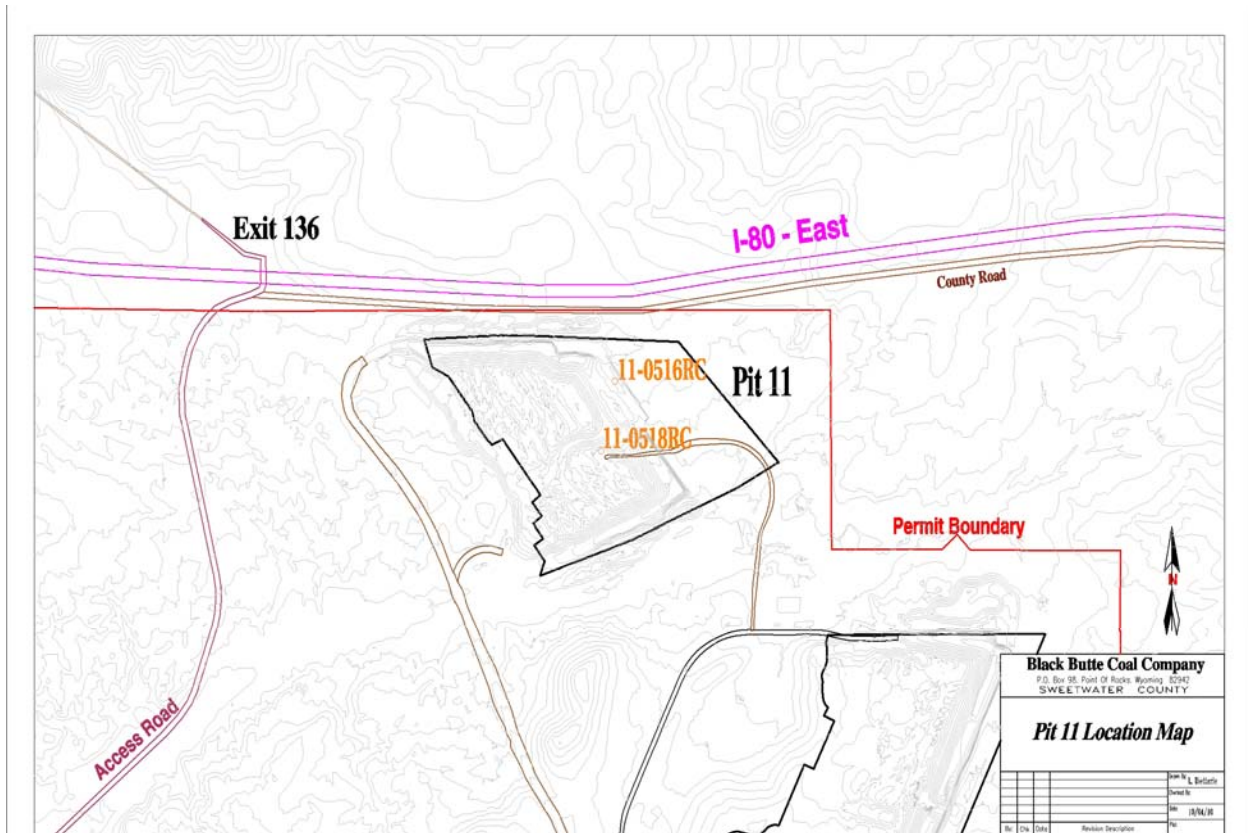


Figure 1: Rock Sample collection location (source: Black Butte Company)

Table 2: Drill Hole Lithology (Source: Black Butte Company)

Raw depths (feet)	Adjusted depths (feet)	Lithology type	Color
0.00-5.00	0.00-5.05	Soil	Yellowbrown
5.00-22.00	5.05-22.21	Sandstone	Greybrown
22.00-25.00	22.21-25.24	Siltstone	Brown
25.00-29.00	25.24-29.27	Sand	Grey
29.00-56.00	29.27-56.53	Siltstone/mudstone	Grey
56.00-61.00	56.53-61.58	Siltstone	Grey
61.00-74.00	61.58-74.70	Mudstone	Grey
74.00-83.00	74.70-83.78	Siltstone	Grey
83.00-85.00	83.78-85.80	Mudstone	Grey
85.00-93.00	85.80-93.88	Siltstone	Grey
93.00-98.00	93.88-98.92	Mudstone	Grey
98.00-129.00	98.92-130.22	Siltstone	Grey
129.00-135.00	130.22-136.27	Mudstone	Grey
135.00-143.00	136.27-144.35	Siltstone	Grey
143.00-144.00	144.35-145.36	Mudstone	Grey
144.00-150.00	145.36-151.42	Sandstone	Grey
150.00-153.20	151.42-154.65	Mudstone	Grey

153.20-155.00	154.65-156.46	Coal	Black
155.00-158.70	156.46-160.20	Carbonaceous mudstone	Brown
158.70-160.00	160.20-161.51	Coal	Black
160.00-168.00	161.51-169.58	Mudstone	Grey
168.00-212.00	169.58-214.00	Sandstone	Grey
212.00-240.20	214.00-241.20	Coal	Black
240.20-245.00	241.20-245.68	Carbonaceous mudstone	Brown
245.00-247.50	245.68-248.01	Coal	Black
247.50-255.00	248.01-255.00	Sandstone/mudstone	Grey

The samples were transported to the lab in containers, and upon arrival their surfaces were cleaned with water and left to dry at room temperature. After drying, all samples were crushed with a jaw crusher and screened with a sieve (mesh opening of 0.185 inch). The retained particles were then mixed several times to obtain representative samples and kept in closed containers until use.

### 3.2 Reference sample

#### 3.2.1 Quantitative analysis

An adapted procedure [17] was partially followed for rock sample digestion in order to screen for the following elements: Ag, As, Ba, Be, Cd, Co, Cr, Cu, Mn, Ni, Pb, Se, V and Zn. The first step of the digestion method involved the addition of 5ml aqua regia (1:3 v/v, HNO<sub>3</sub>: HCl) and 2 ml hydrofluoric acid (HF) to a 0.2g fine powder of sandstone rock sample in a Teflon beaker. The sample mixture was then placed on a hotplate and heated at 100°C until dry. Another 5ml of aqua regia was then added to bring the dissolved metals back to the solution. The resulting mixture was then filtered with Whatman 2 filter paper (pore size: 8µm) and rinsed with deionized (DI) water. The filtrate was then transferred into a 50 ml plastic vial and diluted to its mark. The digestion method was performed three times. The final solutions were analyzed by an ICP-OES Spectrometer (ICAP 6000 series, Thermo Scientific).

### 3.2.2 Apparatus

Two schematic diagrams of continuous and batch percolation extraction set-ups are shown in Figures 2 and 3, respectively; a photo of the actual apparatus (continuous and batch) is shown in Figure 4. The columns are clear PVC columns approximately 7-feet long with an outside diameter (O.D) of 2.5 inches. Each is sufficiently high to contain about 5kg of rock sample (particle size of 0.185 inch), with additional height to contain applied water in the event of poor percolation. Each column has five points evenly spaced for sampling purposes during percolation of the leachate. Only two of these points (3 and 5) were used for sampling collection. A cotton filter medium was placed near each sampling point for easy sample withdrawal. Each column has a punch plate and punch plate support, with the bottoms sealed tightly with bubble caps. An adjustable metering pump was used in the continuous leaching model to ensure a constant flow rate of extraction fluid (water). In the continuous leaching model, containers to hold both influent and effluent liquids were used during extraction.

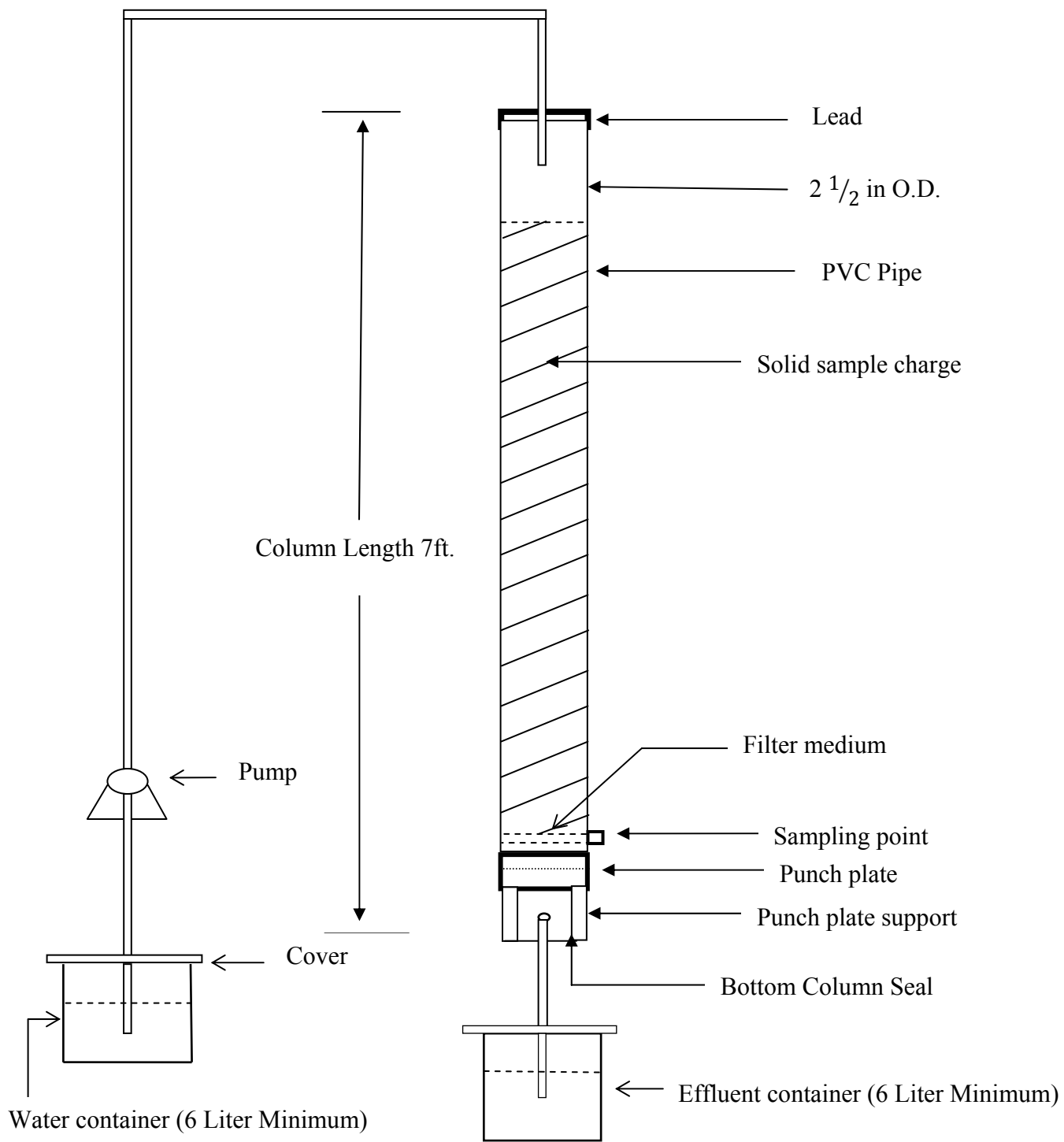


Figure 2: Schematic setup diagram for continuous leaching

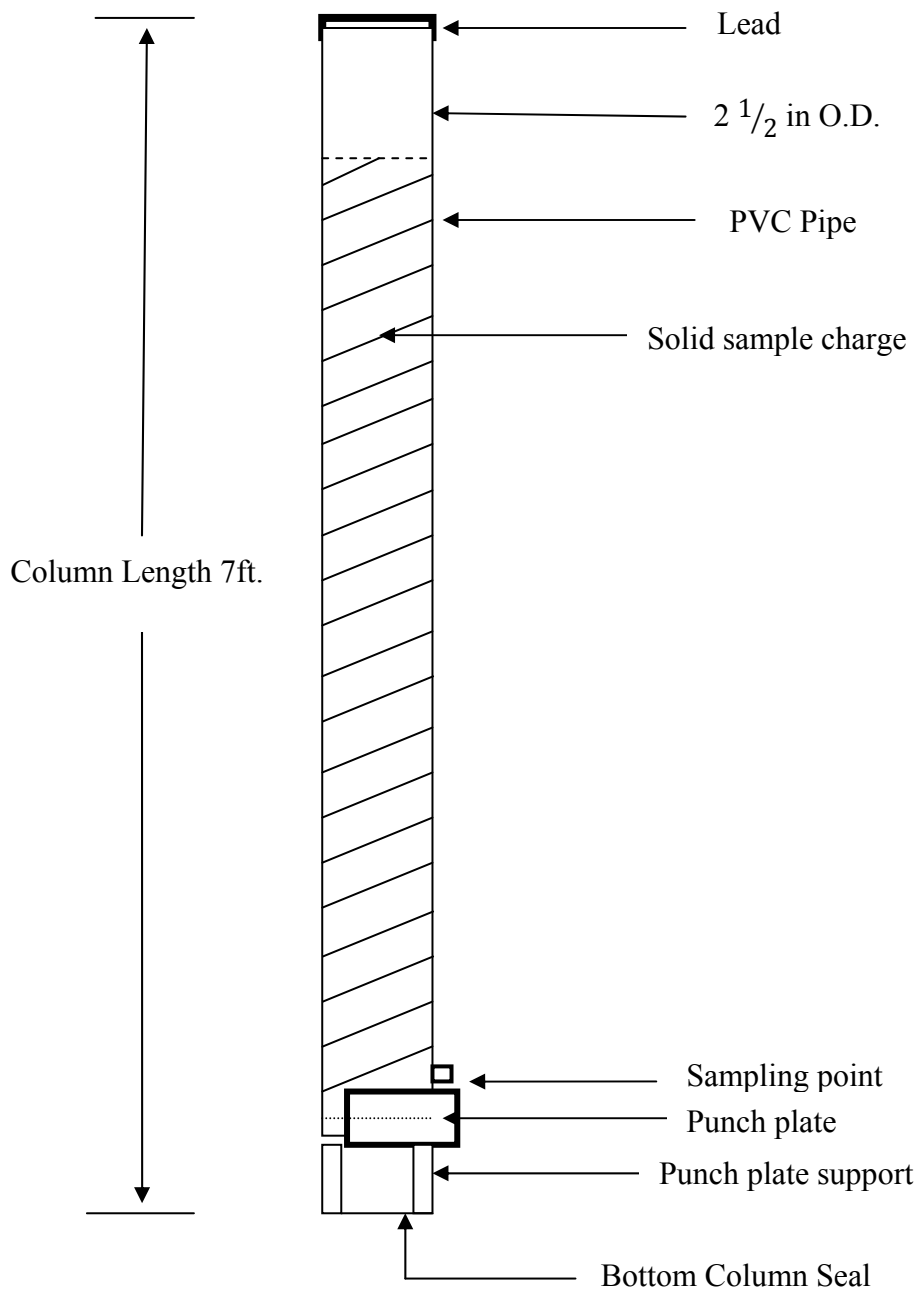


Figure 3: Schematic setup diagram for batch leaching



Figure 4: photo of continuous and batch apparatus

### *3.2.3 Operation Procedure*

## 1. Continuous leaching method

A 5kg dry rock sample was loaded in increments into the PVC column. In order to minimize particle segregation and compaction, the sample increments were carefully loaded without shaking or tamping. Cotton filter medium was inserted into the column near the sampling point in order to withdraw sample effluents using a syringe during the extraction process. Deionized water (DI) was pumped from a container holding a minimum of 6 liters into the column at a specified flow rate using a diaphragm-type metering pump (series 100/150). The initial temperature and pH of the leachate water, as well as the date and starting time of the leaching process, were recorded in accordance with ASTM D 1293[19]. Extraction sample of about 10ml was collected in plastic vials from the sampling point every 8 hours over a 40-hour period. Collected leachate samples were then analyzed for leachable metals using an ICP-OES Spectrometer (ICAP 6000 series, Thermo Scientific). The same procedure was used under different experimental conditions, including flow rate, pH and temperature.

## 2. Batch leaching method

With the exception of the use of a metering pump, a procedure largely similar to method (1) was used to assess the batch leaching method. A set volume of DI water (~1800ml) was added to the column at the start of the leaching process, and small aliquot samples (10ml) were withdrawn and placed into 15 ml vials every 8 hours over a period of 40 hours (unless otherwise specified) from the column sampling point.

## 4. Findings/Results and discussions

#### 4.1 Reference sample analysis

Table 3 presents (in mg/kg) the results of heavy metal concentrations potentially present

Table 3: Metal concentrations in rock sample (sandstone)

Element	Concentration in ppm (mg/Kg)
Arsenic (As)	5.51
Barium (Ba)	206.81
Berillium (Be)	0.93
Cadmium (Cd)	0.85
Cobalt (Co)	4.97
Chromium (Cr)	18.09
Copper (Cu)	8.68
Manganese (Mn)	275.84
Nickel (Ni)	6.19
Lead (Pb)	7.55
Selenium (Se)	5.44
Zinc (Zn)	33.37
Vanadium (V)	38.91

in sandstone rock samples. Because of the chemical composition, matrix complexity, and insolubility of the rock type in mild acidic media (due mainly to a high silica content of approximately 95-97% and various other resistant mineral constituents), the fine powder sample was treated under harsher acidic conditions to ensure complete elemental extraction into the aqueous solution. The method used for the sample dissolution is outlined in section 2.2. In order to minimize errors due to the varying distribution of elements within different rocks, the concentrations shown in Table 3 are based on an average of three representative sandstone

samples. The reported data are based on the average of three independent runs with a calculated relative standard deviation of ~2%. The sandstone samples were found to contain a total of thirteen heavy metals at various concentrations, all within the calibration curve and the ICP detectable range. Compared to the remaining elements, barium (Ba) and manganese (Mn) concentration levels were observed to be highest. However, Ba and Mn are considered less harmful contaminants, and their levels in the sample were far below the allowable limits set by the WHO and EPA for standard potable water. Other more toxic elements such as Cd, As, Be, Co, Cu, Ni, Pb and Se were present as well, but with lower ppm-range concentrations. The remaining elements (Cr, Zn and V) showed moderate ppm concentration levels. Iron appeared to be present in high quantities but showed inconsistency (possibly from the jaw crusher's blades) among the samples, so was not included in this study. Actual Fe concentrations will be included in the next report.

In order to get some clue about the chemical composition of the sandstone sample, a proximately 4 g finely ground sample was pressed into a solid pellet and scanned by XRF (PANalytical Axios XRF analyzer, PANalytical Inc., Almelo, The Netherlands). Table 4 illustrates the concentrations of some major constituents that are present in the sample. Elements in the actual sandstone rocks are tabulated as “metal oxides” and were reported in weight percent (W %) with absolute errors less than 0.080 percent. It can be seen that, alumina “aluminum oxide” ( $\text{Al}_2\text{O}_3$ ) and silica “silicon dioxide” ( $\text{SiO}_2$ ) are predominantly present due to the fact that the rock used in the study is sandstone type. Other metal oxides are present with lower concentrations. P

Table 4: The concentrations of major oxides in rock sample (sandstone)

Compound Name	Concentration in weight (%)	Absolute Error (%)
Al <sub>2</sub> O <sub>3</sub>	16.997	0.035
BaO	0.074	0.001
CaO	3.290	0.0095
CeO <sub>2</sub>	0.023	0.001
Cl	0.033	0.001
Cr <sub>2</sub> O <sub>3</sub>	0.005	0.0005
Fe <sub>2</sub> O <sub>3</sub>	2.708	0.005
K <sub>2</sub> O	2.763	0.0065
MgO	1.549	0.01
MnO	0.054	0.001
Na <sub>2</sub> O	1.122	0.025
Nb <sub>2</sub> O <sub>5</sub>	0.001	0.001
NiO	0.007	0.001
P <sub>2</sub> O <sub>5</sub>	1.886	0.0065
Rb <sub>2</sub> O	0.011	0.001
SO <sub>3</sub>	0.266	0.0025
SiO <sub>2</sub>	68.595	0.08
SrO	0.011	0.001
TiO <sub>2</sub>	0.554	0.0035
Y <sub>2</sub> O <sub>3</sub>	0.003	0.001
ZnO	0.007	0.001
ZrO <sub>2</sub>	0.040	0.001

#### 4.2 Effect of flow rates on metal leaching

Variations in flow rate were examined in order to determine any effects they might have on the fractionation of metals from the sandstone rocks and the dissociation from their counter anions. Aliquots were collected every 8 hours from the column's sampling point over a period of 40 hours and analyzed by ICP. Other experimental parameters such as temperature and pH were kept constant at 21°C and 6, respectively. Water was introduced from the top of the column and

percolated downward through the sandstone particles at four specified constant flow rates. The water flow rates used in the study ranged from 11.67ml/min to 33.33ml/min. Figures 5 to 9 represent (in ppb) concentrations of soluble metals in the leachate tending toward mobilization through the sandstone particles at various flow rates from the bottom column's sampling point; these were collected at the specified sampling periods. The results obtained were generated from the average of three independent experiments. Regardless of the flow rate applied, only five of thirteen elements were observed to have any desorption capability through rocks and dissociation from their minerals under the specified conditions. Their easy fractionation might be attributed to their weak physical or chemical adsorption bonding in their minerals, or might instead be due their solubility tendency relative to the other heavy elements.

The majority of the other heavy metals in the studied rock particles did not show any leaching under the given conditions. Their immobility might possibly owe either to their chemical bonding interactions with the rock's particle surfaces or to the formation of complexes with the rock's minerals. Another explanation could be that some might have leached or desorbed out but formed complexes with minerals in the rock and, as a result, showed no solubility toward water. However, as evidenced by its high concentrations at all flow rates and collection times, one of the leached species, boron (B), showed the highest mobility of all the elements. All plots show that concentrations of B exhibited a direct relationship with flow rate, indicating that its migration or desorption increased as it contacted the water flow. By contrast, the fractionation of other leached elements within the run showed somewhat less mobility based on flow-rate variation.

Figures 5 to 9 also show desorption of these metal species with respect to sampling time. It can be observed that prolonged water contact with the particles' surfaces significantly

impacted the metals' mobility. Maximum concentration levels of leached metals occurred at the first sampling collection time (8hrs); leachate collected at later sampling times (i.e., 16, 24, 32 and 40 hours) showed lower concentrations of leachable metals. Prolonged contact with the water flow caused desorption within shorter time periods, due either to solubility or the weak physical bonding of these species with the rock surface. It is worth noting that all of the leached metals' concentrations at all flow rates were observed to be below the WHO/EPA drinking water standard limits (Table 1). From these findings, it was determined that to complete the remaining task of determining the effects of other parameters (e.g. pH and temperature) on metal leaching, a lower flow rate would be recommended in order to minimize desorption of the leachable metals (especially B and Mn).

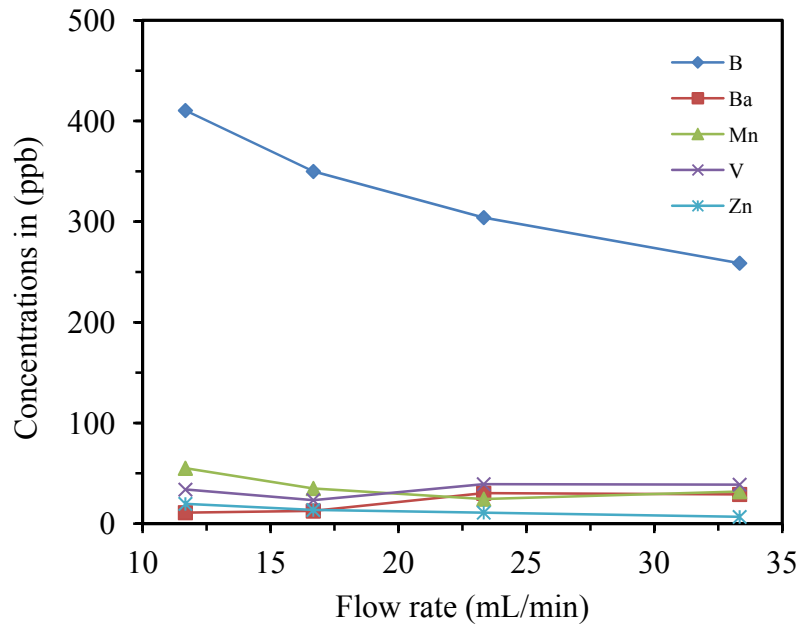


Figure 5: Effect of flow rate on metal leaching (collection time 8 hours)

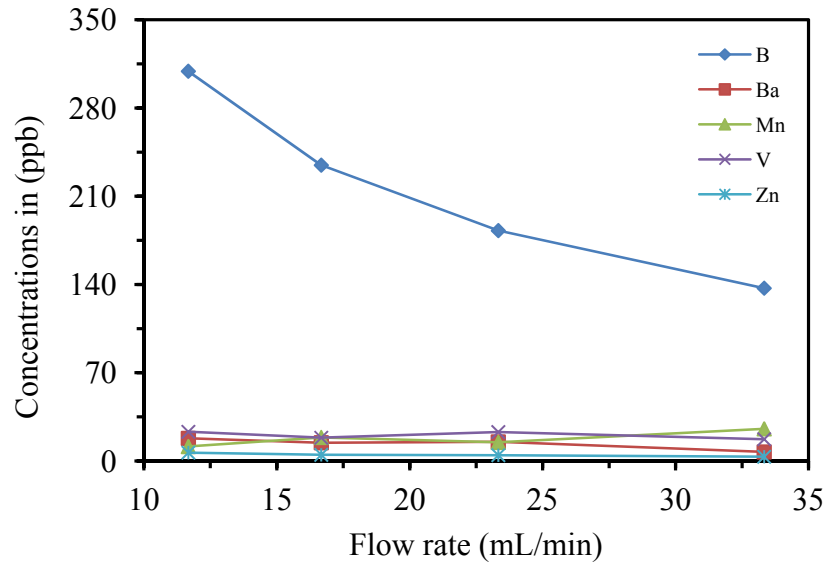


Figure 6: Effect of flow rate on metal leaching (collection time 16 hours)

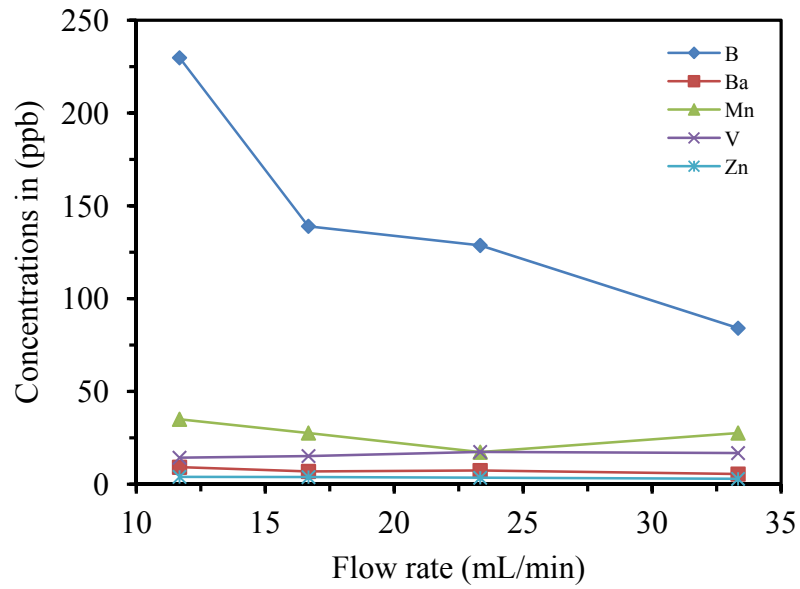


Figure 7: Effect of flow rate on metal leaching (collection time 24 hours)

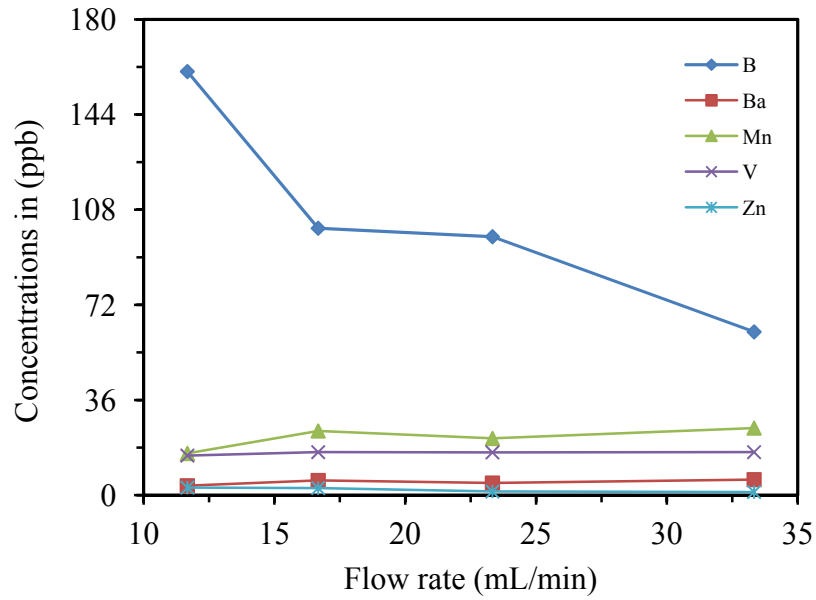


Figure 8: Effect of flow rate on metal leaching (collection time 32 hours)

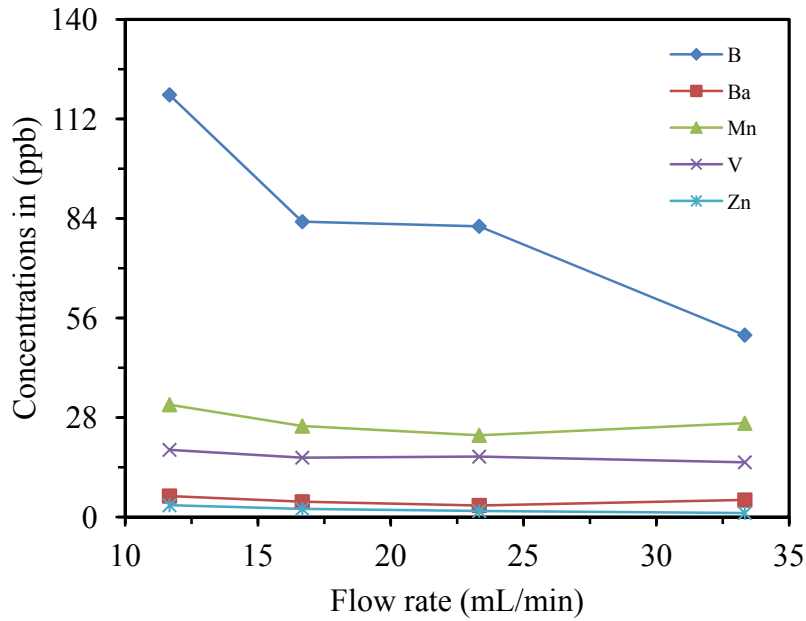


Figure 9: Effect of flow rate on metal leaching (collection time 40 hours)

### 4.3 Continuous vs. batch leaching

A comparison of continuous and batch processes for the leachable heavy metals is presented in Figures 10 and 11, with levels of the extracted amounts shown in ppb concentrations. The concentrations are plotted against collection sampling time periods of 8, 16, 24, 32 and 40 hours. Experiments were conducted at a constant temperature of 21°C and a pH of 6. A water flow rate of 6.33ml/min was used in the continuous leaching. In the case of batch leaching, a quantity of water (about 1900ml) was added from the top of the column sufficient to immerse the 5kg of sandstone particles at the beginning of the process. Samplings were taken periodically every 8 hours. Only four metals (B, Ba, Mn and Zn) appeared to have any mobility in either leaching process. The amounts of Ba and Zn leached were comparable regardless of the leaching process. Steady water contact with the particle surfaces in batch leaching did not cause any noticeable desorption enhancement of the leached metals, rendering extracted metal concentration levels similar to those of the continuous process. However, B was an exception to this finding, evincing a slightly higher mobility in the continuous process compared to the batch process. The reason for this might be due to the flow of water moving downward through the particles, causing the greater mobility of B. By contrast, the behavior of Zn was opposite that of B, due perhaps to the physical interaction or bonding of Zn to the particle surface. Finally, water contact and flow rate were not shown to have any significant effect on leaching of the remaining elements present in the studied rock material.

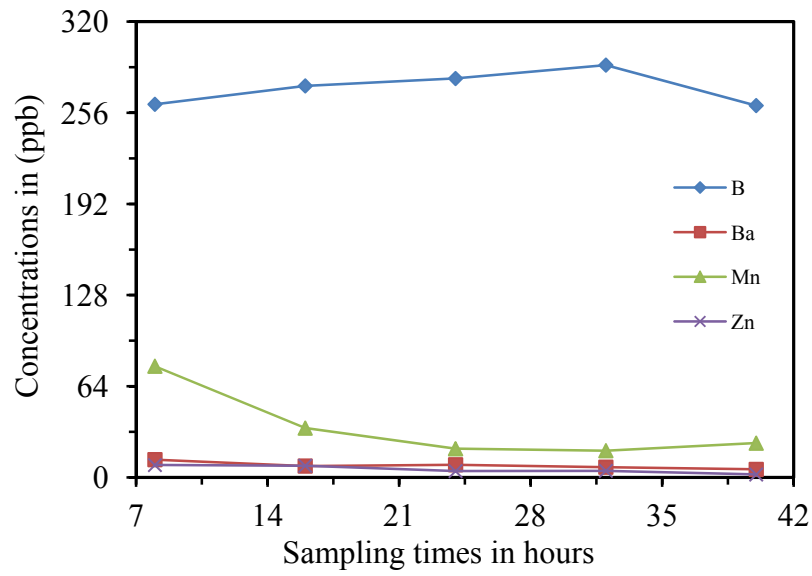


Figure 10: Continuous leaching (flow rate 6.33 ml/min)

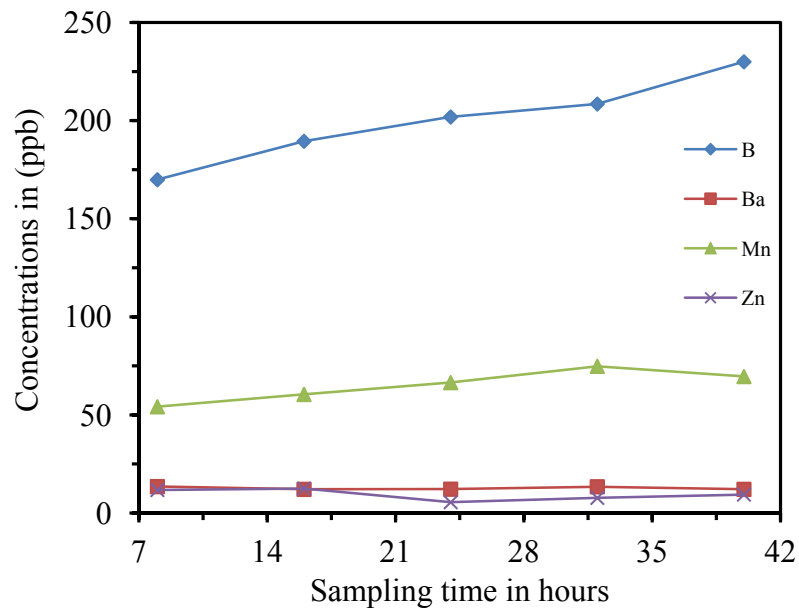


Figure 11: Batch leaching (total volume 1900ml)

#### 4.4 Effect of pH on the heavy metals mobility

Figures 12a to 12d represent leaching of some of the heavy metals that showed their tendency to dissociate from their minerals and their dependency on pH change. Samples were taken every 12 hours over 10 sampling times. Results obtained in the study showed that only four out of the total fourteen heavy metals present in the sandstone rocks were soluble and fall within the detectable range of ICP calibration curve. These are namely boron, barium, manganese, and vanadium. The concentrations of these cations and their degree of pH dependency have some similar trends. All four metals have a higher solubility at lower pH. Increase in the pH tends to gradually decrease their solubility and as a result they become more immobile and hence less leachable. The lower mobility could be attributed to their precipitations and formation of insoluble (i.e. aluminum oxides or iron hydroxides) complexes in the basic media. Prolonged contact did not seem to cause significant effect on the rate of the dissociation of the metals and particularly in the case Mn and V, whereas B indicated some solubility rate increase with contact time. The solubility profiles are not perfectly graphed and this mainly due to the heterogeneity and the less uniformity distribution of the heavy metals within and between the rock samples. Due to the above reason Zn was not present in none of the plots and this could be due to its concentration variation among the rocks or the possibility of its precipitation with iron hydroxides at higher pH's media.

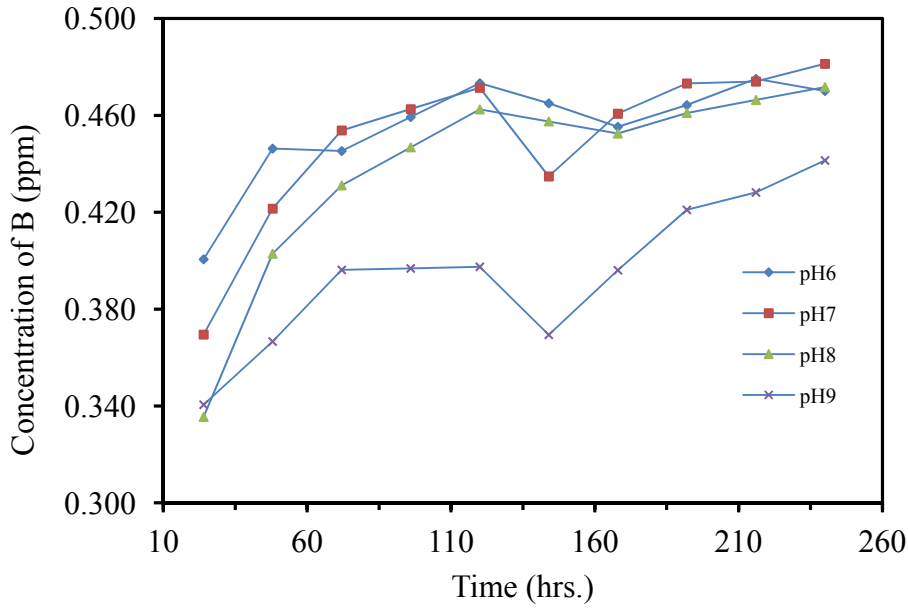


Figure 12. Effect of pH on boron (B) leaching (sample collection time every 12 hours)

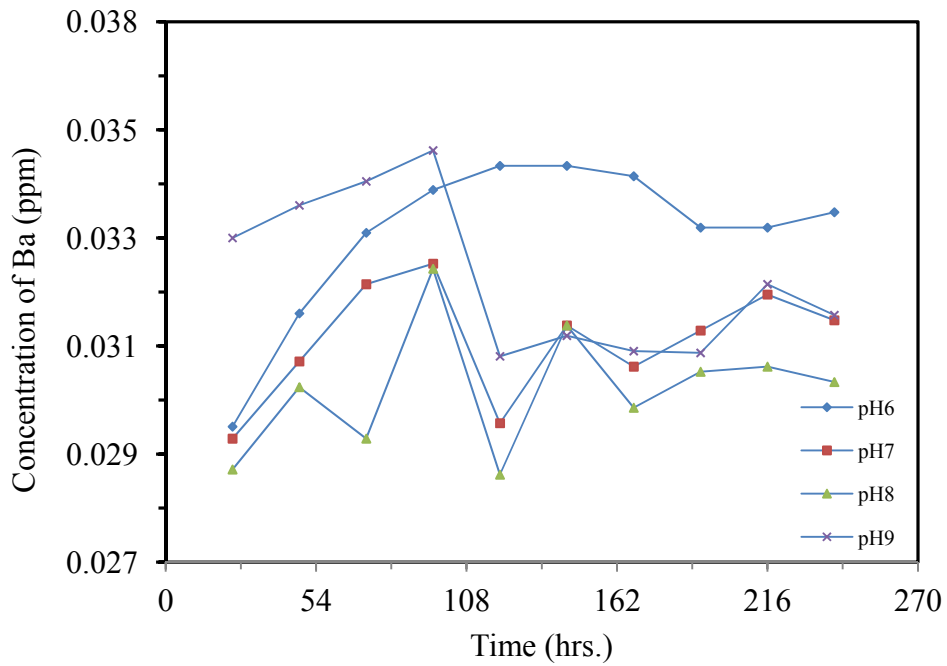


Figure 13. Effect of pH on barium (Ba) leaching (sample collection time every 12 hours)

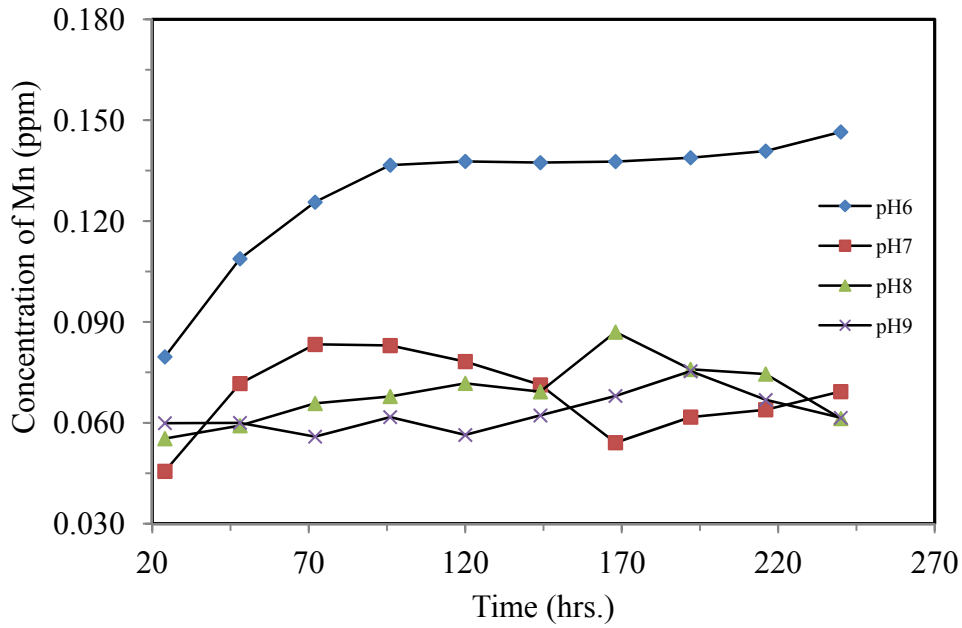


Figure 14. Effect of pH on manganese (Mn) leaching (sample collection time every 12 hours)

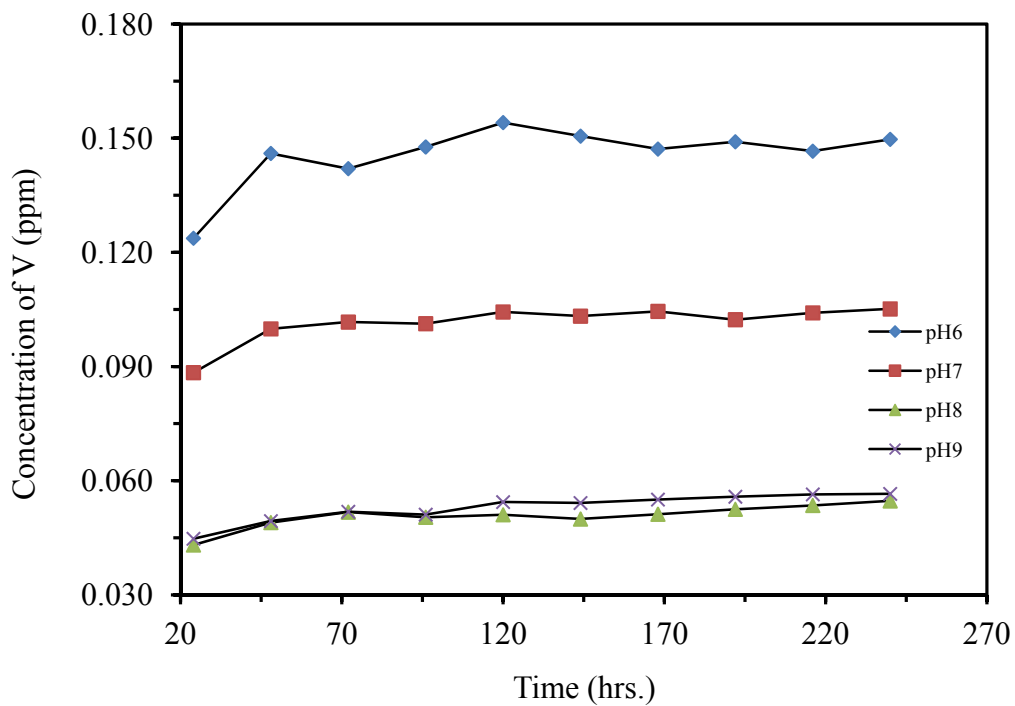


Figure 15. Effect of pH on vanadium (V) leaching (sample collection time every 12 hours)

#### 4.5 Determination of inorganic anions in the leachates

Table 5 lists all possible anions present in the leachate that were collected from the different pH solution media and analyzed via Ion Chromatography (Metrohm 792 IC). In Table 5, sulfate ion has highest concentrations (441-560 mg/L) among all the anions. This indicates that most of the leached heavy metal cations originally bonded with sulfate in minerals. However, Ba tends to have low solubility in the presence of sulfate which forms  $BaSO_4$ , but the presence of chloride ion as the second major ion in the leachate (28-45 mg/L) and nitrate ion (4-17 mg/L) would indicate that Ba could be fractionated or desorbed from minerals that contain chloride or nitrates.  $BaCl_2$  and  $Ba(NO_3)_2$  are known to be more soluble, and the presence of high levels of chloride ion may enable sulfate-rich water to retain more Ba in solution. In the case of Mn, it was mentioned that most of its salts are readily soluble in water, with the exception that its carbonate and phosphate have low solubilities in water. Boron salts are generally soluble, although some boron salts such as boron nitrite are completely insoluble in water. Boron hydrides are soluble in water, which would suggest that boron could be fractionated or desorbed from chloride mineral complexes. The major anions in the leachate are listed in Table 5.

Table 5: Anions in leachate

Sample (mg/L)	#1 pH 6	#2 pH 7	#3 pH 8	#4 pH 9
Flouride	1.5	1.7	1.7	1.7
Chloride	28.4	29.1	30	45
Nitrite as N	1.7	2.0	0.30	2.2
Nitrate as N	5.7	4.4	4.9	17.4
Bromide	.2	0.2	0.10	<0.1
Phosphate	<0.1	<0.1	<0.1	<0.1
Sulfate	484	443	441	560

#### 4.6 Determination of the desorption order of leachable heavy metals

A batch leaching run is presented in Figure 16. Rate of leaching of each individual metal varies with time. B and Mn have similar leaching profiles, where the concentrations show direct increase with time. Similar leaching behaviors were observed for Ba and V. Leaching rates of Ba and V were almost constant. The concentrations of each leached species' were plotted against time. If the leaching data of contaminant species  $i$  fit first order kinetic model gave, then plot of  $-\ln[C_{e,i} - C_t] \sim t$  should be linear with a high regression coefficient. Figures 17-20 are used to establish the reaction orders of B, Ba, Mn, and V. Generally speaking, the leachings of the four species follow first order kinetic model. However, the regression values ( $R^2$ ) for all plots are not very high, which could be attributed to the uneven distribution of heavy metal within the rock particles. Dissociation or desorption rate constant ( $k_{dis.}$ ) for each leached metal can be obtained from the slope of the corresponding plot.

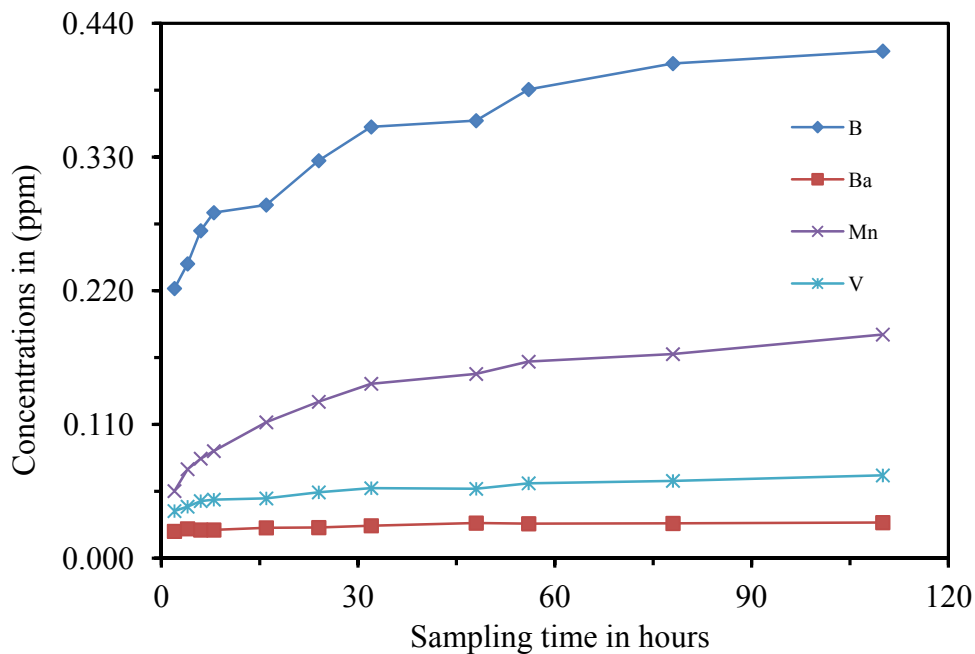


Figure 16: Batch leaching (total volume 2 L)

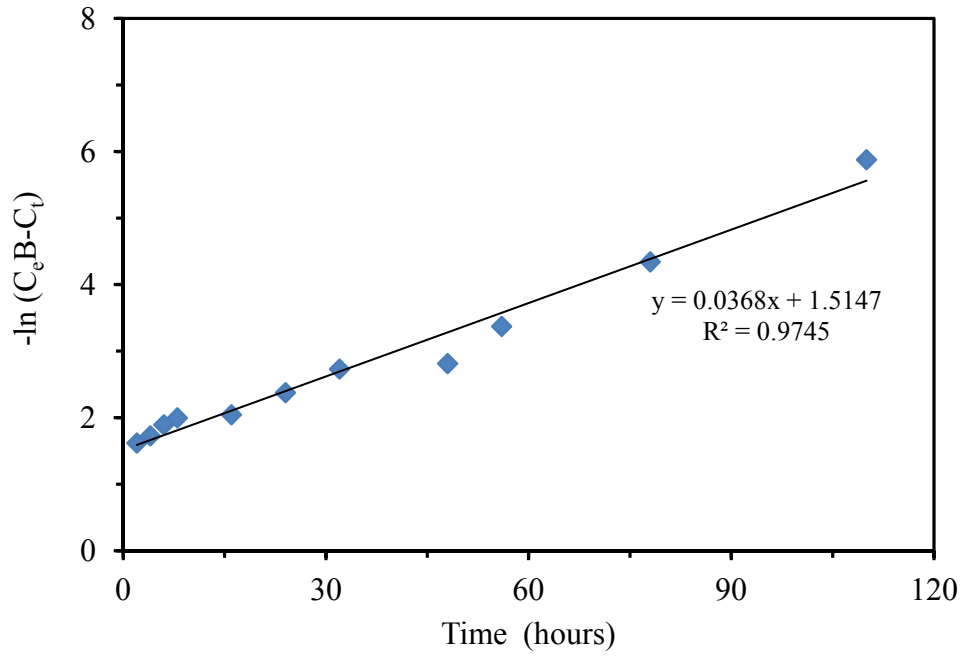


Figure 17. Determination of reaction order of Boron (B)

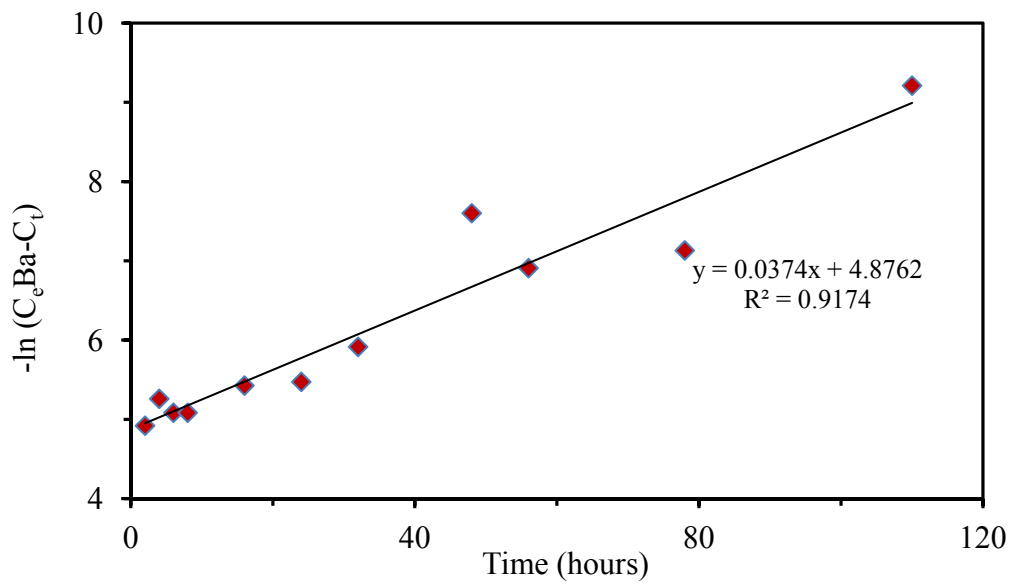


Figure 18. Determination of reaction order of Barium (Ba)

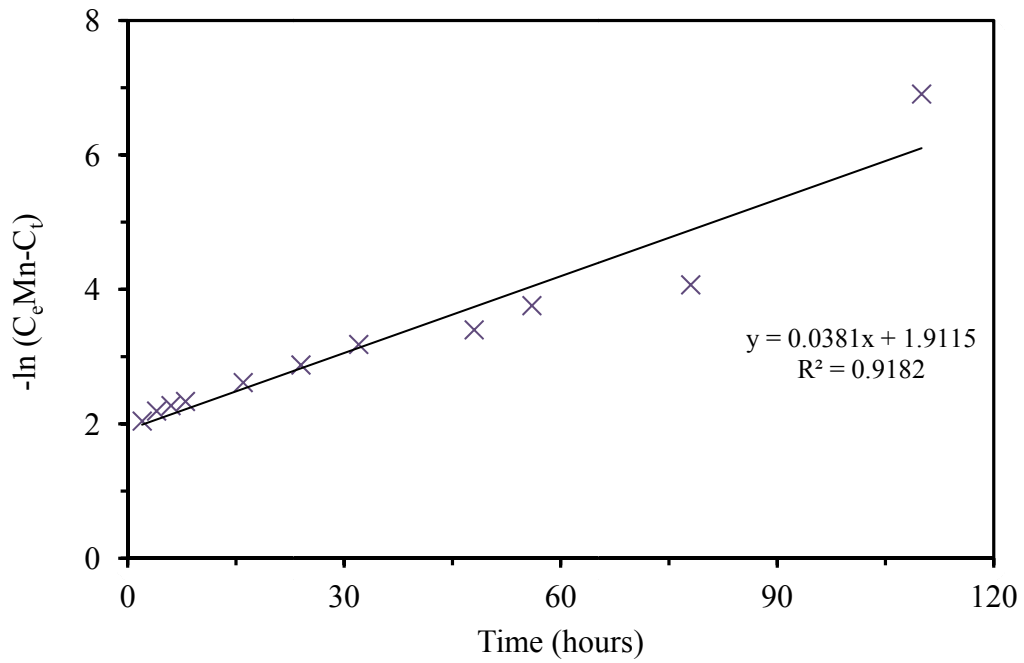


Figure 19. Determination of reaction order of Manganese (Mn)

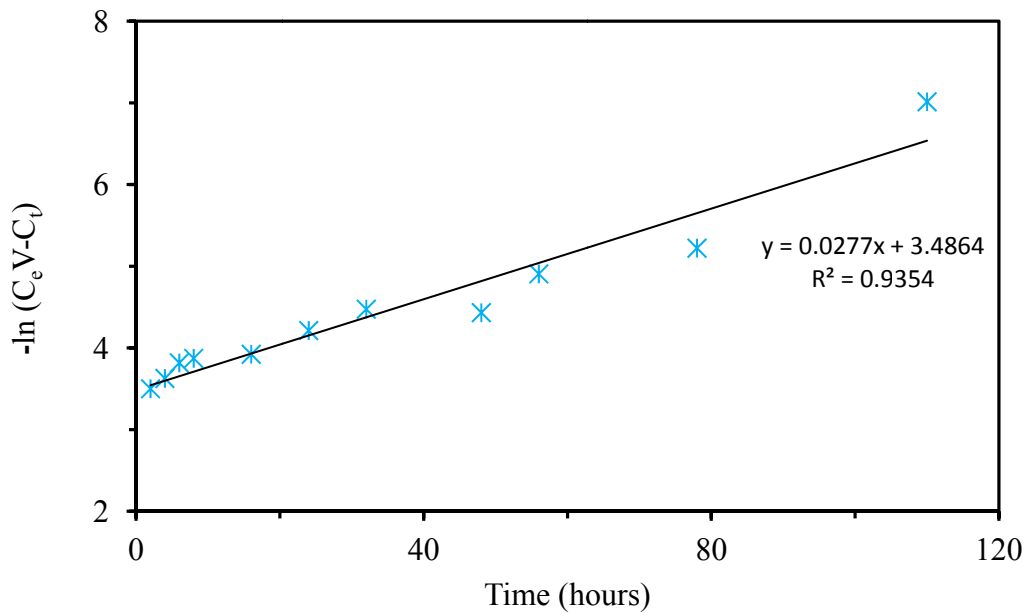


Figure 20. Determination of reaction order of vanadium (V)

#### 4.7 Effect of temperature on the leachability of heavy metals

The work is still being conducted.

### **5. Significance**

On one hand, Wyoming is broadly considered to be in a semi-arid hydroclimatic region. As such, surface water distributions are bi-modal. The vast majority of the time, rivers and streams in the state have little flow although, occasionally during rare events, rivers and streams can swell to almost unbelievable levels. In general, WY has limited sustainable surface water available for use. Moreover, natural disasters such as droughts and tornadoes may unpredictably plague some regions of Wyoming by undermining agricultural, industrial productivity and the well-being and social fabric of communities. Manmade disasters caused by point and nonpoint pollution have been a long-standing concern that may further undermine Wyoming's ability to meet its water needs. It is imperative that Wyoming will not be threatened forever due to the lack of water supply.

In response to the water crisis, Wyoming statute Title 35, Chapter 11, Article 3 (35-11-309) declares that "water is one of the Wyoming's most important natural resources, and the protection, development and management of Wyoming's water resources is essential for the long-term public health, safety, general welfare and economic security of Wyoming and its citizens."

The people are increasingly interested in resorting to aquifer storage and recovery (ASR) to solve the water shortage issue in Wyoming. For instance, the City of Laramie utilizes both surface and groundwater to meet their municipal water needs. The Spur well field is located North of Laramie off of North 9<sup>th</sup> Street. Water levels have been declining at the Spur Well

Field. As a result, the City is investigating the potential for an Aquifer Storage and Recovery (ASR) project to mitigate declining water levels.

ASR would serve to conserve waters that would ultimately go unused. However, the groundwater expansion efforts have met some resistances due to the concerns about aquifer contamination and human health. Acceptance of this potentially important source of drinking water in Wyoming requires solutions to various technical, economic, and regulatory issues, e.g., 1) is contaminant leaching an issue in the application of ASR? 2) do we need to treat the water before it is injected? 3) what monitoring measures should we take to avoid the potential problems? 4) what are the energy costs related to ASR? Obviously many questions need to be answered before ASR technology can be implemented in Wyoming. This project is focused on studying the 1<sup>st</sup> issue mentioned above. Therefore, the project is important to the successful application of ASR.

## **OTHERS**

One graduate student, Abdulwahab M. Ali Tuwati, has been supported by the project. With the support of the project, he successfully finished his MS study in the Department of Chemical and Petroleum Engineering in Spring/2011, and will continue his PhD study in the Department of Chemistry. The progress of the project was presented to Wyoming Water Research Program on Thursday, December 2, 2010, in the WWDC conference room, 6920 Yellowtail Rd, Cheyenne, and to the Department of Chemistry at University of Wyoming on December 8, 2010.

## REFERENCES

- [1] I. McBeth, K. J. Reddy, Q. D. Skinner, Chemistry of trace elements in coalbed methane product water, *Water Res.* 37(2003) 884-890.
- [2] Nevada Mining Association (1996), Meteoric Water Mobility Procedure, *Standardized Column Percolation Test Procedure*, Nevada Mining Association, Reno, NV, 5p.  
  
<http://ndep.nv.gov/bmrr/mobilty1.pdf>
- [3] R. B. Lai, Effect of heavy metal toxicity and exposure on human health, *Indian Journal of Environment and Ecoplanning.* 2(2005) 533-536.
- [4] Water Treatment Solutions, Lenntech. *WHO/EU drinking water standards comparative table*,  
  
<http://www.lenntech.com/who-eu-water-standards.htm>
- [5] Drinking Water Contaminants, National Primary Drinking Water Regulations.  
  
<http://water.epa.gov/drink/contaminants/index.cfm>
- [6] K. A. Mortin, N. M. Hutt, Environmental geochemistry of mine site drainage: Practical and case studies. Minesite Drainage Assessment Group (MDAG) Publishing. (1997) 333.
- [7] J.G. Skousen, Acid mine drainage, *Acid Mine Drainage Control and Treatment: West*

Virginia University and National Mine Land Reclamation center. 91(1995) 12.

- [8] W. Gregg, P. Thomas, Relationship between pyrite stability and arsenic mobility during aquifer storage and recovery., *Environ. Sci. Technol.* 41(2007) 723-730.
- [9] B. Batchelor, Leach models for contaminants immobilized by pH-dependent mechanisms, *Environ. Sci. Technol.* 32(1998) 1721-1726.
- [10] Y. Sun, Z. Xie, J. Xu, Z. Chen, R. Naidu, Assessment of toxicity metal contaminated soils by the toxicity characteristic leaching procedure, *Environmental Geochemistry and Health.* 28(2006) 73-78.
- [11] B. Ludwig, P. Khanna, J. Prenzel, F. Beese, Heavy metal release from different ashes during serial batch tests using water and acid, *Waste Management.* 25(2005) 1055-1066.
- [12] A. Batayneh, Heavy metals in water springs of the Yarmouk Basin, North Jordan and their potentiality in health risk assessment, *Int. J. Phys. Sci.* 5(2010) 997-1003.
- [13] K.M. Banat, F.M. Howari, A.A. Al-Hamad, Heavy metals in urban soils of central Jordan: Should we worry about their environmental risks?, *Environmental Research.* 97(2005) 258-273.
- [14] B.A. Mendez-Ortiz, A. Carrillo-Chavez, M.G. Monroy-Fernandez, Acid rock drainage and metal leaching from mine waste material (tailings) of Pb-Zn-Ag skarn deposit:

environmental assessment through static and kinetic laboratory tests, *Revista Mexicana de Ciencias Geológicas*. 24(2007) 161-169.

[15] G.C. Chen, Z.L. He, P.J. Stoffella, X.E. Yang, S. Yu, J.Y. Yang, D.V. Calvert, Leaching potential of heavy metals (Cd, Ni, Cu and Zn) from acidic sandy soil amended with dolomite phosphate rock (DPR) fertilizers, *Journal of Trace Elements in Medicine and Biology*. 20(2006)127-133.

[16] R. Clemente, A. Escolar, M.P. Bernal, Heavy metals fractionation and organic matter mineralization in contaminated calcareous soil amended with organic materials, *Bioresource*. 97(2006) 1894-1901

[17] J. E. Maskall, I. Thornton, chemical partitioning of heavy metals in soils, clays and rocks at historical lead smelting sites, water, air, and soil pollution. 108(1998)391-409.

[18] M. Bettinelli, U. Baroni, N. Pastorelli, Analysis of coal fly ash and environmental materials by Inductively Coupled Plasma Atomic Emission Spectrometry: comparison of different decomposition procedures, *J. Anal. At. Spectrom.* 2(1987) 485-489.

# Development of GIS-Based Tools and High-Resolution Mapping for Consumptive Water Use for the State of Wyoming

## Basic Information

<b>Title:</b>	Development of GIS-Based Tools and High-Resolution Mapping for Consumptive Water Use for the State of Wyoming
<b>Project Number:</b>	2010WY58B
<b>Start Date:</b>	3/1/2010
<b>End Date:</b>	2/29/2012
<b>Funding Source:</b>	104B
<b>Congressional District:</b>	1
<b>Research Category:</b>	Climate and Hydrologic Processes
<b>Focus Category:</b>	Irrigation, Water Use, Water Supply
<b>Descriptors:</b>	Crop consumptive water use; Evapotranspiration (ET); Reference crop ET; Crop ET; Crop irrigation requirements; and Spatial interpolation of weather data
<b>Principal Investigators:</b>	Gi-Hyeon Park, Mohan Reddy Junna

## Publications

There are no publications.

# **Development of GIS-based Tools and High-Resolution Mapping for Consumptive Water Use for the State of Wyoming**

Final Report

Project Duration: March 2010 to February 2012

**Gi-Hyeon Park (PI)**  
**&**  
**Ryan Rasmussen (Graduate Research Assistant)**

**Department of Civil and Architectural Engineering**  
**University of Wyoming**  
**Laramie, WY**

**May 1, 2012**

# TABLE OF CONTENTS

ABSTRACT.....	1
1. INTRODUCTION .....	1
1.1 Overview .....	1
1.2 Project Objectives .....	2
1.3 Definitions of terms.....	2
1.4 Background .....	2
2.1 Weather Data Interpolation .....	5
2.1.1 Maximum and Minimum Temperature .....	5
2.1.2 Dew Point Temperature.....	7
2.1.3 Wind Speed.....	9
2.1.4 Precipitation.....	11
2.2 Reference ET.....	12
2.2.1 ASCE Standardized.....	12
2.2.2 Hargreaves-Samani.....	14
2.2.3 FAO Blaney-Criddle.....	15
2.3 Crop Coefficients and Land Use .....	16
2.3.1 Group Map.....	16
2.3.2 Land Use Map .....	17
2.3.3 Crop Coefficients.....	18
3. TOOLS DEVELOPED .....	19
3.2 Wyoming ET Calculator .....	19
3.2.1 Model Description .....	19
3.3 Website.....	20
5. PRINCIPAL FINDINGS AND SIGNIFICANCES .....	23
6. PROJECT PUBLICATIONS.....	23
7. STUDENT SUPPORT AND TRAINING.....	23
9. REFERENCES .....	24

## LIST OF FIGURES

Figure 1: Project area (three Wyoming basins) with the SRTM digital elevation.....	5
Figure 2: Location of 1,131 weather stations used in the project. ....	6
Figure 3: An example of spatial interpolation of maximum temperature (TMAX) for July 5, 2010.....	6
Figure 4: An example of spatial interpolation of minimum temperature (TMIN) for July 5, 2010. ....	7
Figure 5: Locations of 56 WBAN stations that provide dew point temperature. ....	7
Figure 6: Bias adjustment for Dew point temperature. (a) TMIN, (b) TDEW, (c) daily TDEW adjustment (TMIN – TDEW).....	8
Figure 7: Spatial interpolation of dew point temperature adjustment: (a) monthly point dew point adjustment and (b) spatially interpolated monthly dew point adjustment. ....	8
Figure 8: Daily Dew point temperature (c) is calculated by subtracting monthly bias of the dew point temperature (b) from spatially interpolated daily dew point temperature (a).....	9
Figure 9: Downscaling of NCEP wind speed. (a) 2 degree NCEP wind speed and (b) Spatially interpolated NCEP wind speed in 0.01 degree resolution. ....	9
Figure 10: Wind bias calculation: (a) NCEP wind speed – (b) observed wind speed at stations = (c) wind speed bias at stations. ....	10
Figure 11: spatial wind bias (b) interpolated from point wind bias (a). ....	10
Figure 12: Final wind speed calculation: (a) NCEP - (b) wind bias = (c) final wind speed.....	11
Figure 13: An example of spatial interpolation of Precipitation for July 5, 2010. (a) Observed daily precipitation at weather stations and (b) spatially interpolated precipitation. ....	11
Figure 14: Precipitation rescaling factor calculation for July. Monthly Rescaling Factor (a) = Monthly PRISM (b) / Monthly Total Average (c).....	12
Figure 15: Final precipitation for July 5, 2010 (Interpolated PRCP x Monthly Rescaling Factor = Final PRCP). ....	12
Figure 16: ASCE standardized grass reference ET (mm) for July 5, 2010. ....	14
Figure 17: Hargreaves-Samani grass reference ET (mm) for July 5, 2010. ....	15
Figure 18: FAO Blaney-Criddle grass reference ET (mm) for July 2010. ....	16
Figure 19: Stations in each group (from Pochop et al., 1992).....	16
Figure 20: Thiessen polygons of group numbers.....	17
Figure 21: Group map for Wyoming. ....	17
Figure 22: National Land Cover Data (NLCD) map for Wyoming.....	18
Figure 23: Default Kc database table.....	18
Figure 24: Wyoming ET Calculator. ....	19
Figure 25: Irrigated area of interest (red polygon).....	21
Figure 26: Graph of the Wyoming ET Calculator and METRIC comparison.....	22
Figure 27: Spatial distribution of July 2009 ET (METRIC on the left and Wyoming ET Calculator on the right). ....	22

## **ABSTRACT**

Accurate estimation of crop consumptive water use is a key component for making decisions in irrigational policy and allocations of water and administration of water rights. State water resources managers utilize crop consumptive water use data to monitor and guide farmers and make a sustainable future plan and decision. This project uses the weather station data in Wyoming and the surrounding states along with Parameter-elevation Regressions on Independent Slopes Model (PRISM) data to produce gridded historical and near real-time daily weather data that are archived in Wyoming State Engineer's Office data server. GIS-based ET calculation tools (an ArcInfo reference ET tool and an ESRI ArcGIS ET calculation tool) and a web-based analysis tool are developed to help water resources managers as well as local water users make operational decisions easier and more accurate than before. The ArcInfo reference ET tools use the daily weather data to calculate the daily reference ET at a spatial resolution of 0.01 x 0.01 degrees. The ArcGIS ET calculation tool, called Wyoming ET Calculator, can be installed on a Windows-based PC and provides a user interface to define parameters (area of interest, crop coefficients, reference ET method, effective precipitation ratios, and water stress factors) for the calculation of potential ET, consumptive irrigational requirement, and actual ET for the area of interest using spatially interpolated weather data.

## **1. INTRODUCTION**

### **1.1 Overview**

Accurate estimations of Evapotranspiration (ET) and Consumptive Irrigation Requirement (CIR) are essential for water resources planning and management. The Wyoming State Engineer's Office (SEO) determines monthly reference evapotranspiration (ET) with an NRCS Spreadsheet ET model (Snyder and Eching, 2003). The main purpose of this project is to replace the NRCS Spreadsheet model with a GIS-based ET calculator, Wyoming ET Calculator. This GIS-based approach uses daily weather data to calculate daily reference ET, CIR, and actual ET, and then aggregate CIR and actual ET into monthly. Among the many reference ET equations available, the ASCE Standardized Reference Evapotranspiration (ASCE, 2005) and the Hargreaves-Samani equations were selected to calculate daily reference ET. Furthermore, the FAO Blaney-Criddle equation was used to calculate monthly reference ET. Data needed for the equations (minimum and maximum temperatures, wind speed, and dew point temperature) were gathered from several sources, such as Natural Resources Conservation Service (NRCS) and the National Centers for Environmental Prediction (NCEP). High resolution (0.01 by 0.01 degree) gridded reference ET maps were produced by spatial interpolation of weather data for the state of Wyoming, including three major river basins in southern Wyoming (North Platte River, Green River, and Bear River basins). Wyoming ET Calculator, a GIS-based ET tool, was developed for

ESRI ArcGIS to calculate daily potential ET, CIR, and actual ET, using daily reference ET, crop coefficients, effective precipitation ratios, and water stress factors.

## 1.2 Project Objectives

The main objectives of this project are to:

- Provide an automatic script to produce spatially interpolated high-resolution (0.01 ° by 0.01 °) weather grid data from available daily weather station data using the inverse distance weighting method and bias correction for each weather variable
- Develop an ArcInfo tool for reference ET calculation to produce high-resolution reference ET maps for Wyoming using the ASCE Standardized, Hargreaves-Samani, and Blaney-Criddle equations
- Develop an ArcGIS ET calculation tool
- Develop a website to serve the data to the public

## 1.3 Definitions of terms

Several terms need to be defined in order to avoid confusion.

- *Potential Evapotranspiration (PET)*: The potential evapotranspiration is the maximum amount of water that would be used as evapotranspiration by crop if water supply is not limited.
- *Reference Evapotranspiration (RET)*: The potential evapotranspiration for the reference crop (either alfalfa or grass).
- *Actual Evapotranspiration (AET)*: Actual evapotranspiration from the field.
- *Effective Precipitation ( $P_e$ )*: The amount of precipitation that would be used for crop evapotranspiration. Some precipitation falling in the field could evaporate directly from the crop surface and excess precipitation would result in runoff.
- *Effective Precipitation Ratio ( $R_{eff}$ )*: The fraction of precipitation that would be used for crop evapotranspiration ( $R_{eff} = P_e / PRCP$ ), where PRCP is precipitation.
- *Consumptive Irrigation Requirement (CIR)*: The amount of water required to meet potential evapotranspiration in addition to the effective precipitation ( $CIR = PET - P_e$ )
- *Water stress factor ( $K_s$ )*: The fraction of water supply with respect to the consumptive irrigation requirement ( $K_s = Actual\ Water\ Supply / CIR$ ).

## 1.4 Background

Evapotranspiration (ET) can be estimated from water balance, energy balance, combined energy and water balance, or measured from the field (Eddy Covariance tower or Lysimeter). Water balance and energy balance models are simpler in calculation but suffer from significant errors due to their insufficient physical descriptions of evapotranspiration processes.

Evapotranspiration is indeed a physical and biological process that is limited by both availability of energy and water as well as crop condition. Therefore, using only water or energy balance is not sufficient for reliable estimates of evapotranspiration. Field measurements can be most accurate at measurement scale, but it is not a feasible solution for measuring evapotranspiration over large area for a long period. The combined energy and water balance methods have been, therefore, widely used in estimating evapotranspiration.

The combined water and energy balance method includes FAO Blaney-Criddle (Brouwer and Heibloem, 1986), SCS TR-21 Modified Blaney-Criddle (Doorenbos and Pruitt, 1977), Hargreaves-Samani (Hargreaves and Samani, 1982), Penman (Penman, 1948), Penman-Monteith (Penman, 1953; Covey, 1959; Rijtema, 1965; and Monteith, 1965), ASCE Standardized Reference ET method (Allen et al., 2005b), and several remote sensing based methods. Satellite based methods, SEBAL (Bastiaanssen et al., 1998a; and Bastiaanssen et al., 1998b) and METRIC (Allen et al., 2005a), have drawn attentions from the community, as they can provide actual ET. However, this method requires high-quality weather data at a minimum of hourly scale and a reliable estimate of the roughness coefficients for crop types. In addition, it is necessary to have trained personnel to process imageries. Therefore, it is widely accepted procedure to use the combined water and energy balance method to estimate long-term consumptive water use in a large area. Among many methods, the Wyoming ET Calculator uses the ASCE Standardized ET, Blaney-Criddle, and Hargreaves-Samani method. The ASCE Standardized ET method is expected to provide most accurate estimates.

Several tools have been developed to make the calculation of ET easier and faster. These include NRCS Excel spreadsheet model (Snyder and Eching, 2003), Ref-ET model (Allen, 1999), the State of Colorado's Consumptive Use Model (StateCU, 2008), ArcE (España et al., 2011), and ArcET (Li et al., 2003).

Ref-ET model calculates RET using FAO and ASCE Standardized ET equations at a point where all required weather data are available. This model is also used in METRIC to calculate reference ET from the weather station. The main deficiency of this model is that it does not account for spatial variability of weather data.

The NRCS Excel Spreadsheet ET model (Snyder and Eching, 2003) uses long-term monthly average weather data at major weather stations, usually available at airports, to calculate monthly reference ET using the standardized Penman Monteith equation. These monthly values are then interpolated into daily reference ET using either linear or cubic functions. This model is therefore limited by the fact that it only uses point data from the nearest weather station to calculate reference ET, even for areas far away from the station, and uses monthly data to get daily data.

The StateCU estimates historical consumptive water use based on user inputs such as water supply condition (diversion), irrigated area, crop patterns, and climate data. It uses SCS

Blaney-Criddle method for monthly scale and the ASCE Standardized ET method for daily scale. Similar to NRCS Spreadsheet model, it also uses nearest weather station(s) to estimate weather data for the location of interest.

To overcome these temporal and spatial limitations in above models, a GIS-based approach can be used. GIS-based ET tools that have been developed for ArcGIS include ArcE (España et al., 2011) and ArcET (Li et al., 2003).

ArcE uses monthly temperature and precipitation from weather stations to calculate monthly PET using the Hargreaves equation. AET is then calculated using the Budyko model for the stations, which must be calibrated. No land use or land cover is taken into account. Similar to other non-GIS models, it only uses monthly point-scale data, and therefore, the limitations mentioned above are not addressed.

ArcET uses a database of meteorological data to interpolate weather data within ArcGIS and then calculate RET. The FAO 56 Penman-Monteith (grass RET), ASCE Standardized Penman-Monteith (short and tall RET), Hargreaves 1985, SCS modified Blaney-Criddle, and the Priestley-Taylor equations are available for reference ET calculation. A land use shape file (only polygon layer) and user-provided crop coefficients are used to get spatial grids of crop coefficients. The reference ET grids are multiplied by the crop coefficient grids to get the potential ET. The total crop PET within the user provided zones is summarized in an ET table. However, CIR and actual ET are not calculated. In addition, ArcET was developed in Visual Basic interface, which will not be supported any more by ESRI in the next version of ArcGIS.

In order to overcome these limitations in the pre-existing tools and facilitate easier and more accurate calculation of consumptive water use, we developed a GIS based ET calculator, Wyoming ET Calculator, for the State of Wyoming. The Wyoming ET calculator is a GIS extension that uses the spatially interpolated weather data from available weather stations. This project also produces same weather data for the future without additional cost, by running an automatic shell script developed for the state of Wyoming. This script collects data from several data servers and produce weather data required for ET calculation. The ArcInfo tool further calculates reference ET for the state of Wyoming. The Wyoming ET calculator was developed using C# and .NET, since ESRI will not support visual Basic interface from the next version of ArcGIS. All data and tools are stored at the SEO data server, which will provide them to the public.

## **2. METHODS AND DATA**

The study area includes the three major basins in southern Wyoming: the North Platte River Basin, the Green River Basin, and the Bear River Basin. These basins, along with the digital elevation model (DEM), are shown in Figure 1. The 90 meter DEM was obtained from Shuttle Radar Topography Mission (SRTM) data and was upscaled to a resolution of  $0.01^\circ$  by  $0.01^\circ$  (approximately 1 km by 1 km), which is the resolution used for all weather data and

reference ET maps. Although most irrigated are located in the three major river basins, we produced high resolution weather data for the State of Wyoming for the other future uses.

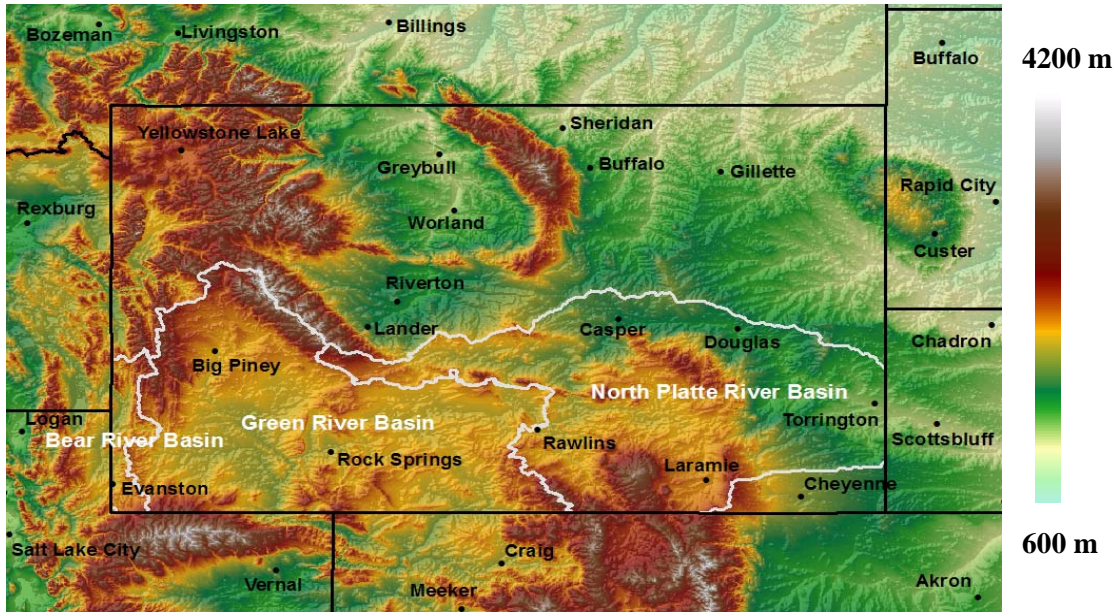


Figure 1: Project area (three Wyoming basins) with the SRTM digital elevation

## 2.1 Weather Data Interpolation

The data needed for the ASCE standardized reference ET equation includes maximum and minimum temperature, wind speed, and dew point temperature at a minimum. These weather data were obtained from various sources in a daily timescale from 1960 to 2010 (a total of 18,628 days). Daily precipitation was also acquired to calculate consumptive irrigation requirement (CIR).

### 2.1.1 Maximum and Minimum Temperature

Maximum and minimum temperature (TMAX and TMIN, respectively) data were obtained from the National Climatic Data Center (NCDC) from January 1960 to December 2010. To get a better interpolation at the boundary of the state of Wyoming, weather data were not limited to Wyoming. Figure 2 shows the 1,135 weather stations in Wyoming and in parts of Colorado, Utah, Idaho, Montana, South Dakota, and Nebraska that were used for the project.

For temperature, inverse distance weighted (IDW) was used to interpolate data into a  $0.01^\circ$  (1 km by 1 km) grid (the same grid as the DEM), while lapsing into it according to elevation using dry adiabatic lapse rate. Examples of this interpolation are shown in Figure 3 and Figure 4.

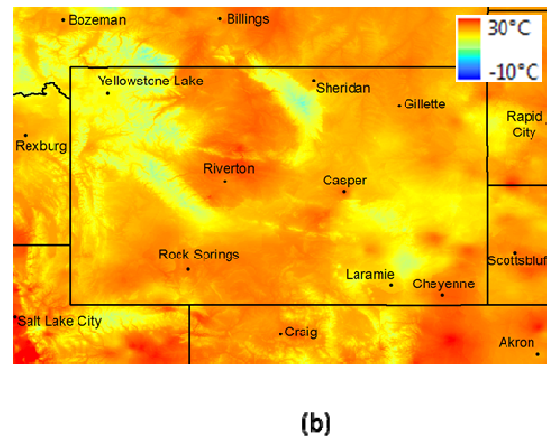
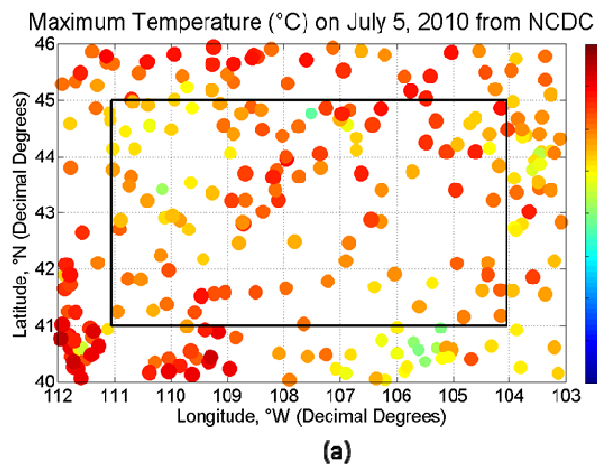
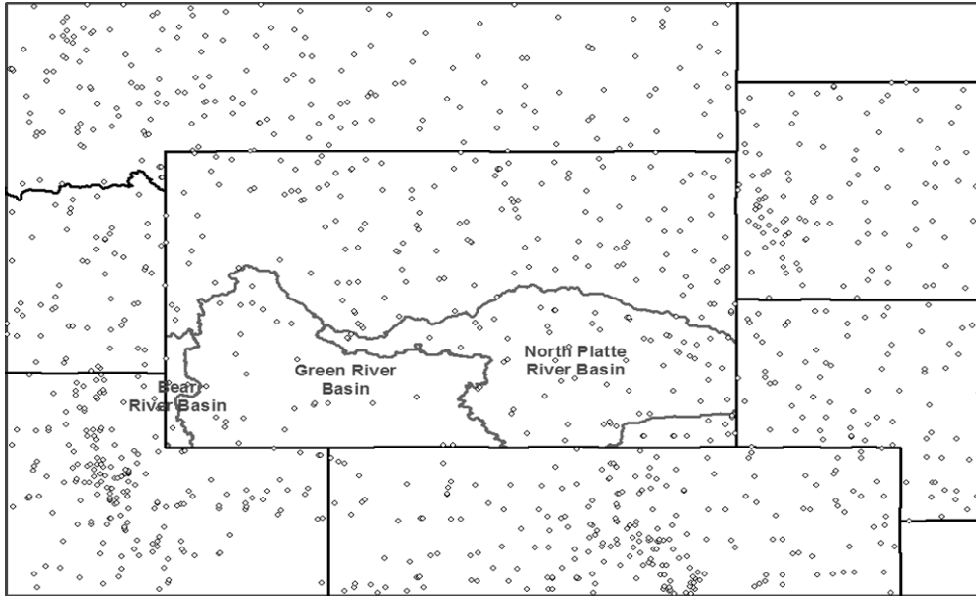


Figure 3: An example of spatial interpolation of maximum temperature (TMAX) for July 5, 2010.

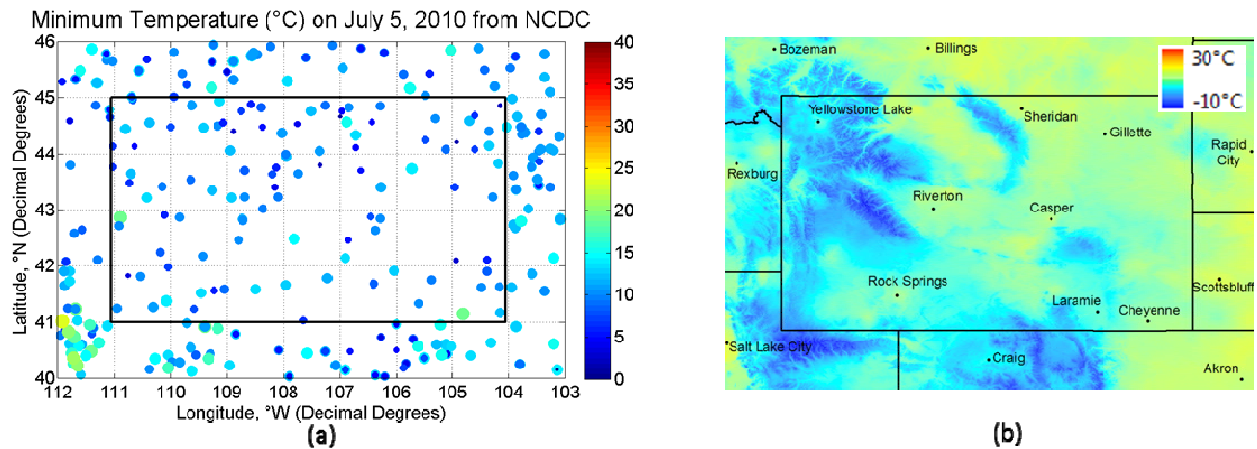
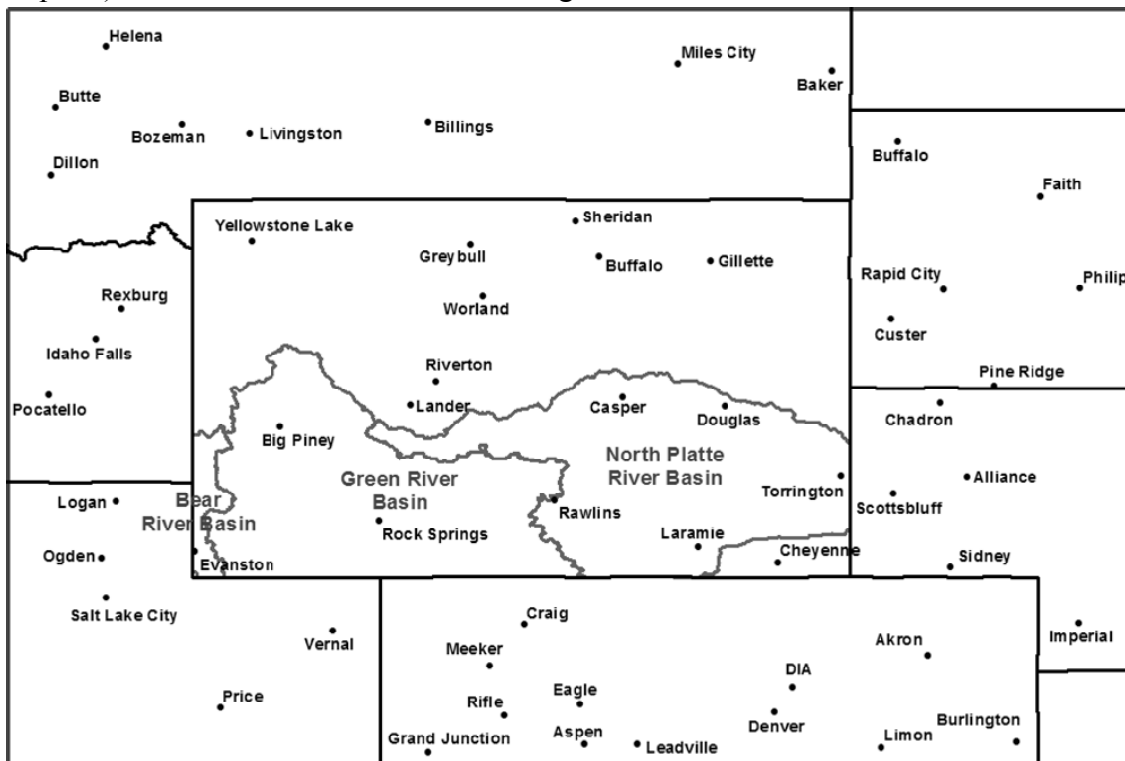


Figure 4: An example of spatial interpolation of minimum temperature (TMIN) for July 5, 2010.

### 2.1.2 Dew Point Temperature

Compared to minimum and maximum temperature data, daily dew point temperature data is very scarce. Daily dew point temperature data were downloaded from Quality Controlled Local Climatological Data (QCLCD) from July 1996 to December 2010. The QCLCD only has records after July 1996 for Weather-Bureau-Army-Navy (WBAN) stations (mostly at the airports). These 56 stations are shown in Figure 5.



The daily dew point temperatures (TDEW) were subtracted from daily TMIN to get a daily TDEW adjustment at 56 stations, as shown in Figure 6.

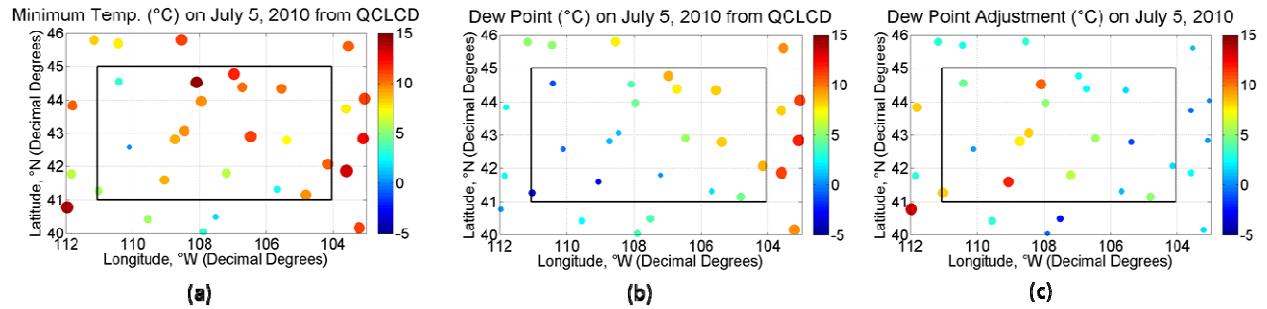


**Figure 6: Bias adjustment for Dew point temperature. (a) TMIN, (b) TDEW, (c) daily TDEW adjustment (TMIN – TDEW)**

The monthly average dew point adjustment was then calculated for each station, resulting in 12 monthly dew point adjustments for each station. These monthly point values were then interpolated using IDW to get monthly grids of dew point adjustment, as seen in Figure 7.

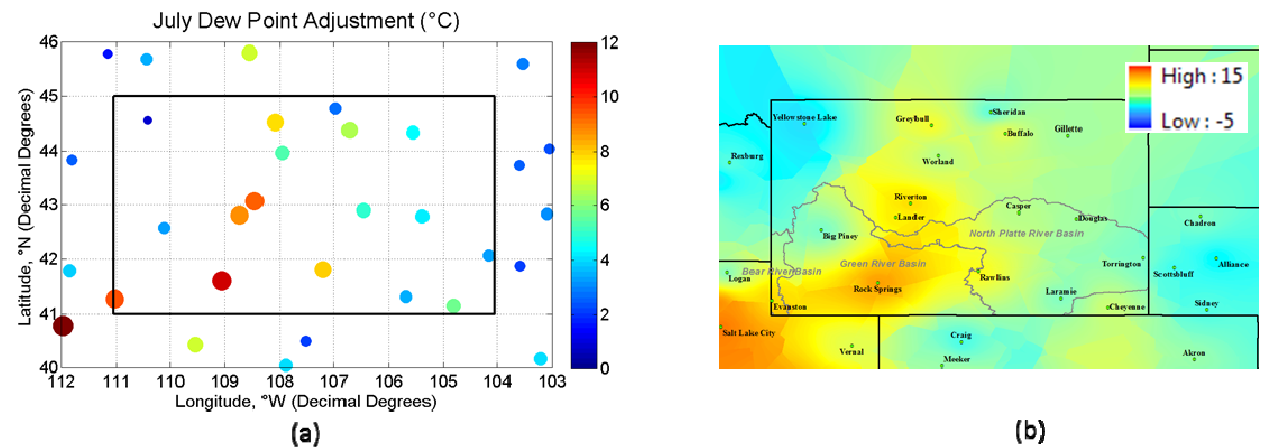


**Figure 7: Spatial interpolation of dew point temperature adjustment: (a) monthly point dew point adjustment and (b) spatially interpolated monthly dew point adjustment.**

The actual dew point grids were calculated by subtracting the appropriate monthly dew point adjustment grid from the daily TMIN grids, as shown in Figure 8.

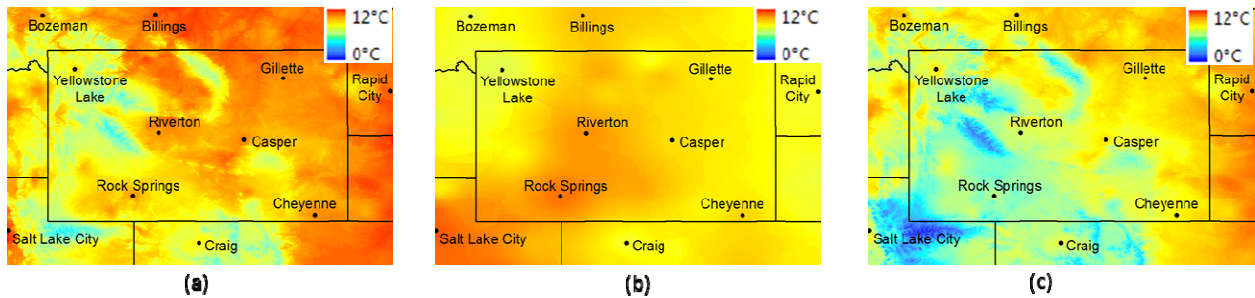


**Figure 8: Daily Dew point temperature (c) is calculated by subtracting monthly bias of the dew point temperature (b) from spatially interpolated daily dew point temperature (a).**

### 2.1.3 Wind Speed

Wind speed Reanalysis I and Reanalysis II data were obtained from National Centers for Environmental Prediction (NCEP). Since these two data sets have a spatial resolution of 2°, it was necessary to downscale them into 0.01°, as shown in Figure 9.

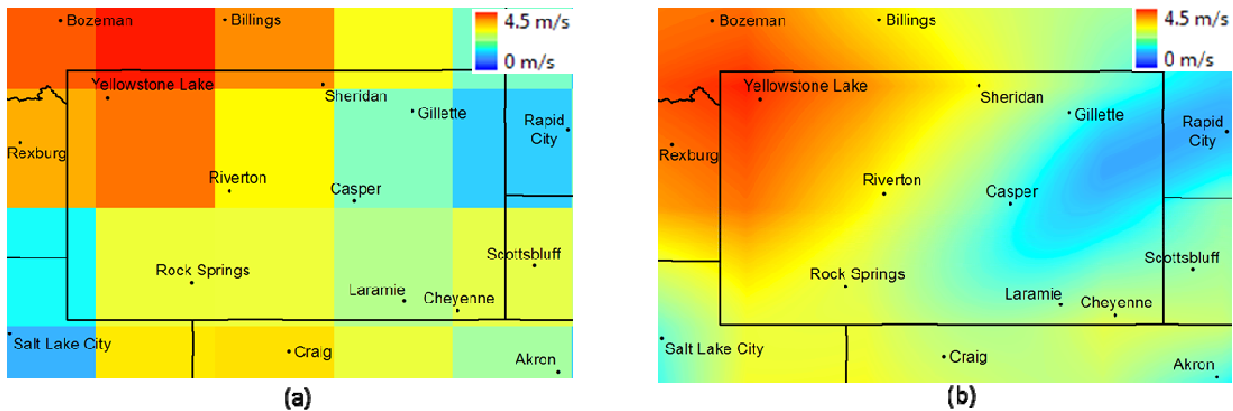


**Figure 9: Downscaling of NCEP wind speed. (a) 2 degree NCEP wind speed and (b) Spatially interpolated NCEP wind speed in 0.01 degree resolution.**

Reanalysis I and II were compared, and it was found that both have a similar pattern, but reanalysis II generally has a higher magnitude. To help determine which data set to use, measured wind speed data were downloaded from NCDC (from January 1984 to June 1996) and from QCLCD (from July 1996 to December 2010) for the same 56 stations that had dew point data. There is no measured wind speed data before 1984. When the measured wind speeds were compared to both reanalysis sets, it was found that the measured wind speeds rarely matched the NCEP values. Therefore, to get a more accurate wind speed grid, it was decided that bias would be calculated and interpolated. Since Reanalysis I data go back to 1948 and Reanalysis II data start in 1979, Reanalysis I was chosen for the bias calculation, as shown in Figure 10.

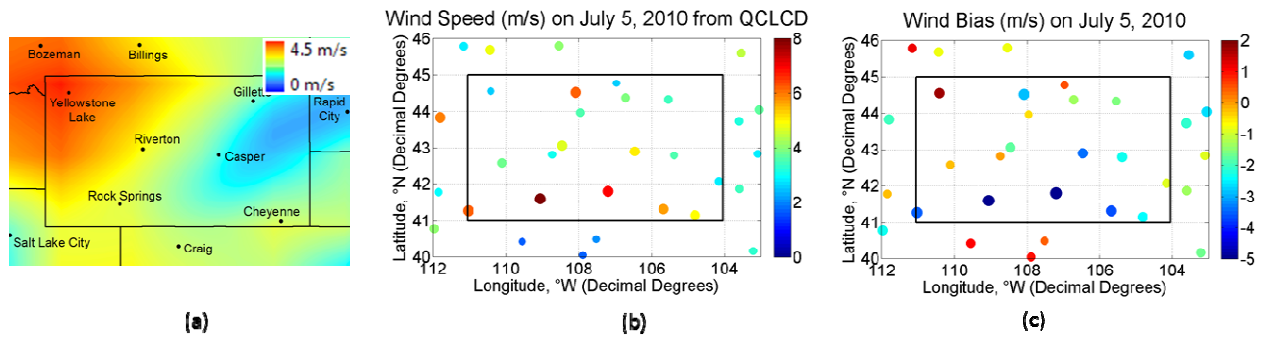


**Figure 10: Wind bias calculation: (a) NCEP wind speed – (b) observed wind speed at stations = (c) wind speed bias at stations.**

The daily bias point values were then interpolated using IDW to get daily bias grids, as shown in Figure 11.

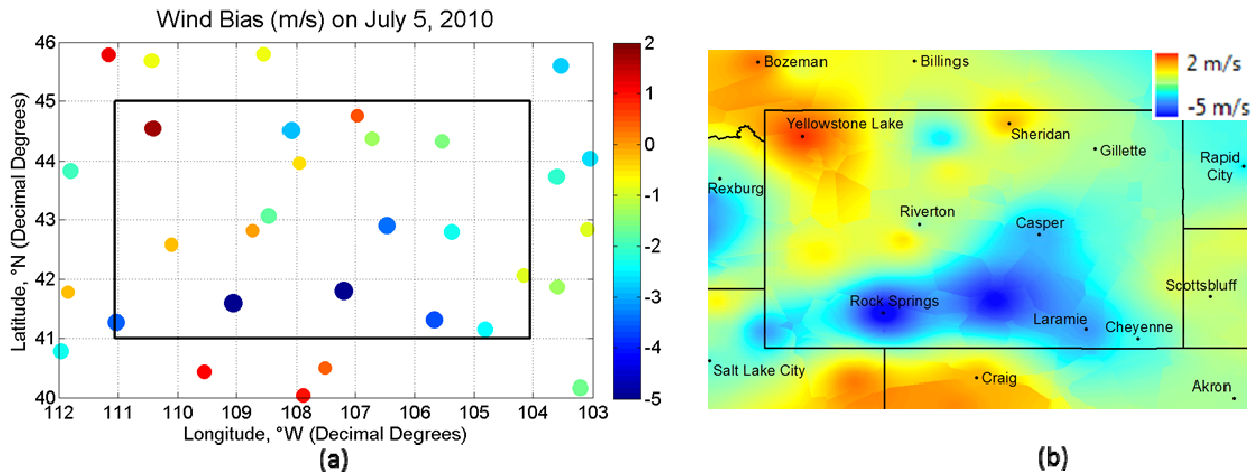


**Figure 11: spatial wind bias (b) interpolated from point wind bias (a).**

The final daily wind speed grids for 1984 to 2010 were calculated by subtracting the daily bias grids from the daily NCEP grids, as seen in Figure 12. Since there are no measured wind speeds before 1984, daily bias cannot be calculated. Instead, average monthly wind bias was calculated by averaging all of the daily bias grids for each month to get 12 monthly bias grids. The final wind speed grids for 1960 to 1983 were calculated by subtracting the appropriate monthly bias grids from each daily NCEP grid. All wind speeds are at a height of 10 meters. Using this procedure, some of the final wind speed grids had small negative values. Any negative wind speeds were replaced with 0.

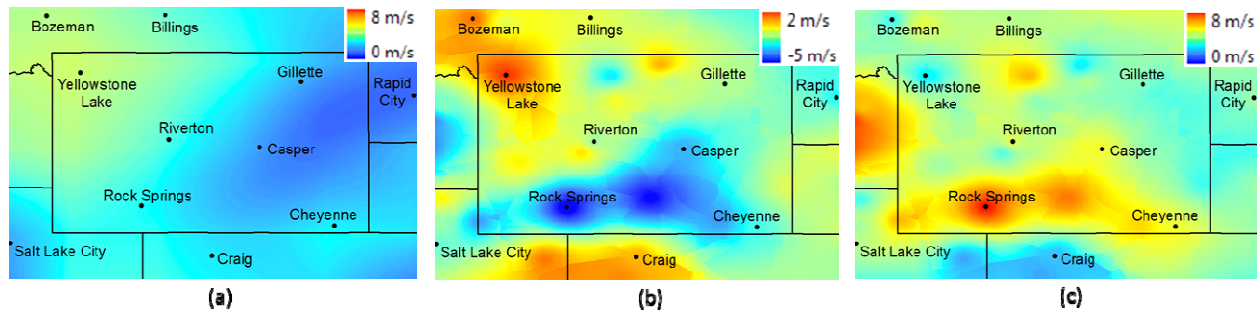


Figure 12: Final wind speed calculation: (a) NCEP - (b) wind bias = (c) final wind speed.

### 2.1.4 Precipitation

Precipitation (PRCP) data were downloaded from NCDC for the same 1,135 weather stations that were used for TMAX and TMIN. PRCP was interpolated the same way TMAX and TMIN were from the weather stations to a grid, except PRCP was not lapsed by elevation. An example of this interpolation is shown in Figure 13.

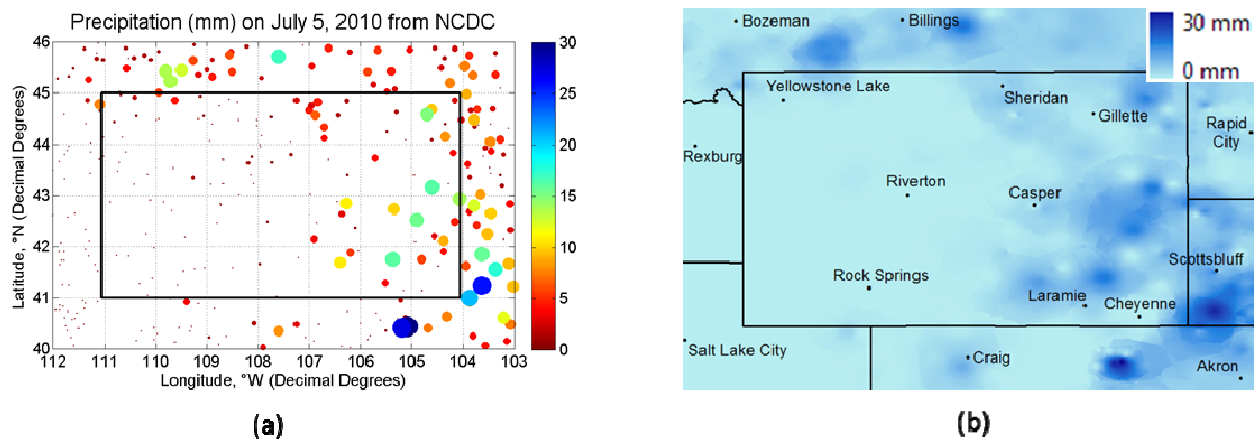
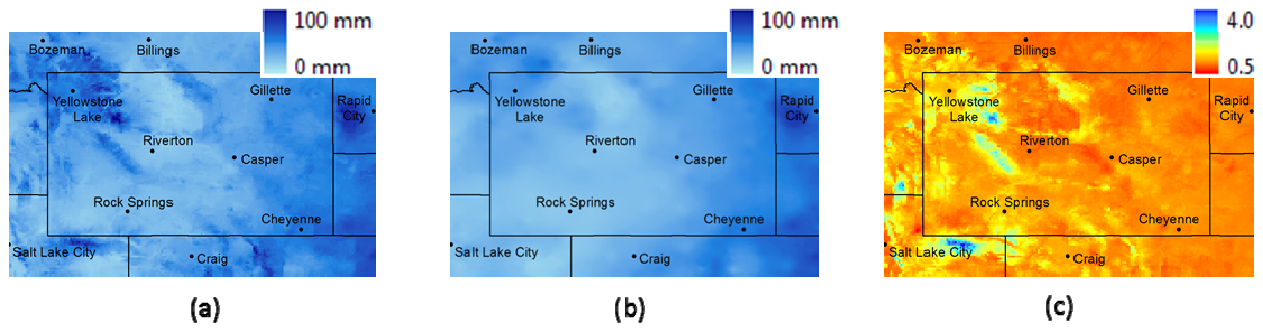


Figure 13: An example of spatial interpolation of Precipitation for July 5, 2010. (a) Observed daily precipitation at weather stations and (b) spatially interpolated precipitation.

To account for elevation, the interpolated PRCP was adjusted using monthly total average PRCP and monthly PRISM data. The monthly total average was calculated by adding up the PRCP on every day for a particular month from 1960 to 2010 and dividing it by the number of months (51). Monthly PRISM data was obtained from the PRISM Climate Group. The rescaling factor was calculated by dividing the PRISM data by the monthly total average, as shown in Figure 14.



**Figure 14: Precipitation rescaling factor calculation for July. Monthly Rescaling Factor (a) = Monthly PRISM (b) / Monthly Total Average (c).**

The final PRCP was then calculated by multiplying the interpolated PRCP and the rescaling factor, as shown in Figure 15.

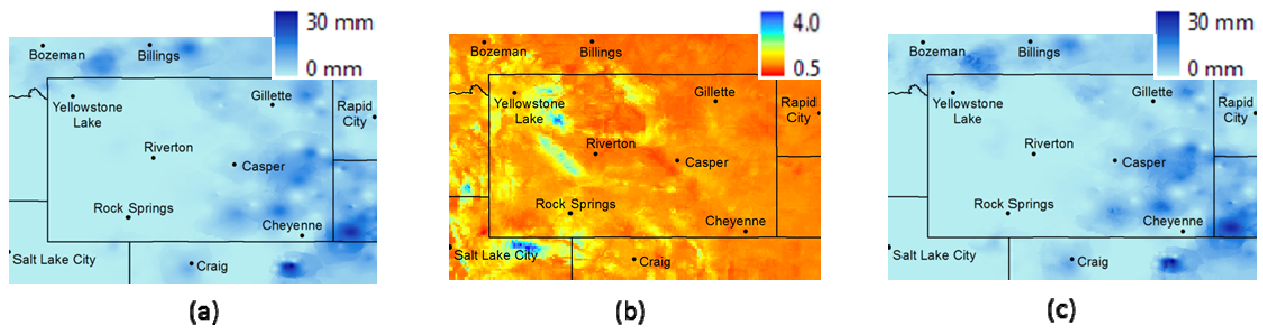


**Figure 15: Final precipitation for July 5, 2010 (Interpolated PRCP x Monthly Rescaling Factor = Final PRCP).**

## 2.2 Reference ET

Among the many reference ET equations available, the ASCE Standardized, Hargreaves-Samani, and the FAO Blaney-Criddle equations were selected for the project. Arc Macro Language (AML) scripts were developed for each equation to calculate the reference ET. For the ASCE Standardized and the Hargreaves-Samani equations, the reference ET is daily from 1960 to 2010. For the Blaney-Criddle equation, the reference ET is monthly from 1960 to 2010 because using the Blaney-Criddle for daily timescales is not recommended by ASCE (2005). Both short (grass) reference ET and tall (alfalfa) reference ET were calculated for this project.

### 2.2.1 ASCE Standardized

The ASCE Standardized reference ET equation is as follows:

$$ET_0 = 0.408 \cdot T_a \cdot (e - a_p) + 0.417 \cdot U_2 \cdot (e - a_p) + 1.6105 \cdot U_2 \cdot T_a$$

where

$ET_{ref}$  = daily standardized reference ET

$\Delta$  = slope of saturation vapor pressure-temperature curve

$R_n$  = net radiation

$G$  = soil heat flux density

$\gamma$  = psychrometric constant

$C_n$  = numerator constant (900 for short reference, 1600 for tall reference)

$T$  = mean temperature

$u_2$  = wind speed at 2 m height

$e_s$  = saturation vapor pressure

$e_a$  = actual vapor pressure

$C_d$  = denominator constant (0.34 for short reference, 0.38 for tall reference)

Within the net radiation calculation, actual incoming solar radiation is required. However, solar radiation measurements were not available. Therefore, incoming radiation was estimated using the Hargreaves-Samani style of radiation prediction:

$$R_s = k_{RS} * \sqrt{T_{max} - T_{min}} * R_a$$

where

$R_s$  = incoming solar radiation

$k_{RS}$  = adjustment coefficient (0.16 for inland locations)

$T_{max}$  = maximum temperature

$T_{min}$  = minimum temperature

$R_a$  = extraterrestrial radiation

An example of an ASCE Standardized reference ET map is shown in Figure 16.

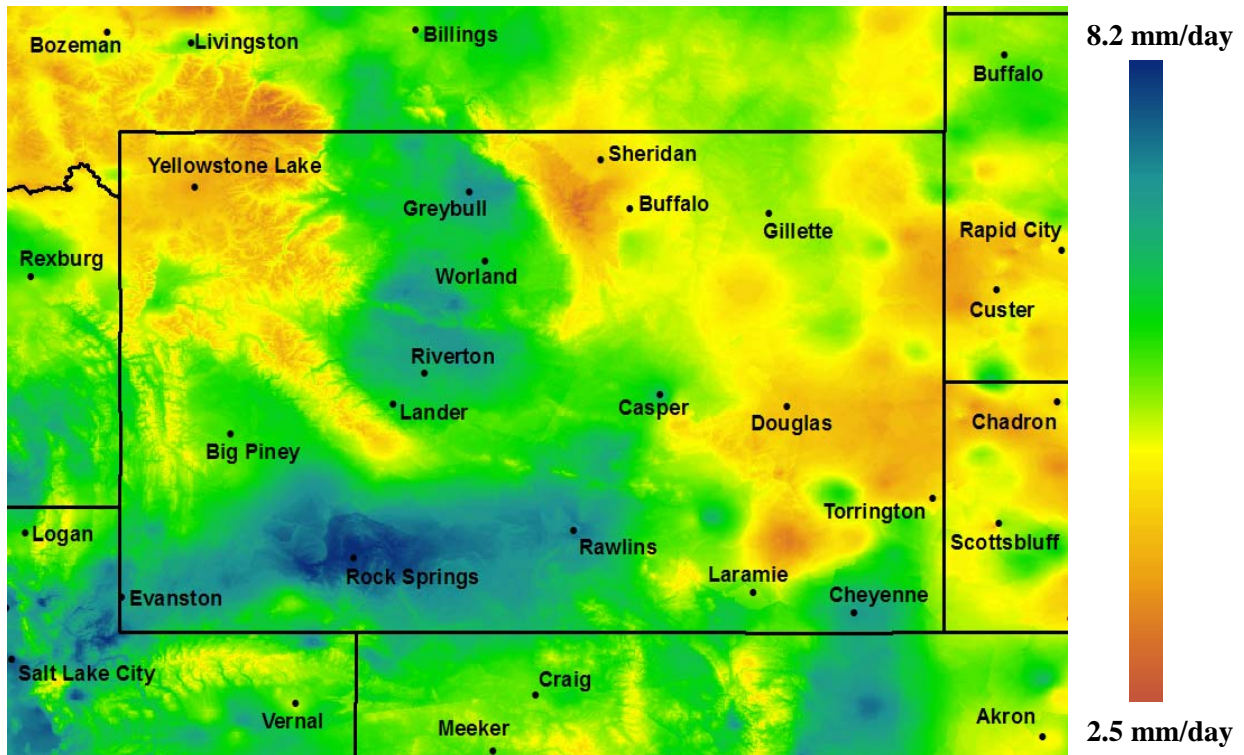


Figure 16: ASCE standardized grass reference ET (mm) for July 5, 2010.

### 2.2.2 Hargreaves-Samani

The Hargreaves-Samani reference ET equation is as follows:

$$RET = \frac{0.0023 \cdot R_a \cdot \sqrt{T_{\max} - T_{\min}} \cdot (T_{\text{mean}} + 17.8)}{2.45}$$

where

RET = daily standardized reference ET

$R_a$  = extraterrestrial radiation

$T_{\max}$  = maximum daily temperature

$T_{\min}$  = minimum daily temperature

$T_{\text{mean}}$  = mean daily temperature

An example of a Hargreaves-Samani reference ET map is shown in Figure 17.

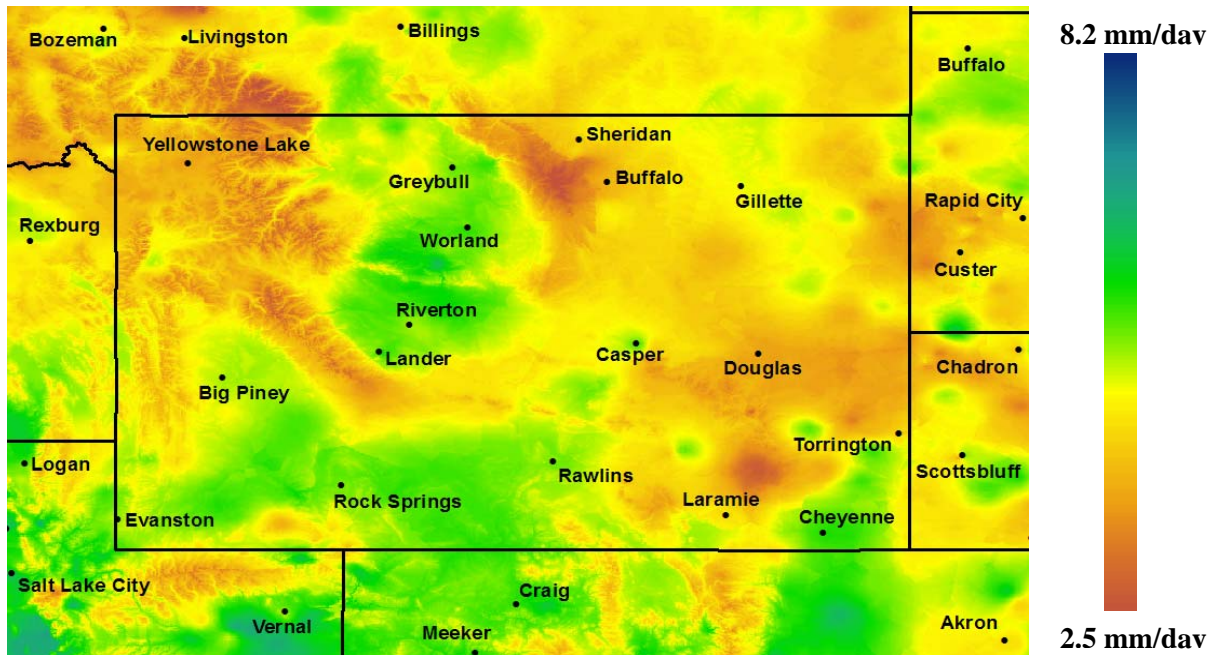


Figure 17: Hargreaves-Samani grass reference ET (mm) for July 5, 2010.

#### 4.2.3 FAO Blaney-Criddle

The FAO Blaney-Criddle reference ET equation is as follows:

$$RET = p \cdot (0.46 \cdot T_{\text{mean}} + 8)$$

where

RET = monthly standardized reference ET

p = mean daily percentage of annual daytime hours

$T_{\text{mean}}$  = mean monthly temperature

The value of p depends on the latitude and month, as shown in Table 1. The values of p were interpolated for each degree. An example of a FAO Blaney-Criddle grass reference ET map is shown in Figure 18.

Table 1: Mean daily percentage of annual daytime hours for different latitudes.

Latitude (Deg. North)	Jan	Feb	Mar	Apr	May	June	July	Aug	Sept	Oct	Nov	Dec
50	0.19	0.23	0.27	0.31	0.34	0.36	0.35	0.32	0.28	0.24	0.20	0.18
45	0.20	0.23	0.27	0.30	0.34	0.35	0.34	0.32	0.28	0.24	0.21	0.20
40	0.22	0.24	0.27	0.30	0.32	0.34	0.33	0.31	0.28	0.25	0.22	0.21
35	0.23	0.25	0.27	0.29	0.31	0.32	0.32	0.30	0.28	0.25	0.23	0.22

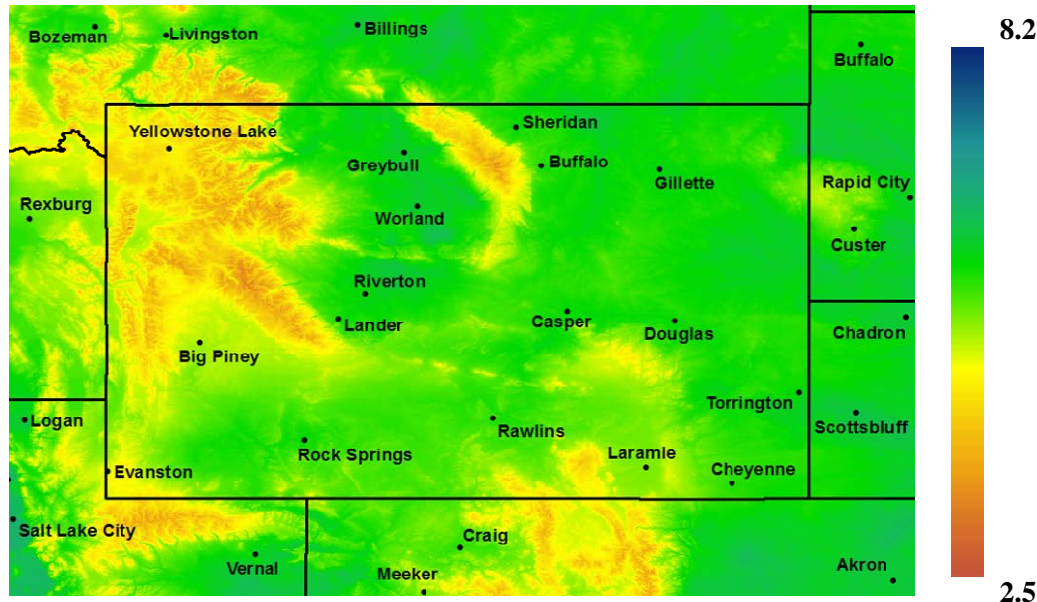


Figure 18: FAO Blaney-Criddle grass reference ET (mm) for July 2010.

## 2.3 Crop Coefficients and Land Use

### 2.3.1 Group Map

Pochop et al. (1992) classified 67 stations in Wyoming into 5 groups, as shown in Figure 19. These groups are based on elevation and growing season length. In order to obtain default growing season for each crop in Wyoming, the group numbers at stations were interpolated using the Thiessen polygon method within each basin for this project. The resulting Thiessen polygons are shown in Figure 20, and the group map is shown in Figure 21.

Group #1 4/1-10/15		Group #2 4/15-10/15		Group #3 4/15-9/30		Group #4 4/15-9/15		Group #5 5/1-9/15	
Albin	Lusk	Double 4 Rch	Centennial	Afton	Big Piney				
Arvada	Midwest	Ft Washakie	Encampment	Alta	L Yellowstone				
Basin	Morrisey	Green River	Evanston	Bedford	Moran				
BoysenDam	Newcastle	Laramie	MedicineBow	Border	Pinedale				
Buffalo	Pathfinder	Moorcroft	Rawlins	Dubois	South Pass				
Casper	Pine Bluffs	Muddy Gap	Saratoga	Farson					
Cheyenne	Powell	Riverton	Seminole Dam	Jackson					
Chugwater	Redbird	Rock Springs	Wamsutter	Kemmerer					
Cody	Sheridan	Sundance		Sage					
Douglas	Ten Sleep	Sunshine		Tower Falls					
Gillette	Thermopolis								
Glenrock	Torrington								
Kaycee	Upton								
LaGrange	Weston								
Midwest	Whalen Dam								
Lander	Wheatland								
Lovell	Worland								

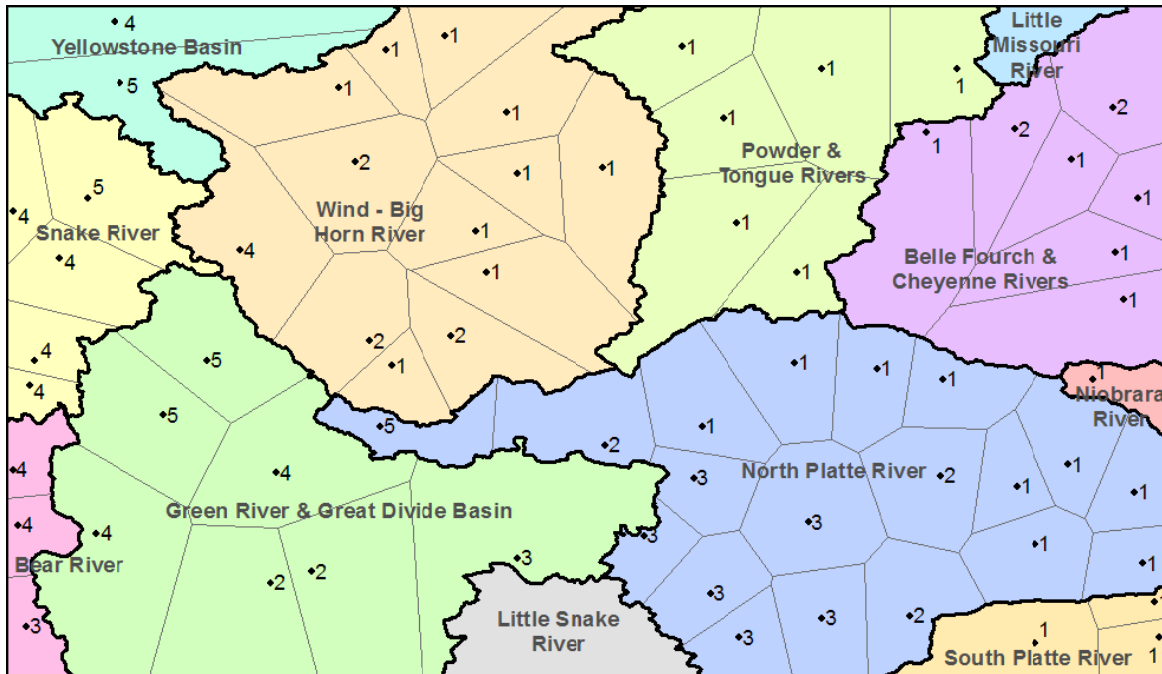


Figure 20: Thiessen polygons of group numbers.

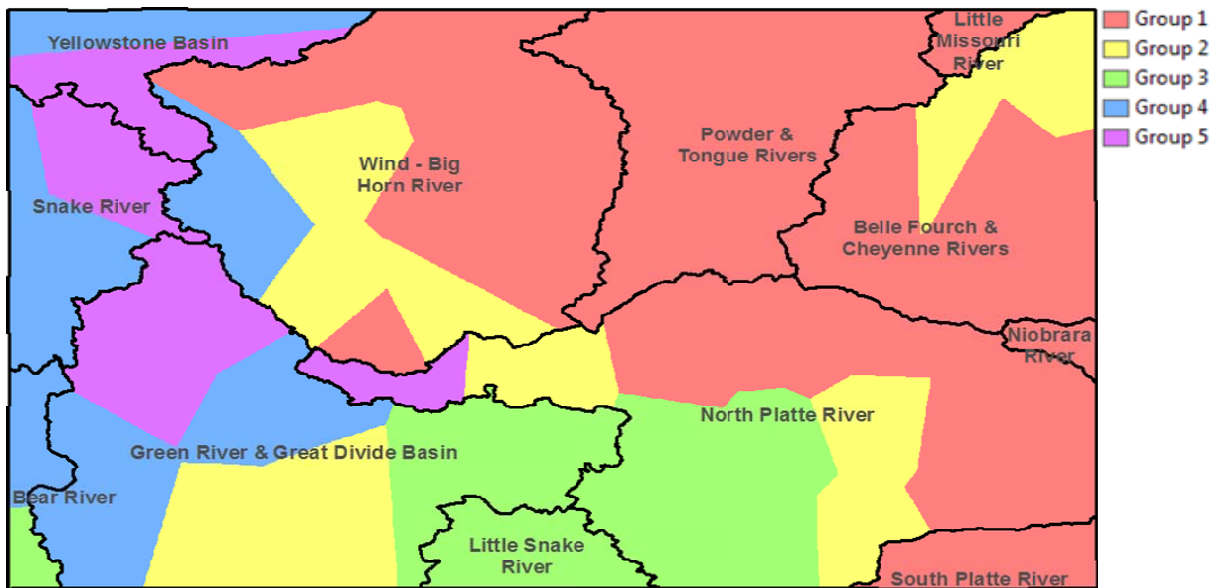


Figure 21: Group map for Wyoming.

### 2.3.2 Land Use Map

The 1992 National Land Cover Data (NLCD) map, seen in Figure 22, was chosen as the default crop type map. However, the users can use their own crop type map, if they desire.



Figure 22: National Land Cover Data (NLCD) map for Wyoming.

### 2.3.3 Crop Coefficients

A database of default crop coefficients ( $K_c$ ) to use in the ArcGIS ET calculation tool was developed. The database contains both actual crops, such as corn and beans, and the land types from the NLCD map, such as evergreen forest and shrublands. For actual crops,  $K_c$  values are obtained from Pochop et al. (1992). For many of Pochop’s crops, there are different  $K_c$  values for each group. Therefore, the entire database is split into 5 groups. Some of the  $K_c$  values for crops also come from FAO's Water Development and Management Unit. This database also contains growing season dates.

The  $K_c$  values for the NLCD land types were much harder to obtain. The values for July are based on a METRIC ET map of July 2009. The values for the other months are found by depreciating the July value a reasonable amount. For these land types, we recommend the user employ their own  $K_c$  values. A small portion of default  $K_c$  database is shown in Figure 23.

GROUP	PROGCROPID	CROP_NAME	PROGLANDID	GS_S_DATE	GS_E_DATE	KC_JAN	KC_FEB	KC_MAR	KC_APR	KC_MAY	KC_JUN	KC_JUL	KC	
1	0	Void	100	NONE	NONE									
1	1	Grass	101	LOCATION	LOCATION				0.87	1.03	1.04	1.03	0.	
1	2	Alfalfa/Grass Mix	102	LOCATION	LOCATION				0.90	1.06	1.07	1.06	0.	
1	3	Alfalfa	103	LOCATION	LOCATION				0.92	1.08	1.09	1.08	0.	
1	4	Small Grains	104	LOCATION	LOCATION			0.40	0.55	0.80	1.00	1.15	0.	
1	5	Corn/Grain Sorghum	105	5/15	9/20					0.48	0.60	1.00	1.	
1	6	Dry Beans	106	6/1	9/15						0.44	1.04	0.	
1	7	Sugar Beets	107	4/24	10/15				0.43	0.48	0.82	1.10	1.	
1	8	Sterile Sorghum/Sudan/Sudex/etc.	108	LOCATION	LOCATION			0.40	0.55	0.80	1.00	1.15	0.	
1	9	Potatoes	109	5/20	10/1						0.45	0.61	1.06	1.
1	10	Grapes	110	5/1	9/15					0.48	0.70	0.83	0.	
1	11	Open Water	111	NONE	NONE	0.60	0.60	0.62	0.62	0.62	0.65	0.65	0.	
1	12	Perennial Ice/Snow	112	NONE	NONE	0.40	0.40	0.40	0.40	0.40	0.40	0.40	0.	
1	21	Low Intensity Residential	121	NONE	NONE	0.25	0.25	0.30	0.45	0.70	0.75	0.80	0.	
1	22	High Intensity Residential	122	NONE	NONE	0.22	0.22	0.27	0.40	0.65	0.70	0.75	0.	
1	23	Commercial/Industrial/Transportation	123	NONE	NONE	0.20	0.20	0.22	0.30	0.58	0.65	0.65	0.	
1	31	Bare Ground/Rock/Sand/Clay	131	NONE	NONE	0.18	0.18	0.20	0.22	0.22	0.25	0.25	0.	
1	32	Quarries/Strip Mines/Gravel Pits	132	NONE	NONE	0.18	0.18	0.20	0.25	0.25	0.30	0.30	0.	
1	33	Transitional	133	NONE	NONE	0.35	0.35	0.45	0.55	0.65	0.70	0.80	0.	
1	41	Forest (Deciduous)	141	NONE	NONE	0.30	0.30	0.40	0.70	0.90	1.00	1.12	1.	
1	42	Forest (Evergreen)	142	NONE	NONE	0.70	0.70	0.80	0.85	0.95	1.00	1.12	1.	
1	43	Forest (Mixed)	143	NONE	NONE	0.50	0.50	0.60	0.78	0.92	1.00	1.12	1.	

Figure 23: Default  $K_c$  database table.

### 3. TOOLS DEVELOPED

The tools developed for this project include a GIS calculator and a website.

#### 3.1 ArcInfo reference ET script

ArcInfo reference model for each equation was written in ArcInfo macro language (AML). The scripts calculate both short and tall reference ET.

#### 3.2 Wyoming ET Calculator

The GIS tool developed for this project, shown in Figure 24, is Wyoming ET Calculator. It is an add-in to ESRI ArcMap and was developed in .NET and C# using Microsoft Visual Studio. The inputs include the gridded reference ET and precipitation maps described above, an area of interest, a timeframe, crop coefficients, effective precipitation ratios, and water stress factors. The main outputs include daily potential ET, CIR, and actual ET. Monthly total and growing season total CIR and ET can also be calculated. See Wyoming ET Calculator's user manual for more information about the interface.

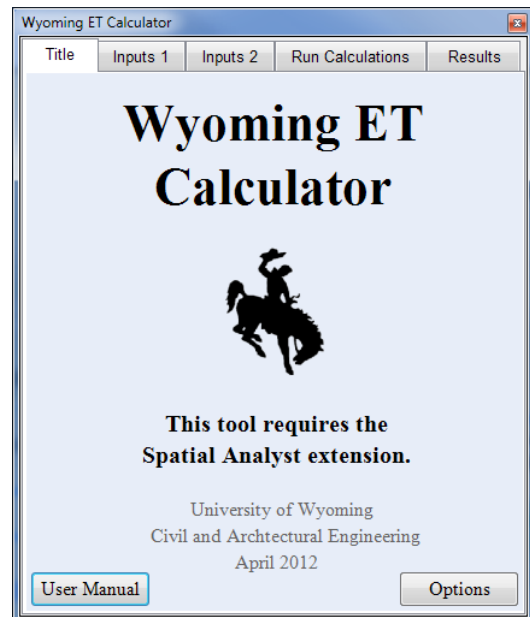


Figure 24: Wyoming ET Calculator.

##### 3.2.1 Model Description

The model performs several calculations on a cell-by-cell basis. These calculations include potential ET (also called crop ET), effective precipitation, CIR, and actual ET (also called consumptive use). Potential ET is the amount of ET that is possible with ample water (the ET demand due to the environment and land type). The calculation is:

$$PET = K_c \cdot RET$$

where

PET = potential ET

$K_c$  = monthly crop coefficient

RET = reference ET

Because not all precipitation that falls will be available to meet ET demand (for example, precipitation can become runoff or infiltrate into the ground), the effective precipitation is needed. The calculation is:

$$P_{\text{eff}} = \text{PRCP} \cdot R_{\text{eff}}$$

where

$P_{\text{eff}}$  = effective precipitation

PRCP = precipitation

$R_{\text{eff}}$  = effective precipitation ratio

CIR is the amount of water a crop needs to meet the ET demand. The calculation is:

$$\text{CIR} = \text{PET} - P_{\text{eff}}$$

where

CIR = consumptive irrigation requirement

PET = potential ET

$P_{\text{eff}}$  = effective precipitation

If effective precipitation is greater than potential ET (meaning CIR is negative), CIR is set to zero. Actual ET includes a factor to account for water stress. The calculation is:

$$\text{AET} = P_{\text{eff}} + \text{CIR} \cdot K_s$$

where

AET = actual ET

$P_{\text{eff}}$  = effective precipitation

CIR = consumptive irrigation requirement

$K_s$  = water stress factor

### 3.3 Website

A website is currently hosted at the University of Wyoming, but will be transferred to the State Engineers' Office. Total of 650 GB of weather data are available to the public, but data download is limited to 2 GB at a time. Users can download monthly data through the ftp server or define a smaller area to subset the data for the area of interest. The website provides spatially interpolated weather data, reference ET, Wyoming ET calculator, and user manual with an example.

#### 4. COMPARISON TO METRIC ET

To evaluate Wyoming ET Calculator, total monthly AET over an irrigated area was compared to total monthly ET found using METRIC for June through September 2009. The area is irrigated lands surrounding the Ocean Lake near Riverton, WY, as shown in Figure 25.

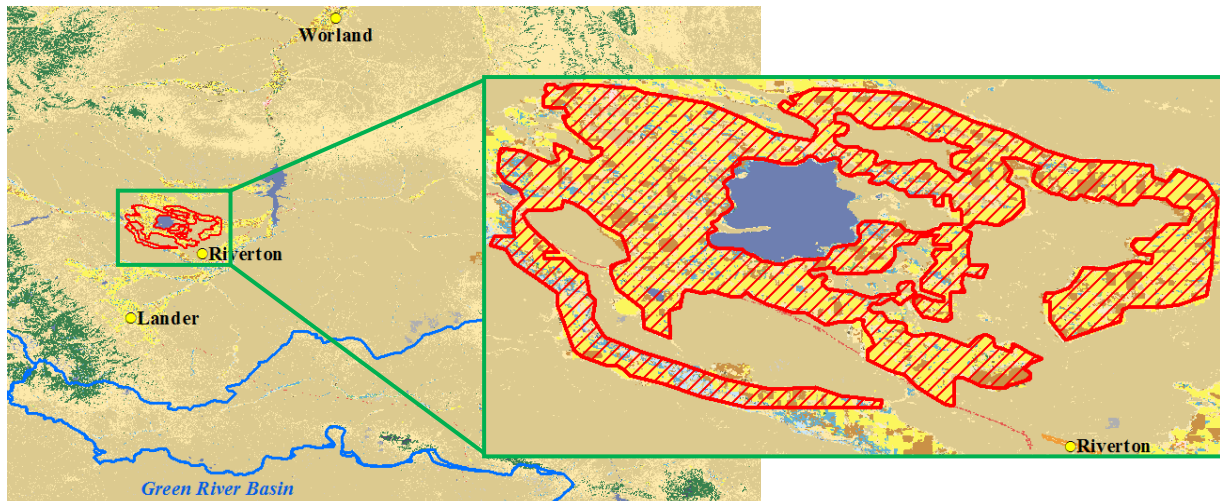


**Figure 25: Irrigated area of interest (red polygon).**

To calculate AET with Wyoming ET Calculator, the model processed daily RET (assuming the entire NLCD crop areas were alfalfa, an effective precipitation ratio of 0.90, and a water stress factor of 1) to get daily AET. This daily AET was then summed to get the monthly AET.

The total monthly ET for METRIC was calculated by linearly interpolating ETrF (ratio of AET to RET) between the days that had satellite imagery to get an ETrf grid for every day. The daily ETrf grids were multiplied by daily ET measured from a station (a point) to get daily grids of ET. Finally, the daily ET grids were summed to get monthly ET grids.

The results, after converting each map from depth to a volume and summing all the cells in the area of interest, are shown in the 2<sup>nd</sup> and third columns of Table 2. These results are shown graphically by the blue and green lines in Figure 26. The fourth column in Table 2 is the METRIC result divided by the Wyoming ET Calculator result. Because the water stress was assumed to be 1 in Wyoming ET Calculator, this represents an actual water stress factor. For June, July, and August, this factor remains very close to a reasonable value of 0.70. The red line in Figure 26 represents the result had a water stress factor of 0.70 been used in Wyoming ET Calculator. The spatial distribution of the volume of ET for July 2009 for both METRIC and Wyoming ET Calculator is shown in Figure 27. Figure 27 shows that ET volume is much more uniform for Wyoming ET Calculator, because there are only a few land types in the NLCD map

over the area of interest, and Wyoming ET calculator uses the same crop coefficient for the same type of crop cover within the same land group.

**Table 2: Results of the Wyoming ET Calculator and METRIC comparison.**

	METRIC (acre-ft)	Wyoming ET Calculator (acre-ft)	Water Stress Factor ( $K_s$ )
<b>June</b>	18,646	26,961	0.692
<b>July</b>	24,976	35,334	0.707
<b>August</b>	18,849	27,635	0.682
<b>September</b>	6,683	15,141	0.441

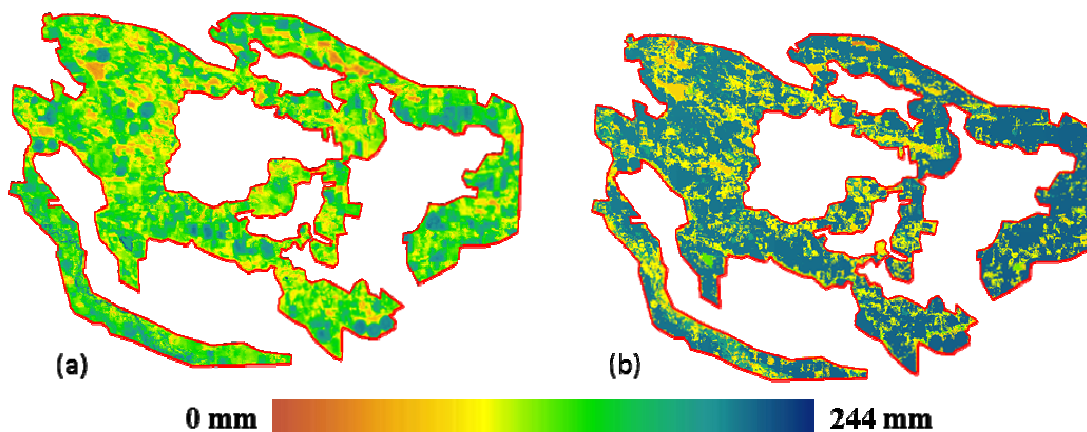
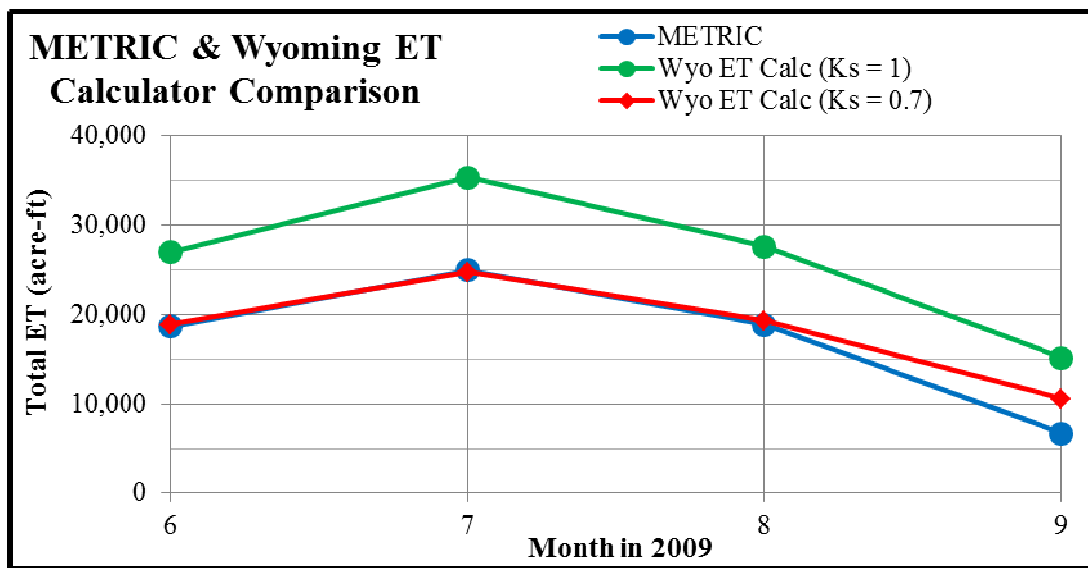


**Figure 27: Spatial distribution of July 2009 ET (METRIC on the left and Wyoming ET Calculator on the right).**

## **5. PRINCIPAL FINDINGS AND SIGNIFICANCES**

- High spatial (0.01 x 0.01 degree) and temporal (daily) weather data for a long-term period (1960-2010) are produced for the state of Wyoming, and they can serve as key information for many hydrological studies.
- More accurate monthly weather data are produced from the daily data.
- Two climate normal data (1971-2000 or 1981-2010) are also produced.
- Reference ET data also are produced for a period from 1960 to 2010.
- Weather data are archived at the SEO's data server, and will serve to the public.
- The Wyoming ET Calculator is installed at SEO's PC, and it will be used as a key tool in estimating consumptive use with user specified scenarios for any given year or for climate normal.
- A webserver hosted at the SEO will serve data and tools to the public and other agencies to facilitate more accurate estimation of consumptive use in the state of Wyoming.
- The Wyoming ET Calculator provides a reliable estimation of ET, compared to METRIC.
- The automatic scripts will continuously produce same quality weather data for the future period without extra cost.

## **6. PROJECT PUBLICATIONS**

Ryan Rasmussen and Gi-Hyeon Park, Estimation of Growing Season ET using Wyoming ET Calculator – AGU meeting December 5-9, 2011 San Francisco, California

Nancy Thoman and Gi-Hyeon Park, Satellite-based Growing Season ET Estimation using a Statistical Transformation – AGU meeting December 5-9, 2011 San Francisco, California

Gi-Hyeon Park, Nancy Thoman, and Ryan Rasmussen, Application of a Statistical Transformation to enhance Satellite-based ET Estimation – 47<sup>th</sup> AWRA Annual Water Resources Conference, November 7-10, 2011 Albuquerque, New Mexico

Ryan Rasmussen and Gi-Hyeon Park, High-resolution mapping of reference ET for the state of Wyoming – AGU meeting December 13-17, 2010, San Francisco, California

## **7. STUDENT SUPPORT AND TRAINING**

Ryan Rasmussen, a M.S. graduate student in Civil and Architectural Engineering at the University of Wyoming was responsible for most of the work included in this project, including data processing, tool development, and web development. He will receive MS degree in Civil Engineering in summer of 2012 and will work for HDR.

Nancy Thoman, a MS student in Civil and Architectural Engineering, was partially supported during the summer of 2011 for processing several LANSAT imageries to estimate ET near Ocean Lake. She was trained for METRIC image processing.

## 9. REFERENCES

- Allen, R.G. 1999. *REF-ET for Windows: Reference evapotranspiration calculator*; version 3.1.08, Univ. of Idaho Research and Extension Center, Kimberly, Idaho. Available at <<http://www.kimberly.uidaho.edu/ref-et>>
- Allen, R.G., A. Morse, M. Tasumi, W.J. Kramber, W. Bastiaanssen, 2005a. Computing and Mapping of Evapotranspiration; Chapter 5 in *Advances in Water Science Methodologies*; U. Aswathanarayana, Ed.; A.A. Balkema Publishers; Leiden, The Netherlands
- Allen, R.G., I.A. Walter, R.L. Elliot, T.A. Howell, D. Itenfisu, M.E. Jensen, and R.L. Snyder. 2005b. *The ASCE Standardized Reference Evapotranspiration Equation*. Published by the American Society of Civil Engineers.
- Allen, R. G., Pereira, L. S., Raes, D., and Smith, M. 1998. "Crop evapotranspiration: Guidelines for computing crop requirements." *Irrigation and Drainage Paper No. 56*, FAO, Rome, Italy.
- Bastiaanssen, W.G.M., M. Menenti, R.A. Feddes and A.A.M. Holtslag, 1998a. The Surface Energy Balance Algorithm for Land (SEBAL): Part 1 formulation, *J. of Hydr.* 212-213: 198-212
- Bastiaanssen, W.G.M., H. Pelgrum, J. Wang, Y. Ma, J. Moreno, G.J. Roerink and T. van der Wal, 1998b. The Surface Energy Balance Algorithm for Land (SEBAL): Part 2 validation, *J. Of Hydr.* 212-213: 213-229
- Brouwer C, Heibloem M. 1986. *Irrigation Water Management: Irrigation Water Needs*. FAO Training Manuel No. 3, Rome, Italy.
- Covey, W. 1959. Testing a hypothesis concerning the quantitative dependence of evapotranspiration on availability of moisture. *Soil Physics*, A. & M. College of Texas, College Station, M.S. Thesis, 58 pp.
- Doorenbos, J., Pruitt, W.O., 1977. Crop water requirements. *Irrigation and Drainage Paper No. 24*, (rev.) FAO, Rome, Italy, 144 pp.
- España, S., Alcalá, F., Vallejos, A., and Pulido-Bosch, A. 2011. *ArcE: A GIS tool for modeling actual evapotranspiration*. *Computers & Geosciences* (2011), doi:10.1016/j.cageo.2011.03.008.
- Hargreaves, G.H., Samani, S. 1982. *Estimating potential evapotranspiration*. *Journal of the Irrigation and Drainage Division* 108(3): 225–230.
- Li, S., Tarboton, D., McKee, M. 2003. *Development of an ArcMap Toolbar for Regional Evapotranspiration Modeling, in ESRI, comp., Proceedings 23<sup>rd</sup> ESRI international users conference. San Diego, California, USA.*
- Monteith, J.L. 1965. Evaporation and environment. pp. 205-234. In G.E. Fogg (ed.)

Symposium of the Society for Experimental Biology, *The State and Movement of Water in Living Organisms*, Vol. 19, Academic Press, Inc., NY.

Penman, H.L. 1953. The physical basis of irrigation control. *Rep. 13th Intl. Hort. Congr.*, 2:913-914.

Pochop, L., Teegarden, T., Kerr, G., Delaney, R., Hasfurther, V. 1992. *Consumptive Use and Consumptive Irrigation Requirements in Wyoming*, Laramie, Wyoming.

Rijtema, P.E. 1965. Analysis of actual evapotranspiration. Agric. Res. Rep. No. 69, Centre for Agric. Publ. and Doc., Wageningen, 111 p.

Snyder R.L. and Eching S, 2003. PMday, Penman-Monteith daily. The Regents of the Univ. California, Davis, California. Available from <http://biomet.ucdavis.edu/evapotranspiration/PMmonXLS/PMmon.xls>.

StateCU, 2008. State Consumptive Use. Available from <http://cdss.state.co.us/software/Pages/StateCU.aspx>

# Treatment of High-Sulfate Water Used for Livestock Production Systems

## Basic Information

<b>Title:</b>	Treatment of High-Sulfate Water Used for Livestock Production Systems
<b>Project Number:</b>	2010WY59B
<b>Start Date:</b>	3/1/2010
<b>End Date:</b>	2/29/2012
<b>Funding Source:</b>	104B
<b>Congressional District:</b>	1
<b>Research Category:</b>	Water Quality
<b>Focus Category:</b>	Agriculture, Treatment, Water Quality
<b>Descriptors:</b>	Sulfate, Water Treatment, Livestock, Health
<b>Principal Investigators:</b>	Kristi Cammack, Kathy Austin, Ken C Olson, Cody L Wright

## Publication

1. Jons, A.M, K.L. Kessler, K.J. Austin, C. Wright, and K.M. Cammack, 2011. Iron carbonate supplementation of lambs administered high-sulfur water. J. Anim. Sci. 89(E-Suppl.):694.

# Treatment of High-Sulfate Water used for Livestock Production Systems

## FINAL REPORT (04/20/2012)

### Principal Investigators:

Kristi M. Cammack, Ph.D., Assistant Professor, University of Wyoming  
[kcammack@uwyo.edu](mailto:kcammack@uwyo.edu)

Kathy J. Austin, M.S., Senior Research Scientist, University of Wyoming  
[kathyaus@uwyo.edu](mailto:kathyaus@uwyo.edu)

Ken C. Olson, Ph.D., Associate Professor, South Dakota State University  
[kenneth.olson@sdstate.edu](mailto:kenneth.olson@sdstate.edu)

Cody L. Wright, Ph.D., Associate Professor, South Dakota State University  
[cody.wright@sdstate.edu](mailto:cody.wright@sdstate.edu)

**Abstract:** Reliable drinking water sources that meet minimum quality standards are essential for successful livestock production. Recent surveys have shown that water sources throughout the semi-arid rangelands of the U.S. are not of sufficient quality to support optimum herd/flock health and performance. Water sources high in sulfur (S) concentrations, usually in the form of sulfate ( $\text{SO}_4^{2-}$ ), are problematic in many western regions. High  $\text{SO}_4^{2-}$  concentrations in water sources can arise from several factors. First, water sources can be naturally high in  $\text{SO}_4^{2-}$ . Second, drought conditions can cause  $\text{SO}_4^{2-}$  to be concentrated within the water source. Third, conventional oil and gas production can also increase  $\text{SO}_4^{2-}$  content within the water source. Many of these water sources are used for livestock production systems, especially throughout the western states. High- $\text{SO}_4^{2-}$  water has been shown to reduce performance and cause secondary health and immunity complications in exposed livestock. Additionally, high  $\text{SO}_4^{2-}$  levels in drinking water are a primary cause of polioencephalomalacia (PEM) in ruminant livestock. Sulfur-induced PEM (sPEM) is a disease state in ruminant animals that can cause 25% morbidity and 25-50% mortality in affected populations, resulting in substantial economic losses to the livestock producer. Currently, there are no available treatments for affected livestock, and frequent and stringent testing of drinking water sources for levels of  $\text{SO}_4^{2-}$  and other S compounds, a costly and time-consuming process, is the best prevention strategy. In addition, methods for  $\text{SO}_4^{2-}$  removal from the water source are neither cost-effective nor practical. Ferrous carbonate ( $\text{FeCO}_3$ ) is a soluble iron salt that is routinely used in water treatment plants to bind S. We hypothesize that treatment of high- $\text{SO}_4^{2-}$  water with  $\text{FeCO}_3$  would bind excess S, enabling such sources to be used for livestock production. Our objectives were to 1) determine the effectiveness of  $\text{FeCO}_3$  treatment in binding S in high- $\text{SO}_4^{2-}$  water, and 2) determine if treatment of high- $\text{SO}_4^{2-}$  water with  $\text{FeCO}_3$  prevents the reduced performance and poor health normally observed in livestock consuming high- $\text{SO}_4^{2-}$  water. Briefly, wether lambs ( $n = 80$ ) were assigned to one of four treatments in a randomized complete block design with 20 wethers per treatment replicated over 2 pens per treatment. Treatments included: 1) control feed and low-S

water (57 mg SO<sub>4</sub><sup>2-</sup>/L; LS); 2) control feed and high-S water (2,250 mg SO<sub>4</sub><sup>2-</sup>/L; HS); 3) low-Fe (250 ppm FeCO<sub>3</sub>) feed and high-S water (2,250 mg SO<sub>4</sub><sup>2-</sup>/L; HSLI); and 4) high-Fe (500 ppm FeCO<sub>3</sub>) feed and high-S water (2,250 mg SO<sub>4</sub><sup>2-</sup>/L; HSHI) for a 50 d trial period. All wethers received *ad libitum* access to feed and water. Body weights and blood samples were taken on d -1, 25, and 50, and rumen H<sub>2</sub>S gas was measured on d -1 and 50. Lambs were slaughtered after the trial period for liver and muscle sample collections. There were no differences in ADG between treatment groups ( $P = 0.351$ ). Daily water intake was also not different ( $P = 0.305$ ) between treatment groups, nor was daily feed intake ( $P = 0.116$ ). Mineral analyses showed no treatment effects ( $P \geq 0.214$ ) on plasma concentrations of Fe or Zn, or on hepatic concentrations of Se, Fe, Mo, Mn, or Zn ( $P \geq 0.094$ ). However, both plasma and hepatic Cu concentrations were different ( $P \leq 0.023$ ) between the LS and HSLI groups, with LS wethers having greater concentrations of Cu than HSLI wethers. Production of H<sub>2</sub>S gas was increased ( $P < 0.001$ ) during the trial, with the LS group having lower ( $P \leq 0.012$ ) H<sub>2</sub>S concentrations in the rumen than the HS, HSHI, and HSLI groups. Real-time RT-PCR was performed on 23 genes to assess potential changes at the molecular level. Genes identified as differentially expressed ( $P \leq 0.05$ ) in response to treatment were *SLC26A2*, *GNMT*, *ITGB2*, *PRKACA*, *APEX1*, *EPB41*, *TG2*, *PCNA*, and *PIPOX*. Genes identified as having a tendency to be differentially expressed ( $P \leq 0.10$ ) in response to treatment included *TGFβ1*, *SOD1*, *TUSC3*, and *TJPI*. Genes that were differentially expressed between treatments were consistently upregulated in the HSHI group compared to the other treatment groups. These differentially expressed genes are involved in immune function, oxidative damage, apoptosis, tumor suppression, and tight junctions, suggesting that high dietary Fe, perhaps in combination with high dietary S, influences cellular functions in wethers consuming high-S water. In summary, results of this study suggest that supplementation of an Fe compound to ruminant animals exposed to high-S drinking water was not effective at preventing H<sub>2</sub>S gas accumulation in the rumen, and would likely not prevent the negative effects associated with high dietary S.

**Title:** Treatment of High-Sulfate Water used for Livestock Production Systems  
**FINAL REPORT**

**Statement of Critical Regional or State Water Problem: *Need for Project.*** Reliable drinking water sources that meet minimum quality standards are essential for successful livestock production. However, recent surveys have shown many water sources, especially throughout the semi-arid rangelands of the U.S. and Wyoming, are not of sufficient quality to support optimum herd/flock health and performance [1]. Many of these low quality sources are dangerously high in S and S compounds, especially SO<sub>4</sub><sup>2-</sup>, due to underlying soil conditions, drought conditions, and(or) manmade contaminants (e.g. conventional gas and oil water; CBM water). However, because of limited water resources throughout the western regions, many of these high-SO<sub>4</sub><sup>2-</sup> water sources are still used in livestock production systems. Ruminant livestock consuming high-SO<sub>4</sub><sup>2-</sup> water are prone to poor growth and performance and health complications, including polioencephalomalacia (sPEM), a neurological disorder typically terminating in death. Outbreaks of sPEM can cause 25% morbidity and 25-50% mortality in affected populations. This in combination with the losses in growth and performance results in significant economic losses to producers. Currently, there are no available treatments for livestock affected by high-SO<sub>4</sub><sup>2-</sup> water consumption (including sPEM), and frequent and

stringent testing of drinking water sources for levels of  $\text{SO}_4^{2-}$  and other S-compounds, a costly and time-consuming process, is the best prevention strategy. Methods for removal of  $\text{SO}_4^{2-}$  from the water source include reverse osmosis, distillation, and ion exchange, none of which are cost-effective or practical for livestock producers.

**Who Would Benefit and Why.** Many water sources high in  $\text{SO}_4^{2-}$  are still used for livestock production due to lack of alternative available sources. Additionally, in many of these areas it is neither feasible nor practical to haul in water low in  $\text{SO}_4^{2-}$ . Therefore, identification of an effective treatment for high- $\text{SO}_4^{2-}$  water sources would 1) prevent the health and performance problems associated with livestock consuming high- $\text{SO}_4^{2-}$  water, and 2) allow producers to use available water resources despite high  $\text{SO}_4^{2-}$  concentrations.

**Statement of Results or Benefits: Information to be Gained.** Ferrous carbonate ( $\text{FeCO}_3$ ) is a soluble iron salt with potential to bind S. We hypothesized that treatment of high- $\text{SO}_4^{2-}$  water with  $\text{FeCO}_3$  will bind excess S and ultimately prevent the poor performance and health (i.e. sPEM) of livestock consuming high- $\text{SO}_4^{2-}$  water. We expected to determine 1) if  $\text{FeCO}_3$  treatment of high- $\text{SO}_4^{2-}$  water sufficiently binds S and reduces it to levels within the recommendations for livestock production, and 2) if  $\text{FeCO}_3$  treatment of high- $\text{SO}_4^{2-}$  water prevents the decreased performance and poor health that livestock typically experience when administered high- $\text{SO}_4^{2-}$  water. Identification of a practical, water-applied treatment for high- $\text{SO}_4^{2-}$  water would offer livestock producers a means by which such sources could be used for livestock production without compromising herd/flock health and performance.

**How Information Was Used.** The information garnered from this research was used to 1) determine if treatment of high- $\text{SO}_4^{2-}$  water with  $\text{FeCO}_3$  lowers S concentrations to within the recommended levels for livestock production, and 2) determine if the  $\text{FeCl}_2$  water treatment prevents the reduced performance and poor health normally observed in livestock consuming high- $\text{SO}_4^{2-}$  water. Unfortunately, our results suggested that Fe does not effectively lower S concentrations, nor did it positively affect animal performance. Further research is needed to identify other potential treatments for high- $\text{SO}_4^{2-}$  water. *Our long-term goal is to develop a practical, water-applied treatment for high- $\text{SO}_4^{2-}$  water sources that will bind S and reduce it to levels acceptable for livestock consumption, enabling such sources to be used in livestock production systems.*

**Nature, Scope, and Objectives of the Project:** The basic nature of the proposed research was to identify a water-applied treatment for high- $\text{SO}_4^{2-}$  water that producers can affordably and practically apply to those high- $\text{SO}_4^{2-}$  water sources used for livestock production. This research is especially important for livestock producers in the western regions of the U.S., including Wyoming, where high- $\text{SO}_4^{2-}$  water sources are prevalent. The objectives of this project were to 1) determine if  $\text{FeCO}_3$  treatment of high- $\text{SO}_4^{2-}$  water reduces S to levels within the accepted recommendations for livestock production, and 2) determine if treatment of high- $\text{SO}_4^{2-}$  water with  $\text{FeCO}_3$  prevents the reduced performance and poor health normally observed in livestock consuming high- $\text{SO}_4^{2-}$  water. Health was assessed by incidence of sPEM and changes in hepatic gene regulation; performance was assessed by measures of feed intake, feed efficiency, and gain. This project was completed over a two year period by one M.S. student (Amanda Jons).

**Methods, Procedures, and Facilities:** Cattle and sheep are both ruminant livestock affected by high-SO<sub>4</sub><sup>2-</sup> water. Sheep are commonly used as a model species, as they are the most economical ruminant farm animal available. This study used ram lambs (n = 80; 6 months of age) maintained at the University of Wyoming's Stock Farm. The Stock Farm houses a GrowSafe Feed Intake and Behavior Monitoring system, the only system to-date specifically designed to collect feed intake and behavior data of individual sheep in group settings.

Rams were allowed a 10 d adjustment period to become accustomed to the GrowSafe system. Prior to treatment, drinking water was analyzed for concentrations of total dissolved solids, S, and S compounds. Ram lambs were randomly assigned to one of four treatments for the 60 d trial period: low-SO<sub>4</sub><sup>2-</sup> water (57 mg SO<sub>4</sub><sup>2-</sup>/L water; n = 20); high-SO<sub>4</sub><sup>2-</sup> water (2,250 mg SO<sub>4</sub><sup>2-</sup>/L water; n = 20); high-SO<sub>4</sub><sup>2-</sup> water + low FeCO<sub>3</sub> (2,250 mg SO<sub>4</sub><sup>2-</sup>/L + 250 mg FeCO<sub>3</sub>/L; n = 20); or high-SO<sub>4</sub><sup>2-</sup> water + high FeCO<sub>3</sub> (2,250 mg SO<sub>4</sub><sup>2-</sup>/L + 500 mg FeCO<sub>3</sub>/L; n = 20). This level of SO<sub>4</sub><sup>2-</sup> administration has been shown to cause performance and health deficiencies in previous studies conducted by the PI and co-PIs. All lambs were administered the same diet throughout the experimental period. Lambs were allowed *ad libitum* access to feed and water. Weights were recorded on d -2 and -1, d 29 and 30, and d 60 and 61, and averaged for more precise estimates of initial, mid, and final BW, respectively. Blood samples were collected in conjunction with BW on d -2, d 29, and d 60 for serum Fe, copper (Cu<sup>2+</sup>), and molybdenum (Mo) analyses. High SO<sub>4</sub><sup>2-</sup> acts as a Cu<sup>2+</sup> antagonist in ruminants, irreversibly binding Cu<sup>2+</sup> and rendering it unavailable for utilization. Additionally, Mo is involved in the binding of Cu<sup>2+</sup> through the formation of thiomolybdates in high-S environments. Because excess H<sub>2</sub>S gas production is causal to sPEM, rumino-centesis was performed on d -2 and d 60 to obtain measures of, and changes in, ruminal H<sub>2</sub>S gas production. Ruminal gas was collected via the rumen gas caps and aspirated through H<sub>2</sub>S detector tubes.

Traits measured for each individual ram using the GrowSafe system included daily feed intake, residual feed intake (a measure of feed efficiency), daily feeding time, and rate of feed intake. In addition, average daily gain was estimated for each lamb. Lambs were closely monitored for clinical signs of sPEM. No lambs exhibited severe signs of sPEM and had to be removed from the trial. All lambs were euthanized at the end of the trial period for liver collection; muscle samples were also collected to determine S accumulation in muscle tissues. Multiple subsamples of each liver were collected for mineral and gene expression analyses.

Results indicated that there were no differences in ADG ( $P = 0.351$ ), daily water intake ( $P = 0.305$ ), or daily feed intake ( $P = 0.116$ ) between treatments. Mineral analyses showed no treatment effects ( $P \geq 0.214$ ) on plasma concentrations of Fe or Zn, or on hepatic concentrations of Se, Fe, Mo, Mn, or Zn ( $P \geq 0.094$ ). Production of H<sub>2</sub>S gas was less ( $P \leq 0.012$ ) in low-S control lambs compared to lambs in the high-S treatment groups; no differences in H<sub>2</sub>S gas production were detected between high-S treatment groups. These production results suggested that Fe was not effective in countering the effects of high dietary S (through the drinking water in this instance) in lambs.

**Gene Expression Analyses.** The liver plays a key role in sulfide (S<sub>2</sub>) detoxification. Previous studies in our laboratory have shown chronic exposure to high-SO<sub>4</sub><sup>2-</sup> water induces changes in hepatic gene regulation (Table 1). Many of these genes are integral to immune function, indicating that liver health is affected by high-S water. Assessment of those genes in the present

study may determine any changes in health due to the FeCO<sub>3</sub> treatment at a molecular level. Assessment at the molecular level is essential to determine if the FeCO<sub>3</sub> treatment causes any changes not readily detectable at the phenotypic level. Real-time RT-PCR was performed to determine if treating high-SO<sub>4</sub><sup>2-</sup> water with FeCO<sub>3</sub> causes molecular changes and alters liver function. Briefly, RNA was extracted from liver subsamples from each animal, reverse transcribed into cDNA, and quantified relative to a standard housekeeping gene. Genes identified as differentially expressed in response to treatment were *SLC26A2* (*P* = 0.004), *GNMT* (*P* = 0.032), *ITGB2* (*P* = 0.030), *PRKACA* (*P* = 0.016), *APEX1* (*P* = 0.024), *EPB41* (*P* < 0.001), *TG2* (*P* = 0.002), *PCNA* (*P* = 0.033), and *PIPOX* (*P* = 0.029). Genes identified as having a tendency to be differentially expressed in response to treatment included *TGFβ1* (*P* = 0.097), *SOD1* (*P* = 0.070), *TUSC3* (*P* = 0.077), and *TJPI* (*P* = 0.059). Genes that were differentially expressed between treatments were consistently upregulated in the high-SO<sub>4</sub><sup>2-</sup> water/high FeCO group compared to the other treatment groups. These differentially expressed genes are involved in immune function, oxidative damage, apoptosis, tumor suppression, and tight junctions, suggesting that high dietary Fe, perhaps in combination with high dietary SO<sub>4</sub><sup>2-</sup>, influences cellular functions in wethers consuming high SO<sub>4</sub><sup>2-</sup> water.

Gene(s)	Function
MHC Class I Heavy Chain	Immune system
MHC Class II, DQ alpha 5, DQ beta, and DRB3, TGF beta 1	Immune system; Stimulus response
Regakine 1 and Integrin, beta 2	Immune system; Stimulus response; Binding
Inhibin, Beta A	Immune system; Binding
Interleukin 8 Receptor, Beta	Response to stimulus
ZFP 385A, Interleukin 1 Rc, HOP Homeobox, Pyrroline-5 CR 1, Cys-rich EGF-like 2	Binding
Tubulin beta 4, Protein Kinase (cAMP-dependent, catalytic, alpha)	Cytoplasmic function; Binding
Transglutaminase 2	Cation binding
Lysosomal-associated Protein Transmembrane 4 Alpha	Cytoplasmic function
Glycine N-Methyltransferase	Hepatic S-adenosylmethionine function
Aldo-keto Reductase Family 1, Member B10	Oxidoreductase activity
Pyruvate Carboxylase, Uncoupling Protein 2	Cell/membrane function

**Significance.** Results suggested that Fe does not effectively lower S concentrations, nor did it positively affect animal performance or health. Further research is needed to identify other potential treatments for high-SO<sub>4</sub><sup>2-</sup> water.

**Student Training.** This project served as the thesis project of a M.S. student (Amanda Jons) in the Department of Animal Science, with PI Cammack as the advisor for the student. The student was trained in the areas of animal production, toxicity, genomics, and water quality, and was responsible for carrying out all aspects of this research project, including both the animal and laboratory components. Together with the PIs, the student prepared manuscripts that will be submitted shortly. The M.S. student prepared two Annual Reports for the Department of Animal Science describing her experiment and presenting results. She presented her work at the American Society of Animal Science national meeting in the summer of 2011 in New Orleans; the abstracted was published in the meeting proceedings. Amanda also presented a poster summarizing her work at the Colorado Ruminant Nutrition Roundtable. Finally, Amanda presented her work at the Department of Animal Science's spring seminar series, and defended her thesis work successfully in the summer of 2011. Amanda continued to work in the PIs

laboratory following her graduation, and is currently seeking a research position. This research was also an opportunity for undergraduate training. A number of undergraduate students assisted with this project, giving them the opportunity to gain hands-on animal care and laboratory experience. Two of the undergraduates helping with project will be starting graduate school themselves in the fall of 2012.

### **Publications.**

- Jons, A.M., K.L. Kessler, K.J. Austin, C. Wright, and K.M. Cammack. 2011. Iron carbonate supplementation of lambs administered high-sulfur water. *J. Anim. Sci.* 89(E-Suppl.):694.
- Jons, A.M., K.J. Austin, K.L. Kessler and K.M. Cammack. 2011. Effects of  $\text{FeCO}_3$  supplementation on hepatic gene expression of wethers administered high-S water. Colorado Nutrition Roundtable. Fort Collins, CO.
- Jons, A.M., K.L. Kessler, K.J. Austin, C. Wright, and K.M. Cammack. 2012. Effects of iron carbonate supplementation on performance of lambs administered high-sulfur water. *Small Ruminant Research*. In preparation.
- Jons, A.M., K.L. Kessler, K.J. Austin, C. Wright, and K.M. Cammack. 2012. Effects of iron carbonate supplementation on hepatic gene expression of lambs administered high-sulfur water. *Small Ruminant Research*. In preparation.

**Related Research.** The current NRC recommendation for dietary S is  $< 0.3\%$  dry matter (DM), with the maximum tolerable concentration estimated at  $0.4\%$  DM [2]. Sulfur content in water, however, is typically reported in parts per million (ppm), and the most common form of S in water is  $\text{SO}_4^{2-}$ . Polioencephalomalacia is associated with water  $\text{SO}_4^{2-}$  concentrations of  $\geq 2,000$  mg/L, which when combined with a typical  $0.2\%$  DM S feedstuff results in  $0.53\%$  DM total dietary S [3]. Therefore, when S or  $\text{SO}_4^{2-}$  content of water is included in the estimation of dietary S, the total dietary S is often much higher than anticipated. *Mechanism:* Sulfate and  $\text{S}_2$  together form a recycling system, as absorbed  $\text{S}_2$  is oxidized into  $\text{SO}_4^{2-}$  in the liver. Levels of  $\text{H}_2\text{S}$  gas increase with greater dietary S. The excess production of  $\text{H}_2\text{S}$  inhibits cytochrome oxidase in the electron transport system, reduces ATP production, and ultimately causes necrosis in the brain [4]. The  $\text{S}_2$  ion is also capable of binding to hemoglobin and forming sulfhemoglobin, reducing the ability of the blood to deliver oxygen to the body [5].

**Sources of High-S Water:** Survey and field data have consistently shown surface and subsurface water can be high in  $\text{SO}_4^{2-}$ , particularly throughout the western regions of the U.S. The Water Quality for Wyoming Livestock & Wildlife review [6] reported that of  $> 450$  forage and water collection sites located throughout the U.S.,  $11.5\%$  exceeded the dietary S concentrations considered safe for livestock. Of those sites,  $37\%$  were located in the western U.S., including Wyoming. Drought further exacerbates the high  $\text{SO}_4^{2-}$  problem, as  $\text{SO}_4^{2-}$  is concentrated in the water due to greater evaporation and reduced moisture recharge [7]. In addition, conventional gas and oil produced water discharge can be high in  $\text{SO}_4^{2-}$ , particularly in arid regions such as the Big Horn Basin (John Wagner, personal communication). Of five water discharge sites sampled in the Big Horn Basin, two exceeded  $2,000$  mg  $\text{SO}_4^{2-}$ /L [8], well above the limit considered safe for livestock consumption. Although many CBM water sources are low in  $\text{SO}_4^{2-}$ , including those in the Powder River Basin, there have been reports of high and variable  $\text{SO}_4^{2-}$  concentrations (hundreds to thousands of mg/L) in CBM waters from the Fort

Union Formation in Campbell County [9]. Because of the limited availability of water resources in those regions, many of those sources high in  $\text{SO}_4^{2-}$  are still used for livestock production.

***High-S Water and Performance:*** Poor performance of animals exposed to drinking water sources with high levels of  $\text{SO}_4^{2-}$  is common. Declines in average daily gain in cattle consuming high-  $\text{SO}_4^{2-}$  water have been reported in both grazing and confined environments [1,10]. Also, decreases in feed consumption and body weight gain in ruminant livestock exposed to high- $\text{SO}_4^{2-}$  drinking water are consistently reported. *High-S Water and PEM:* Polioencephalomalacia is characterized by necrosis of the cerebral cortex and remains one of the most prevalent central nervous system diseases in cattle and sheep [2,11]. Clinical signs of PEM may include head pressing, blindness, incoordination, and recumbency accompanied by seizures [2], with young ruminants the most commonly affected [12]. The limited amount and availability of quality water is problematic for producers, especially when livestock consuming  $\text{SO}_4^{2-}$  contaminated water are also exposed to forages with moderately elevated S levels [3].

### ***References.***

- [1] Patterson, T. 2003. Challenges with water: Implications to animal performance and health. Colorado Nutrition Roundtable.
- [2] Gould, D.H. 1998. Polioencephalomalacia. *J. Anim. Sci.* 76:309-314.
- [3] Gould, D.H., D.A. Dargatz, F.B. Garry, D.W. Hamar and P.F. Ross. 2002. Potentially hazardous sulfur conditions on beef cattle ranches in the United States. *J. Am. Vet. Med. Assoc.* 221:673-677.
- [4] Karamjeet, P. 2000. Polioencephalomalacia in cattle. *Kansas Vet. Quarterly.* 3:2.
- [5] Kung, Jr., L., J.P. Bracht, A.O. Hession, and J.Y. Tavares. 1998. High sulfate induced polioencephalomalacia (PEM) in cattle – burping can be dangerous if you are a ruminant. Pacific Northwest Nutrition Conference, Vancouver, BC, Canada.
- [6] Raisbeck, M.F., S.L. Riker, C.M. Tate, R. Jackson, M.A. Smith, K.J. Reddy, and J.R. Zygmunt. A review of the literature pertaining to health effects of inorganic contaminants. *Water Quality for Wyoming Livestock & Wildlife.* B-1183.
- [7] Wright, C. 2006. Monitor water quality for healthy livestock. South Dakota State Drought.
- [8] Ramirez, Jr., P. 2002. Oil field produced water discharges into wetlands in Wyoming. U.S. Fish & Wildlife Service. Region 6. Contaminants Program. Project #97-6-6F34.
- [9] Rice C.A., M.S. Ellis, and J.H. Bullock, Jr. 2000. Water co-produced with coalbed methane in the Powder River Basin, Wyoming: Preliminary compositional data. USGS Report. 00-372.
- [10] Loneragan, G.H., J.J. Wagner, D.H. Gould, F.B. Garry, and M.A. Thoren. 2001. Effects of water sulfate concentration on performance, water intake, and carcass characteristics of feedlot steers. *J. Anim. Sci.* 79:2941-2948.
- [11] Olkowski, A.A. 1997. Neurotoxicity and secondary metabolic problems associated with low to moderate levels of exposure to excess dietary sulphur in ruminants: a review. *Vet. Human Toxicol.* 39:355-360.
- [12] Ramos, J.J., C. Marca, A. Loste, J.A. García de Jalón, A. Fernández, and T. Cubil. 2003. Biochemical changes in apparently normal sheep from flocks affected by polioencephalomalacia. *Vet. Res. Comm.* 27:111-124.

# Multi-Century Droughts in Wyoming's Headwaters: Evidence from Lake Sediments

## Basic Information

<b>Title:</b>	Multi-Century Droughts in Wyoming's Headwaters: Evidence from Lake Sediments
<b>Project Number:</b>	2010WY60B
<b>Start Date:</b>	3/1/2010
<b>End Date:</b>	2/28/2013
<b>Funding Source:</b>	104B
<b>Congressional District:</b>	1
<b>Research Category:</b>	Climate and Hydrologic Processes
<b>Focus Category:</b>	Drought, Water Supply, Climatological Processes
<b>Descriptors:</b>	drought, lakes, water volumes, long-term climate change
<b>Principal Investigators:</b>	Bryan N Shuman, Thomas A Minckley, Jacqueline J Shinker

## Publications

1. Shinker, J.J., B.N. Shuman, T.A. Minckley, and A.K. Henderson, 2010. Climatic Shifts in the Availability of Contested Waters: A Long-term Perspective from the Headwaters of the North Platte River, *Annals of the Association of American Geographers* (Special Issue on Climate Change), 100 (4), 866-879.
2. Shuman, B., P. Pribyl, T.A. Minckley, and J.J. Shinker, 2010. Rapid hydrologic shifts and prolonged droughts in Rocky Mountain headwaters during the Holocene, *Geophysical Research Letters*, DOI:10.1029/2009GL042196.

## **Multi-Century Droughts in Wyoming's Headwaters: Evidence from Lake Sediments**

March 2011-February 2012, Annual Report, Year 2 of 3

Bryan Shuman, J. J. Shinker, and Thomas Minckley

### **Abstract**

Wyoming has historically experienced extended periods of drought, which have had significant economic and social impacts. Tree-ring records and archeological evidence indicate that past centuries have contained multi-decadal “megadroughts” far more severe than any drought of the past 150 years. This project has been studying past dry periods, which likely exceeded even the severity of multi-decadal “megadroughts” in Wyoming watersheds. In doing so, we are building upon funding from a previous Wyoming Water Research Program grant, and have found evidence of consistent moisture histories across the water-producing regions of the state. Evidence derives from prehistoric shoreline elevations in lakes in the Medicine Bow, Wind River, and Bighorn Mountains, and shows that climatic shifts can rapidly generate new hydrologic regimes that persist for centuries to millennia. Aridity at least as severe and extensive as during the AD 1930s Dust Bowl prevailed from >8000-5500, 4500-3000, and 2800-2000 years before AD 1950). The lake-shoreline elevations as well as watershed moisture budget calculations indicate that at least portions of the North Platte and Bighorn River systems were probably ephemeral for several millennia when dune activity was common across parts of Wyoming, Colorado, and Nebraska. Work in 2011 included 1) additional surveys of lakes in the Bighorn drainage basins, using sub-surface radar, to determine the extensiveness of past periods of low lake levels, 2) sediment core collection and analysis, including radiocarbon dating and fossil analyses, of representative lakes in the Bighorn and Beartooth Ranges to date and quantify past climate conditions, and 3) hydroclimatic analysis, comparing paleoclimate estimates with modern climatic and stream flow data, to examine the factors that contributed to the periods of prolonged drought. Additionally, collaboration with UW archeologists has revealed that the human history of the Bighorn Basin was strongly linked to the changes in regional water supplies over the past 13,000 years. This work involved several graduate students, undergraduates, and high school interns in different activities from field work to data analysis and presentation.

## **Progress**

### Objectives

Water in the western United States, and Wyoming in particular, has long been a source of conflict within the region (e.g., long-running Supreme Court cases regarding the allocation of the North Platte, Green and Bighorn Rivers), and the past century has revealed that the availability of water can change significantly over time. Climate change is likely to exacerbate uncertainties in water supplies, including the potential for hydroclimatic changes to persist beyond reasonable resource planning horizons. Yet, water is critical for energy development, agriculture, urban use, and recreation in Wyoming, and planning requires estimates of the potential range of future availability. Long-term records of drought history, therefore, are needed to provide empirical data regarding past variability, particularly as a means to test predictive models (e.g., correlations with oceanic variability).

Our previous work in the northern Wind River Range and in the southern portions of the Platte River basin indicates centennial to millennial periods since the last ice age when lakes across the region were lower than today – and when rivers such as the North Platte probably had ephemeral flows (Shuman et al., 2010; Shinker et al., 2010). Historic observations, therefore, do not adequately represent the full range of natural climate variability. Tree-ring data are also limited by biological and methodological constraints, which cause long-term trends to be undetected or perhaps underestimated, and this project aims to enhance the long-term record of drought in Wyoming by generating new records of water-level changes in lakes across northern portions of the state particularly in the mountain ranges that ring the Wind-Bighorn and Green River watersheds.

To reach our goal, the project incorporates four activities:

1. **Confirm the extent and magnitude of past droughts**: are drought-history reconstructions from new study sites consistent with our prior results in terms of the estimated magnitude of past aridity? How geographically consistent or patterned were past droughts?
2. **Compare the lake sediment records of drought with dendroclimatic reconstructions**: at the locations of recent dendroclimatic studies in the Bighorn and Green River basins, do lakes capture similar long-term variations?
3. **Examine the predictability of drought**: Was the timing of past drought in Wyoming consistent with the histories of Pacific and Atlantic sea-surface temperatures and with water balance in other hydrologic basins as expected from historic relationships.
4. **Reconstruct in-stream flow** based on lake sediment analyses from areas of high flow contributions: did the Green and Bighorn Rivers have prolonged periods of extremely low flows such as we have reconstructed for the North Platte?

### Methods

Previous studies have demonstrated that small lakes, such as kettle and moraine-dammed lakes in glaciated areas, can produce consistent records of climate-controlled lake-level fluctuations (e.g., Shuman et al., 2010; Shinker et al., 2010). In such lakes, the water table of the surrounding aquifer is exposed at the surface, and the lake level generally reflects the climate-controlled water budget of the aquifer. Therefore, we are analyzing shore-to-basin transects of sediment cores (Fig. 1) and sub-surface profiles (Fig. 2) from multiple lakes to determine past shoreline elevations and measure regional moisture balance.

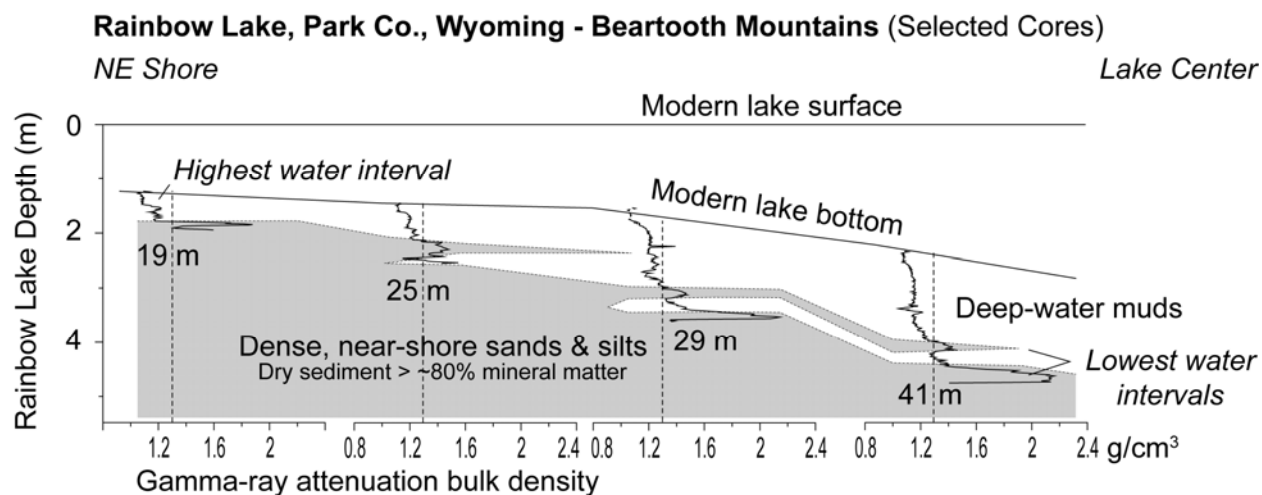


Figure 1. Sediment characteristics (such as sediment density above) in a transect of sediment cores collected perpendicular to shore can be used to track shifts in a lake's shoreline over time. Here, cores collected in July 2011 from Rainbow Lake show layers of sand associated with periods of low water when the shoreline moved toward the lake center.

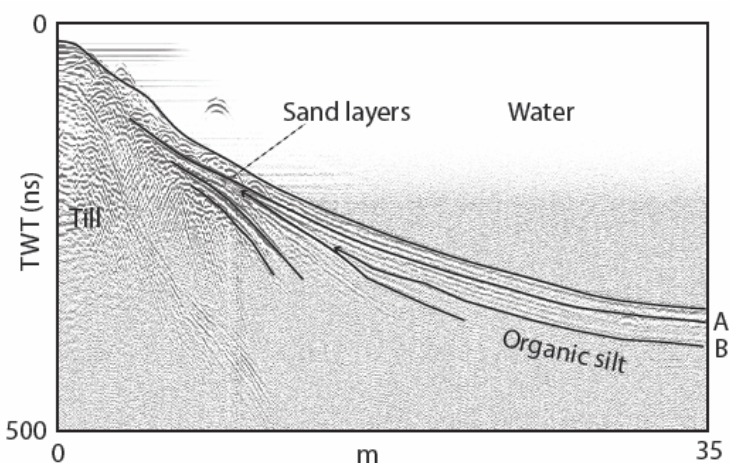


Figure 2. Ground-penetrating radar profiles show submerged paleoshorelines (sand layers marked by the convergence of stratigraphic layers and large amplitude radar reflections) in Lower Paintrock Lake. This profile spans the area of core locations (see Fig. 1), and confirms that the sand layers in the cores are associated with episodes of near-shore erosion (truncation of off-shore layers, such as layer B, at arrows). Data are presented in

nanoseconds of the two-way travel time (TWT) of the radar signal, which is a function of depth.

In 2010 and 2011, we surveyed multiple lakes throughout the Bighorn River drainage with a ground-penetrating radar (GPR), as was previously done at Lake of the Woods in the northern Wind River Range and elsewhere (Shuman et al., 2010; Shinker et al., 2010), and identified changes in the geometry of the sediments that indicate past shifts in shoreline position (Fig. 2). We assume that sandy, macrophyte-rich substrates expanded toward the center of the lake and that sedimentation slowed near shore when lake levels were low (Fig. 1, 2).

Sediment cores were collected at representative lakes in 2010 (Upper Medicine Lodge and Lower Paintrock Lake in the west-central Bighorn Mountains, Fig. 1) and 2011 (Duncan Lake in the north-central Bighorn Mountains and Rainbow and Lily Lakes in the Beartooth Range). The cores have enabled us to date past shoreline deposits (Fig. 3). Shifts in sediment composition and

grain size have been assessed using loss on ignition, magnetic susceptibility, grain-size analysis, and other core logging techniques that can be conducted in the UW Geology and Geophysics Department, using equipment in Shuman's lab. To date the sedimentary changes, one-cm wide slices were removed from sediment cores and sieved to find plant macrofossil material for AMS radiocarbon dating. At Paintrock Lake, we used standard pollen analysis techniques to reconstruct vegetation composition during periods of long-term drought, as we also have done at one site in the Medicine Bow Mountains (Minckley et al., 2012), and using existing data from other lakes in the region, we have used pollen data infer regional temperature trends (Shuman et al., 2012; Kelly et al., in review).

We have focused our coring on lakes with well-defined watersheds, with limited additional groundwater inputs, because such lakes can be used to estimate long-term moisture-balance changes. To calculate long-term  $\Delta P-E$  (e.g., Fig. 3), we have developed a new method for systematically estimating elevational shifts in each lake's shoreline from the maximum depths of the paleoshoreline sediments compared to the water depths of similar sediment today (Pribyl and Shuman, in review). We then calculate changes in lake volume by accounting for lake size and bathymetry, and divide by the watershed area and 365 days to obtain a  $\Delta P-E$  value for the watershed in mm/day as we did previously for only certain snap-shots of the past (Shuman et al., 2010; Shinker et al., 2010). This approach allows for a more systematic comparison of results across the region, and has enabled us to compare with a) data from Colorado to evaluate north-south storm track shifts (Shuman et al., in prep.) and b) archeological data from the Bighorn Basin (Kelly et al., in review).

### 2011 Activities

- Fieldwork: GPR profiles collected from multiple lakes in Bighorn and Beartooth Ranges; and sediment cores were collected from one lake in the Bighorns and two lakes in the Beartooth Range.
- Lab work: In-depth core analyses of Lower Paintrock Lake (Bighorn Co.), including loss-on-ignition, grain-size, sediment density, sedimentary charcoal, macrofossils and radiocarbon analyses, as well as preliminary sediment analyses (e.g., density) of the cores from Duncan, Rainbow, and Lily Lakes.
- Analyses: Compiled core data from Lower Paintrock Lake to build a robust lake-level reconstruction; compared quantified moisture history datasets with results from other regions and with regional archeological data.
- Paper writing: See list of publications and manuscripts below.
- Outreach: Presentation was given to the Wyoming Water Association annual meeting.

### Principal Findings

Findings to date parallel our primary questions:

1. **The extent and magnitude of past droughts**: Our new methodology (Pribyl and Shuman, in review) enabled us to systemically produce time series of water-level changes from our sediment core data, and then calculate watershed hydrologic balance based on these data. In this way, we have produced reconstructions of the balance of precipitation and evaporation

for two different watersheds: one on the northern side of the Medicine Bow Mountains (around Little Windy Hill Pond) and one at the northern end of the Wind River Range (at Lake of the Woods). The two reconstructions agree well in terms of both magnitude and timing of past dry episodes (Fig. 3, blue lines).

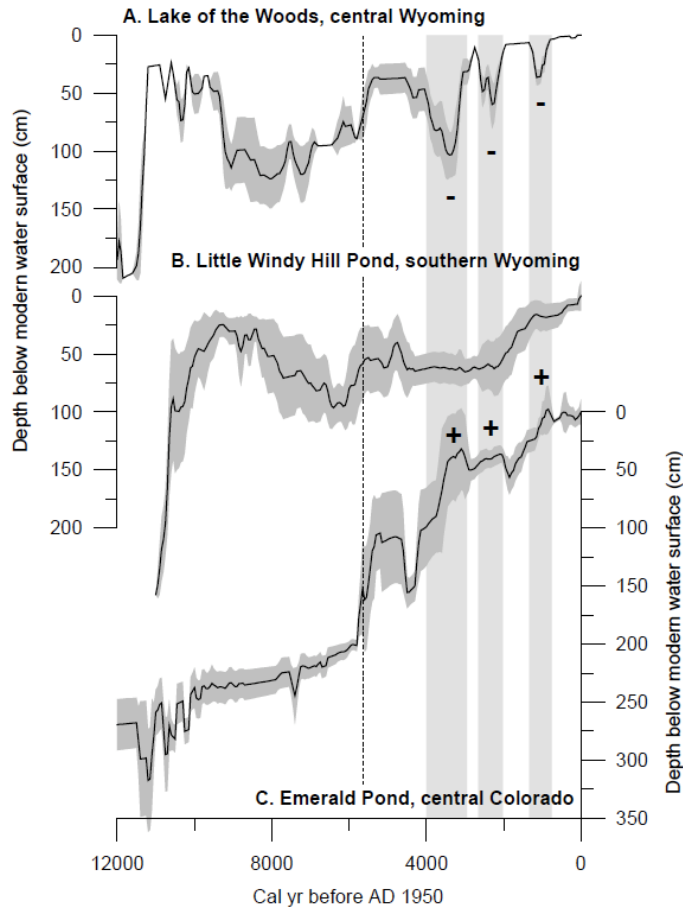


Figure 3. Sediment core density data (left) from 15-m south of shore at Paintrock Lake, Bighorn Co., show intervals of low density deep-water sediment interrupted by dense, sand layers typical of ancient shoreline (low water) deposits. Black dots (plotted versus time on the right) mark the stratigraphic position of radiocarbon ages (1-sigma uncertainty listed) that provide constraints on the timing of low water intervals at the lake. The timing of sand deposition appears to agree well with that of dry periods reconstructed at Little Windy Hill Pond (Medicine Bow Range; blue dashed line plotted as reconstructed precipitation minus evaporation over time) and Lake of the Woods (Wind River Range, thin blue line), as well as with episodes of loess deposition (dune activity) in Nebraska.

Preliminary data from Lower Paintrock Lake in the Bighorn Mountains appear to show episodes of severe aridity at similar times as the other sites (Fig. 3), which indicates that much of the high-elevation snow-dominated areas of the state had similar moisture histories. The results show prolonged periods of  $>50$  mm/yr reductions in annual moisture balance from ca. 8000-5500, 4500-3000, and 2800-2000 years before AD 1950; these episodes overlap in time with other evidence of aridity, such as periods of dune activity recorded by loess deposition in Nebraska's Sand Hills (Fig. 3, symbols in upper right).

The consistency of the timing of events is well represented by the similarities of radiocarbon dates bracketing the paleoshorelines (sand layers) formed in each lake during arid periods. For example, at Lower Paintrock Lake (Bighorn Co.), the uppermost pair of sand layers in core 15A began to form at 4800-4576 years before AD 1950 (Fig. 3); similar sand layers formed at Lake of the Woods (Fremont Co.), Little Windy Hill Pond (Carbon Co.), and Upper Big Creek Lake (Jackson Co., Colorado) above respective radiocarbon ages of 4812-4625, 4806-4529, 4808-4584 years before AD 1950. Likewise, a synchronous interval of

loess deposition in western Nebraska buried a soil formed during the previous wet period, which radiocarbon dates to 4810-4550 years before AD 1950 (Miao et al., 2007).

2. **The predictability of drought:** The timing of past drought in Wyoming appears to be linked to the histories of Pacific and Atlantic sea-surface temperatures, but the related changes in precipitation appear to be superimposed on long-term trends driven by changes in temperature-driven evaporation rates (Fig. 4, 5). Over the past 11,000 years, the temperature and evaporation trends resulted from slow orbital change that produced high temperatures and high evaporation from ca. 9000-6000 years before AD 1950. Based on these relationships, 1 degree C of warming has produced a ~75 mm/yr reduction in available water (equivalent to a 230,000 acre-ft/yr reduction on the Platte River).

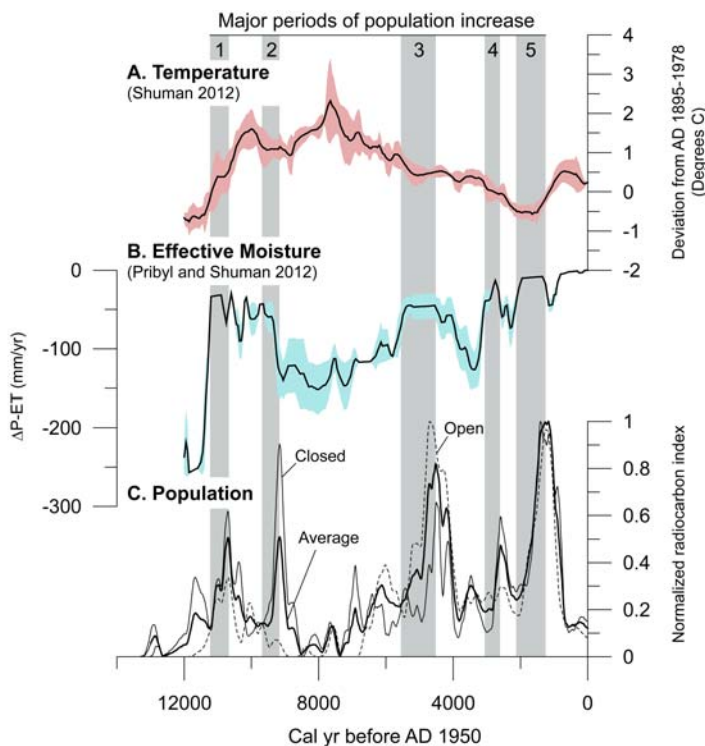


Figure 4. Wyoming temperature (A, red) and moisture reconstructions (B, plotted in blue as change in precipitation minus evaporation,  $\Delta P-E$ , versus time) have variations consistent with documented orbital change. Before ca. 8000 years before AD 1950, the presence of the Laurentide Ice Sheet in central Canada (A, dashed line) likely contributed to wet conditions in Wyoming. Since then, high temperatures have produced periods of low  $\Delta P-E$ , as have additional phases of oceanic variation (e.g., ca. 4000 yrs ago). The human population of the Bighorn Basin (C) appears to have grown and shrunk in response to changes in water supply. The population grew during wet/cool

phases (gray bars) with occupations at both open (dashed line) and cave (closed; thin line) sites, but collapsed with the onset of dry phases.

Additional work by Shinker and students has examined the atmospheric dynamics and circulation associated with dry episodes in Wyoming to help explore the mechanistic linkages that may have been the underpinning to the events of the past 10000 years.

3. **Significant reductions in in-stream flow:** Based on lake sediment analyses from Lower Paintrock Lake, which today overflows into Paintrock Creek and ultimately the Bighorn River, past arid periods may have substantially reduced regional river flow. Sand layers, which mark the periods of low water, date to the same intervals as changes in the North Platte River watershed when the river was likely ephemeral (Shinker et al., 2010). The layers also lie at elevations (Fig. 2) below the modern outlet of Lower Paintrock Lake (<50 cm

below the modern lake surface), and indicate periods of reduced overflow when archeological data indicate significant reductions in the regional human population.

### Significance

Our results are confirming that climatic processes, including variability in temperature and the state of the global oceans, can drive large and persistent changes in the availability of water in Wyoming. Severe dry episodes have lasted for centuries to millennia across much of the state's water producing regions, including 1) the North Platte River headwaters in the Snowy Range of southeastern Wyoming and the Park Range of northern Colorado, 2) the convergence of the Snake (Columbia), Green (Colorado), and Bighorn (Missouri-Mississippi) River watersheds on the Continental Divide in the Wind River Range, and 3) the eastern Bighorn River watershed in the Bighorn Mountains. Evidence that lakes that today overflow into these major river systems have not overflowed in the past indicates that climate changes can dramatically reduce flow rates in rivers that are already fully allocated to various uses. The lack of human occupations in the Bighorn Basin during the warmest and driest intervals of the past appears to confirm the significance of these reductions in water supply (Fig. 4).

### **Publications and Presentations (\* Student Author):**

#### Published in 2010

Shinker, J. J., Shuman, B. N., Minckley, T. A., and Henderson, A. K.\*, 2010. "Climatic Shifts in the Availability of Contested Waters: A Long-term Perspective from the Headwaters of the North Platte River," *Annals of the Association of American Geographers (Special Issue on Climate Change)*, 100 (4), 866-879.

Shuman, B., Pribyl, P.\*, Minckley, T. A., and Shinker, J. J., 2010. "Rapid hydrologic shifts and prolonged droughts in Rocky Mountain headwaters during the Holocene," *Geophysical Research Letters*, DOI:10.1029/2009GL042196.

#### Published in 2012

Minckley, T.A., R.K. Shriver\*, and B. Shuman. Resilience and regime change in a southern Rocky Mountain ecosystem during the past 17000 years. *Ecological Monographs*.

- *Includes detailed reconstruction of moisture availability in the Medicine Bow Mtns*

Minckley, T.A., and R.K. Shriver. Vegetation response to different fire-types in a Rocky Mountain forest. *Journal of Fire Ecology*.

#### Submitted publications

Pribyl, P.\*, and B. Shuman. Changes in moisture availability during the Holocene at the Colorado-Columbia-Missouri River headwaters, central Wyoming. In revision following reviews from *Earth and Planetary Science Letters*. Peer Reviewed.

Shuman, B., A. K. Henderson\*, and C. Plank\*. Moisture Patterns in the United States and Canada over the Past 15,000 Years: A New Synthesis of Lake Shoreline-Elevation Data. In revision following reviews from *Quaternary Science Reviews*. Peer Reviewed.

Kelly, R., T. Surovell, and B. Shuman. Strong climatic influence on human populations in the central Rocky Mountains over the past 13,000 years. In revision following reviews from *Proceedings of the National Academy of Sciences*. Peer Reviewed.

### Publications in preparation

Pribyl, P.\*, and B. Shuman. Severe regional river-flow reductions during the Younger Dryas and mid-Holocene, northern Colorado. Plan to submit to *Geology*. Peer Reviewed.

Shuman, B., J. Marsicek\*, P. C. Newby\*, G. Carter\*, D. D. Hougardy\*, P. Pribyl\*, S. Brewer, J. P. Donnelly, D. Foster, and W. Wyatt Oswald (B). From Causes to Impacts of Holocene Moisture Variation in Mid-Latitude North America. Plan to submit to *Nature Geosciences*. Peer Reviewed.

### Presentations (\*undergraduate; \*\*graduate student)

#### 2010

Shuman, B. N., J.J. Shinker and T. A. Minckley. 2010. "Millennial-scale hydroclimatic variation and prolonged episodes of ephemeral river flow in the Rocky Mountains during the Later-Quaternary," Geological Society of America, Denver, CO.

Shinker, J. J., B. N. Shuman, T. A. Minckley, and A. K. Henderson\*\*. 2010. "Climatic shifts in the availability of contested waters: A long-term perspective from the headwaters of the North Platte River," Poster presenter, American Quaternary Association, Laramie, WY.

Shinker, J. J., B. N. Shuman, T. A. Minckley, and A. K. Henderson\*\*. 2010. "Climatic shifts in the availability of contested waters: A long-term perspective from the headwaters of the North Platte River," Association of American Geographers, Washington, DC.

Shinker, JJ. 2010, Women in Science Conference, Career Panelist, University of Wyoming.

#### 2011

Shinker, J. J., 2011, Spatial Heterogeneity of Western U.S. Climate Variability. Association of American Geographers, Seattle, Washington.

Heyer, J.\* and Shinker, J.J., 2011. "An Investigation of Climatic Controls in the Upper Laramie River Watershed During Low Stream Flow Years", at UW Undergraduate Research Day, April, 2011.

Serravezza, M.\*\*, 2011. "Ground-penetrating radar as a tools for reconstructing past droughts in

Wyoming,” UW Roy J. Shlemon Center for Quaternary Studies, Quaternary Research Symposium, Fall 2011.

## 2012

Heyer, J.\*, Fredrickson, J.\*\* and Shinker, J.J., 2012. *Climate, drought and low stream flow in the headwaters of the North Platte River*. Annual meeting of the Association of American Geographers, New York City.

Fredrickson, J.\*\* and Shinker, J.J., 2012. Hydroclimatic variability and drought in Wyoming headwater regions. Annual meeting of the Association of American Geographers, New York City.

### **Student Involvement**

Marc Serravezza, a Ph.D. student in Geology & Geophysics, was supported by this grant and took the lead on analyses of the sediment cores from Lower Paintrock Lake, Bighorn Co., as well as the field work to collect new cores from Rainbow, Duncan, and Lily Lakes. Marc was supported in this work by recent UW undergraduates, Devin Hougardy and Paul Haselhorst, and other Geology Ph.D. students, John Calder, Grace Carter and Jeremiah Marsicek. All five contributed to field work in the Bighorn and Beartooth Mountains in summer 2011.

Joshua Fredrickson, a Geography/Water Resource master’s student was supported through the Geography Department to analyze climate data associated with recent low stream flow events in the Bighorn and Colorado River drainages. Geography undergraduate Joshua Heyer also contributed to this work.

# Impact of Bark Beetle Outbreaks on Forest Water Yield in Southern Wyoming

## Basic Information

<b>Title:</b>	Impact of Bark Beetle Outbreaks on Forest Water Yield in Southern Wyoming
<b>Project Number:</b>	2010WY61B
<b>Start Date:</b>	3/1/2010
<b>End Date:</b>	2/28/2013
<b>Funding Source:</b>	104B
<b>Congressional District:</b>	1
<b>Research Category:</b>	Climate and Hydrologic Processes
<b>Focus Category:</b>	Hydrology, Surface Water, Water Quantity
<b>Descriptors:</b>	bark beetles, water budget, water yield
<b>Principal Investigators:</b>	Brent E. Ewers, Holly Barnard, Elise Pendall, David Williams

## Publications

There are no publications.

# Impact of bark beetle outbreaks on forest water yield in southern Wyoming

## Annual Report, Year 2 of 3

PIs: Brent E Ewers, Elise Pendall and David G Williams

### Abstract

A Rocky Mountain Region outbreak of bark beetles and their associated fungi from British Columbia to New Mexico is having profound impacts on forest function and ecosystem services. These forests are key components of major river watersheds which could magnify any impacts on downstream users of water including those in Wyoming. Current and ongoing research is documenting the potential extent, causes and impacts on carbon exchange and evapotranspiration but less is known about how water yields will be impacted on short to long time scales. This project will enhance preliminary measurements of evapotranspiration and soil moisture from a mid-elevation lodgepole pine forest undergoing infestation by 1) reasonably closing stand water budgets to better quantify and thus predict water yield and 2) extending replicate measurements and analyses to post-infection management to facilitate future scaling to landscape water yield. New stands will be established in mid elevation former lodgepole pine that has been clearcut after infestation. We will provide complete water budgets that are closed on a stand basis by measuring 1) spatially explicit snow accumulation and loss, 2) detailed liquid canopy interception and stem flow, 3) appropriately scaled transpiration from living, dying and dead trees' water use (or lack thereof) through sap flow and leaf gas exchange, 4) soil hydraulic characteristics and modeling and runoff for water yield and 5) stable isotopes of soil, plant and atmospheric water as a further test of water budget component closure. Our proposed data collection and analysis will provide highly probable predictions of water yield during the first 5 to 10 years of the outbreak and provide the basis for first order predictions of the next 10 to 100 years of impact. The results of this project will be communicated with State and Federal agency personnel, providing data necessary for future water management decisions in all areas of Wyoming impacted by the bark beetle outbreak.

### Objectives

- 1) Quantify how precipitation is partitioned into evapotranspiration, throughfall, stemflow, soil storage and water yield across forest types (including a clearcut) as trees die and the forests begin initial recovery from bark beetle-induced mortality
- 2) Determine errors and associated uncertainty in closing a water budget across forest types

### Methodology

All components of forest stand water budgets are being measured at the lodgepole pine bark beetle sites with a select group of major components at the higher elevation spruce and fir bark beetle site. Some of the following measurements are being partially or fully funded by ongoing National Science Foundation project and a completed UW Agriculture Experiment Station grant. **Precipitation** is being measured with multiple approaches to obtain incoming liquid and frozen precipitation as well as throughfall and

snowpack depth and density prior to infiltrating or running over soil. **Drainage** is being estimated by combining soil physical properties with soil water storage measurements. Piezometers are measuring **streamflow** out of the forests at multiple spatial locations. **Evapotranspiration** being measured using eddy covariance methods at the lodgepole pine, clear cut lodgepole pine and spruce and fir forests. **Tree transpiration** is being measured in nearly 50 trees representing a range of bark beetle infestation and responses of trees to forest management such as thinning or clear cutting. Stable isotope measurements of water vapor fluxes are being used to partition evapotranspiration into transpiration and **evaporation**. Measurements of leaf gas exchange and plant hydraulic conductance have been made to test mechanisms of tree mortality in response to the bark beetle epidemic. A spatial grid of 144 plot level measurements of tree and understory characteristics was sampled to scale up plot level flux measurements to watersheds.

### **Progress**

We now have data from all the major measurements outlined in the methods. Stable isotope data has been received from UW SIF lab and has been compared to water fluxes. Tree physiology mechanisms from leaf gas exchange and hydraulic conductance have been tested. A conceptual overview of the impact of bark beetle mortality on carbon, water and nutrient cycles from these forests is in press. Manuscripts from graduate students have been submitted on error analysis of eddy covariance measurements, energy budget closure of bark beetle impacted stands and the change in evapotranspiration and carbon exchange of a high elevation spruce forest before and after the bark beetle outbreak. Manuscripts are now in preparation on carbon and water exchange from lodgepole pine forest

### **Principal Findings**

Our significant results to date are 1) transpiration and evapotranspiration decline measurably in the first year and precipitously in the second year of an outbreak, 2) water fluxes from the stands decline faster than carbon uptake, 3) soil moisture increases with the decline in transpiration and evapotranspiration strongly suggesting increased streamflow, 4) soil N increases after the outbreak due to reduced vegetation activity, 5) energy balance closure is low (~50%) unless spatial heterogeneity and energy storage changes from mortality are included then closure is higher (~80%), 6) common sonic anemometers likely underestimate sensible and latent heat fluxes, 7) increased soil moisture does not appear to increase streamflow likely due to a) earlier snow melt with declining canopy structure, b) increased evaporation indicated by stable isotopes of water, c) potential storage effects at the watershed scale.

### **Significance**

This work is providing measurements and analysis of stand-level water balance that are critical to developing forecasting tools for determining the impact of bark beetles on streamflows from primary streams to major river systems. We are testing mechanisms of bark beetle impacts on water yield by conducting investigations at the stand and ecosystem level. Our work shows that predictive tools should be based on mechanistic understanding of first-order beetle impacts which can then be scaled appropriately and

tested by comparison against streamflow data as part of future research efforts beyond the scope of this project.

Our proposed research will apply the stand water and energy balance approach to sites that cover the major land and management cover types in the Medicine Bow Mountains, maximizing applicability to both forest and water managers (see multiple presentations to forums with managers below), while improving basic knowledge of disturbance effects on water cycling and providing quantitative, hands-on training to graduate and undergraduate students. Finally, our research data is now being sought by many investigators from multiple science fields further illustrating the high impact nature of the work.

### **Students Supported**

Julia Angstmann, PhD student, helped establish research sites, graduated before project began

Tim Aston-PhD student, helped set up sap flux measurements, no direct support from project beyond logistics

Bujidma Borkhoo-PhD student, main responsibilities are soil measurements and assistance with atmospheric measurements.

John Frank-PhD student, main responsibilities are all of the flux measurements from the spruce and fir bark beetle site (note: John Frank is a full time employee of the USFS RM Exp St in Ft. Collins, and does not receive any salary support from this project). Support from this project is used for field visits and site maintenance through a USFS subcontract.

David Reed-PhD Student, main responsibilities are the atmospheric and streamflow measurements

Faith Whitehouse-MS Student, main responsibilities are the tree physiology measurements

Claire Hudson-Undergraduate Student, main responsibilities were assisting with soil trace gas measurements and lab processing and vegetation measurements. Now a graduate student at UW working on an MS in Alaskan Forests.

Margo Hamann-Undergraduate Student, main responsibilities are assisting with tree physiology field measurements and lab processing

### **Publications (*Students and Post-Docs are italicized*)**

**Reed D**, BE Ewers, E Pendall, R Kelley. In Review. Bark Beetle Mortality Increases Energy Imbalance in Eddy Covariance Measurements Due to Canopy Heterogeneity. *Agriculture and Forest Meteorology*.

**Frank, J**, W Massman, BE Ewers. In Review. Underestimates of sensible heat flux due to vertical velocity measurement errors in non-orthogonal sonic anemometers. Agriculture and Forest Meteorology.

Edburg, SL, JA Hicke, PD Brooks, EG Pendall, BE Ewers, U Norton, D Gochis, and E Gutmann. 2012. Cascading Impacts of Bark Beetle-Caused Tree Mortality to Coupled Biogeophysical and Biogeochemical Processes, Frontiers Ecology and Environment. In press.

**Presentations (*Students and Post-Docs are bolded*)**

(Invited) Ewers BE. Temporal and Spatial Scaling of Evapotranspiration Using Plant Hydraulic Theory. Penn State. Critical Zone Observatory Distinguished Speaker Series. Mar. 23, 2012

Ewers BE. Impact of Bark Beetle Outbreaks on Precipitation Processing by Forests. Wyoming Weather Modification Technical Advisory Team, Meeting, Cheyenne, WY Jan. 18, 2012.

**Frank, J**, B Massman, B Ewers. Errors in measured sensible heat flux due to vertical velocity measurements in non-orthogonal sonic anemometers. Front Range Student Ecology Symposium, CSU, Ft. Collins, CO Feb. 22, 2012.

**Frank, J**, B Massman, BE Ewers. Net ecosystem exchange of carbon dioxide and evapotranspiration response of a high elevation Rocky Mountain (Wyoming, USA) forest to a bark beetle epidemic. UW Program in Ecology Symposium, Feb. 17, 2012.

**DE Reed**, BE Ewers, E Pendall, RD Kelly. Mountain Pine Beetle epidemic effects on the carbon, water, and energy fluxes of lodgepole pine ecosystems. UW Program in Ecology Symposium, Feb. 17, 2012.

Mackay, DS, BE Ewers, DE Roberts, NG McDowell, E Pendall, **JM Frank**, **DE Reed**, WJ Massman, B Mitra. A coupled carbon and plant hydraulic model to predict ecosystem carbon and water flux responses to disturbance and environmental change. American Geophysical Union Meeting, San Francisco, CA, Dec. 2011.

Brooks, PD, HR Barnards, JA Biederman, **B Borkhuu**, SL Edburg, BE Ewers, DJ Gochis, ED Gutmann, AA Harpold, JA Hicke, E Pendall, **DE Reed**, AJ Somor, PA Troch. Water, Carbon, and Nutrient Cycling Following Insect-Induced Tree Mortality: How well do plot-scale observations predict ecosystem-scale response. American Geophysical Union Meeting, San Francisco, CA, Dec. 2011.

(Invited) Ewers, BE, E Pendall, D Reed, H Barnard, F Whitehouse, J Frank, W Massman, P Brooks, J Biederman, K Nathan, B Mitra, DS Mackay. Use of plant hydraulic theory to predict ecosystem fluxes across mountainous gradients in environmental controls and insect disturbance. American Geophysical Union Meeting, San Francisco, CA, Dec. 2011.

**Frank, JM**, WJ Massman, BE Ewers. Net ecosystem exchange of carbon dioxide and evapotranspiration response of a high elevation Rocky Mountain (Wyoming, USA) forest to a bark beetle epidemic. American Geophysical Union Meeting, San Francisco, CA, Dec. 2011.

Norton, U, E Pendall, BE Ewers, **B Borkhuu**. Trace gas emissions from a chronosequence of bark beetle-infested lodgepole pine (*Pinus contorta*) forest stands. American Geophysical Union Meeting, San Francisco, CA, Dec. 2011.

**DE Reed**, BE Ewers, E Pendall, RD Kelly. Mountain Pine Beetle epidemic effects on the carbon, water, and energy fluxes of lodgepole pine ecosystems. American Geophysical Union Meeting, San Francisco, CA, Dec. 2011.

Gochis, DJ, ED Gutmann, PD Brooks, DE Reed, BE Ewers, E Pendall, JA Biedermann, AA Harpold, HR Barnard, J Hu. Diagnosing the influence of model structure on the simulation of water, energy and carbon fluxes on bark beetle infested forests. American Geophysical Union Meeting, San Francisco, CA, Dec. 2011.

(Invited) Ewers, BE. Plant Hydraulic Theory and Mountains. Mountain Research Institute, Berkeley, CA, Dec. 2011.

(Invited) Ewers, BE, E Pendall, H Barnard, D Williams, U Norton, **D Reed**, P Brooks, D Gochis, A Harpold, **J Frank**, W Massman, F Whitehouse, **B Borkhuu**, **J Angstmann**. Impact of Bark Beetle Outbreaks on Forest Ecosystem Processes. Wyoming Environment and Natural Resources Speaker Series, Jackson, WY, Dec. 2011.

(Invited) Ewers, BE, E Pendall, H Barnard, D Williams, U Norton, **D Reed**, P Brooks, D Gochis, A Harpold, **J Frank**, W Massman, **F Whitehouse**, **B Borkhuu**, **J Angstmann** . Impact of Bark Beetle Outbreaks on Forest Water Yield. Wyoming Water Development Commission. Cheyenne, WY, Nov. 2011.

(Invited) Ewers, BE, E Pendall, H Barnard, D Williams, U Norton, **D Reed**, P Brooks, D Gochis, A Harpold, **J Frank**, W Massman, **F Whitehouse**, **B Borkhuu**, **J Angstmann** . Impact of Bark Beetle Outbreaks on Forest Water Yield. Joint Agriculture Committee of the Wyoming Legislature. Afton, WY, Oct. 2011.

Ewers, BE, E Pendall, U Norton, **D Reed**, **J Frank**, **B Borkhuu**, **F Whitehouse**, **N Brown**, H Barnard, P Brooks, **T Aston**, **J Angstmann**, W Massman, D Williams, A Harpold, J Biederman, S Edburg, A Meddens, D Gochis, J Hicke. Cascading effects of bark beetles and blue stain fungi on coupled water, C and N cycles. UW Dept. Botany. Sept. 2011.

(Invited) Ewers, BE, E Pendall, H Barnard, D Williams, U Norton, **D King**, **D Reed**, P Brooks, D Gochis, A Harpold, **J Frank**, W Massman, **F Whitehouse**, **B Borkhuu**, **J Angstmann**. The challenge of predicting the interacting effects of weather modification

and bark beetles on forest water yield. Wyoming Weather Modification Technical Advertiser Team Meeting. Lander, WY, July 2011.

**Borkhuu, B**, E Pendall, U Norton, BE Ewers. Effects of mountain pine bark beetle infestation on soil CO<sub>2</sub> efflux in lodgepole forests in Southeastern Wyoming. Soil Science Society Western Meeting, Laramie, WY. June 2011.

(Invited) Ewers, BE. Testimony on bark beetle impacts on forest hydrology. Joint meeting of the Select Water Committee of the Wyoming Legislature and the Wyoming Water Development Commission. Cheyenne, WY, June 2011.

Ewers, BE, E Pendall, H Barnard, **F Whitehouse**, **D Reed**, **J Frank**, P Fornwalt, T Aston, J Angstmann, U Norton, A Harpold, P Brooks. Sap flux measurements quantify the timing of transpiration loss due to fungal xylem occlusion following bark beetle attack and subsequent ecosystem consequences. VIII International Sap Flow Meeting, Volterra, IT, May, 2011.

(Invited) Ewers, BE, E Pendall, H Barnard, D Williams, U Norton, **D Reed**, P Brooks, D Gochis, A Harpold, **J Frank**, W Massman, F Whitehouse, **B Borkhuu**, J Angstmann. Impact of Bark Beetle Outbreaks on Forest Water Yield. Wyoming Water and Environmental Law Conference, Cheyenne, WY, Apr. 2011.

**Frank, J**, WJ Massman, BE Ewers. Evapotranspiration response of a high elevation Rocky Mountain (Wyoming, USA) forest to a bark beetle epidemic. Bark Beetle-Water Symposium, Boulder, CO 2011.

Harpold, AA, PD Brooks, JA Biederman, A Somor, P Troch, D Gochis, E Gutmann, H Barnard, **D Reed**, E Pendall, BE Ewers. Quantifying the effects of tree dieoff from mountain pine beetles on hydrologic partitioning at the catchment-scale. Bark Beetle-Water Symposium, Boulder, CO 2011.

Gochis, D, E Gutmann, AA Harpold, PD Brooks, JA Biederman, H Barnard, **D Reed**, E Pendall, BE Ewers. Multi-model assessment and verification of bark beetle impacts on land surface-atmosphere energy and water exchanges. Bark Beetle-Water Symposium, Boulder, CO 2011.

**Frank J**, W Massman, BE Ewers. Response of high elevation rock mountain forest evapotranspiration to a bark beetle epidemic. CSU Hydrology Days, Ft. Collins CO. Feb. 2011.

**Reed D**, Kelly R, Ewers B, Pendall E. Energy Closure of a Heterogeneous Forest Canopy. Ameriflux Annual Meeting, Feb. 2011

**Frank J**, W Massman, BE Ewers. Response of high elevation rocky mountain (Wyoming, USA) forest carbon dioxide and water vapor fluxes to a bark beetle epidemic. Ameriflux Annual Meeting, Feb. 2011.

BE Ewers, E Pendall, U Norton, **D Reed, J Franks, T Aston, F Whitehouse**, HR Barnard, PD Brooks, J Angstmann, WJ Massman, DG Williams, AA Harpold, J Biederman, SL Edburg, AJ Meddens, DJ Gochis, JA Hicke. The Rocky Mountain epidemic of bark beetles and blue stain fungi cause cascading effects of coupled water, C and N cycles. AGU, San Francisco, CA, Dec, 2010.

**DE Reed**, RD Kelly, BE Ewers, E Pendall. The mountain pine beetle epidemic contributes to increased spatial and temporal variability and decoupling of carbon and water fluxes from lodgepole pine. AGU, San Francisco, CA, Dec, 2010.

DJ Gochis, PD Brooks, AA Harpold, BE Ewers, E Pendall, HR Barnard, **D Reed**, PC Harley, J Hu, J Biederman. Measuring and modeling changes in land-atmosphere exchanges and hydrologic response in forests undergoing insect-driven mortality. AGU, San Francisco, CA, Dec, 2010.

PD Brooks, AA Harpold, AJ Somor, PA Troch, DJ Gochis, BE Ewers, E Pendall, JA Biederman, **D Reed, HR Barnard, F Whitehouse, T Aston, B Borkhuu**. Quantifying the effects of mountain pine beetle infestation on water and biogeochemical cycles at multiple spatial and temporal scales. AGU, San Francisco, CA, Dec, 2010.

BE Ewers (invited) E Pendall, **D Reed, F Whitehouse, J Frank, T Aston, J Angstmann**, D Williams, H Barnard, WJ Massman, U Norton. Impacts of a bark beetle epidemic on forest hydrology. Wyoming Water Forum, Cheyenne, WY, Nov. 2010.

BE Ewers E Pendall, U Norton, **B Borkhu, T Aston, D Reed, J Frank, J Anstmann**, WJ Massman, PD Brooks, DJ Gochis, HR Barnard, D Williams. First and higher order impacts of bark beetles on ecosystem processes of Rocky Mountain Forests. Ecological Society of America Meeting, Pittsburgh, PA, Aug. 2010.

## Fate of Coalbed Methane Produced Water in Disposal Ponds in the Powder River Basin

### Basic Information

<b>Title:</b>	Fate of Coalbed Methane Produced Water in Disposal Ponds in the Powder River Basin
<b>Project Number:</b>	2011WY74B
<b>Start Date:</b>	1/1/2010
<b>End Date:</b>	2/28/2013
<b>Funding Source:</b>	104B
<b>Congressional District:</b>	1
<b>Research Category:</b>	Water Quality
<b>Focus Category:</b>	Geochemical Processes, Groundwater, Solute Transport
<b>Descriptors:</b>	Infiltration, Pond sediments, Sodicity, Salinity
<b>Principal Investigators:</b>	Thijs Kelleners, Katta J Reddy

### Publications

There are no publications.

# **FATE OF COALBED METHANE PRODUCED WATER IN DISPOSAL PONDS IN THE POWDER RIVER BASIN**

FY 11 Annual Report, Year 1 of 2

T.J. Kelleners, Assistant Professor Soil Physics  
K.J. Reddy, Professor of Environmental Quality  
R. Drapeau, MS Graduate Student, Soil Science

Department of Ecosystem Science and Management, University of Wyoming

Reporting period: 03/01/2011 – 02/29/2012

## **1. Abstract**

The Powder River basin (PRB) in Wyoming has seen a rapid increase in coalbed methane (CBM) production over the past decade. Product water from the ~20,000 active CBM wells is mostly released in surface ponds. The product water may be high in total dissolved solids, be sodium dominated, and may contain trace elements that are toxic to humans, livestock, and wildlife. The fate of the pond water is generally unknown. Infiltration of pond water could lead to the contamination of shallow groundwater and surface water. Concentration of pond water due to evaporation could lead to unacceptable high trace element concentrations. Previous studies suggest that pond water infiltration reduces with time because of soil dispersion related to the high sodium content of the CBM water. We propose to examine the relationship between soil type, CBM water quality, and infiltration rate for a variety of unlined ponds across the PRB. We are particularly interested in determining the time frame over which the infiltration rate reduces as compared to the total lifetime of the ponds. This type of information is currently lacking for the PRB and would greatly benefit pond operators, landowners, and agencies in assessing the environmental impact of the ponds (i.e. groundwater contamination versus concentration of pond water constituents). Infiltration experiments conducted in the laboratory will be supplemented with numerical modeling of subsurface water flow and solute transport to assess the practical implications of the measured infiltration rates.

## **2. Progress**

### **2.1 Objectives**

The study examines the relationship between soil type, CBM produced water quality, and infiltration rate for unlined disposal ponds in the PRB. The specific objectives are:

- (1) Identify combinations of soil type and CBM water quality that are representative for conditions in the PRB;
- (2) Measure saturated soil hydraulic conductivity as a function of time during CBM water infiltration in the laboratory;
- (3) Model water flow and solute transport for typical PRB CBM ponds over an assumed 10-year lifetime.

## 2.2 Methodology

Objective (1): The proposed study uses a network of water quality measurement sites across the PRB that were established by the research group of KJ Reddy. The network covers 26 sites located in five PRB watersheds (Tongue River, Powder River, Little Powder River, Belle Fourche River, and Cheyenne River). The geochemistry of wellhead water and pond water has been determined annually at these sites from 2003 to 2007. Detailed soil information for the PRB and the 26 sites is available from the Natural Resource Conservation Service. The geochemistry and soils data are used to identify up to ten representative combinations of soil type and CBM water quality for the PRB.

Objective (2): Soil samples are collected from selected sites and taken to the laboratory for the infiltration experiments. The sampled soil is used to represent pre-CBM discharge soil conditions for the pond area. The infiltration experiments are conducted using CBM well water which is collected at the time of soil sampling. The infiltration experiments are conducted in the laboratory by packing the soil in PVC columns with metal screens at the bottom. At the start of the experiment, the columns are wetted from the bottom up with tap water to drive all the air out. Subsequently, well water is applied to the top of the columns at a constant head using a mariotte bottle and outflow quantity and quality is monitored at the bottom of the columns. The saturated soil hydraulic conductivity is calculated as a function of time using the Darcy equation. Soil water quality inside the columns is analyzed upon completion of the infiltration experiment. The CBM water infiltration results are compared to “baseline” tap water infiltration results for the same soils to assess the impact of the saline-sodic well water.

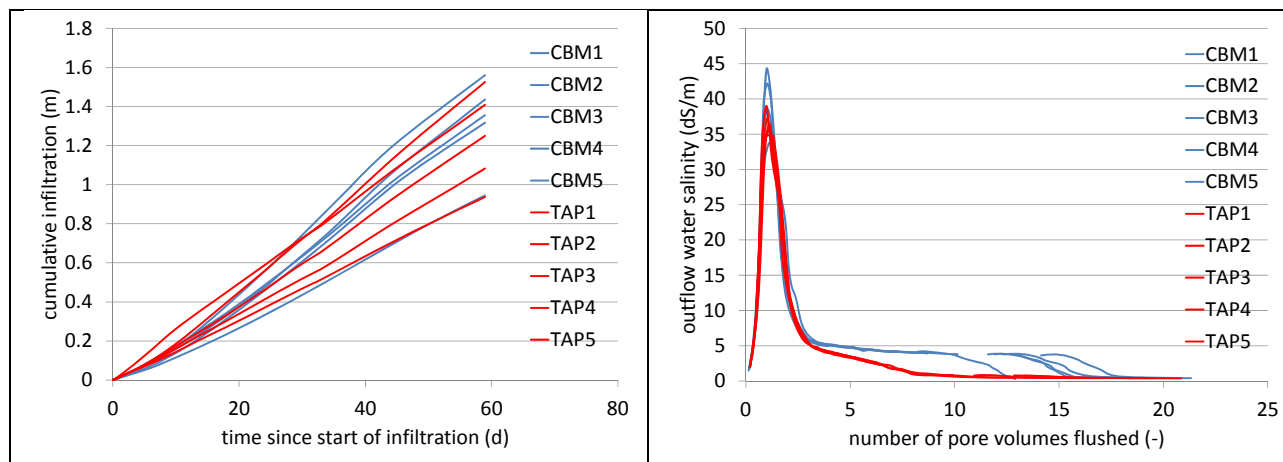
Objective (3): The practical implications of temporal variations in the saturated hydraulic conductivity of the pond sediments are studied using the Hydrus-2D model for water flow and solute transport in variably-saturated porous media. The model is applied in axisymmetric mode to describe a vertical cross section of the pond sediments. A sensitivity analysis is conducted for a number of idealized pond settings to quantify the effect of reduced hydraulic conductivity on water flow and solute transport over the assumed 10-yr lifetime of the ponds.

## 2.3 Principal Findings

The landowners / pond operators that had previously allowed data collection as part of KJ Reddy’s water quality studies were contacted during summer 2011. It was found that many of the original wells had stopped pumping (the amount of water pumping decreases as the well ages). Two field trips were conducted to the Gillette / Sheridan area to collect soil and water samples from two wells that had continued to operate. Other landowners / pond operators that manage newly installed wells / disposal ponds were contacted to supplement the Gillette / Sheridan wells. Carrie Steinhorst of the Wyoming Department of Environmental Quality was contacted to aid with the identification of new sites.

A first set of infiltration experiments was completed for the Gillette site (CBM water  $EC = 3.3 \text{ dS m}^{-1}$ ; CBM water  $SAR = 6.3 \text{ mmol}_c^{0.5} \text{ l}^{-0.5}$ ). Columns were infiltrated with CBM water (5 replicates) and tap water (5 replicates). Cumulative infiltration versus time, and outflow salinity versus number of pore volumes flushed are shown in the figure below. Towards the end of the

infiltration experiment (after ~10 pore volumes), when the outflow salinity had stabilized, the CBM water columns were infiltrated with good quality stream water to see whether the low salinity water would induce soil dispersion.



The results show that: (1) On average, infiltration is highest for the CBM water columns; (2) infiltration rates for the CBM and tap water columns remains relatively constant with time; (3) large quantities of salts are flushed from the soil at the onset of infiltration, reflecting the saline nature of PRB soils; (4) the tap water columns reduce to a lower outflow salinity than the CBM water columns; and (5) infiltrating the CBM water columns with good quality stream water does not trigger soil dispersion, judging from the unchanged trend in cumulative infiltration. Results from the Sheridan site and others will be used to see whether the above findings hold for the entire PRB.

## 2.4 Significance

The fate of CBM water in the unlined ponds is not well understood. Both infiltration and evaporation are likely. Infiltration of pond water may lead to contamination of the shallow groundwater and to degradation of streams that are fed by the groundwater. The contamination is caused by the solutes in the pond water and by the mobilization of solutes already present in the soil. Evaporation of pond water may lead to the concentration of trace elements to levels that are toxic for livestock and wildlife that use the pond for drinking water. The infiltration characteristics of the soil determine whether infiltration will be dominant, or, in case of low infiltration rates, evaporation. Previous studies suggest that pond water infiltration reduces with time because of soil dispersion related to the high sodium content of the CBM water. The results from the column infiltration studies for the Gillette site seem to contradict this as no drop in infiltration rate with time is observed. Additional column infiltration studies, covering the range of soils and CBM water qualities present in the PRB, will be conducted to provide a more comprehensive picture. This type of information is currently lacking for the PRB.

### **3. Publications**

As part of the study, one oral presentation was given during the 2011 UCOWR/NIWR annual conference as part of a technical session on Energy & Water, moderated by Michael Campana of Oregon State University:

Kelleners, T.J. The effects of coal-bed natural gas produced water on infiltration. Oral presentation at the UCOWR/NIWR annual conference, July 11-14, 2011, Boulder, CO.

### **4. Student Support Information**

MS student Robert Drapeau has been hired for the duration of the 2-year project. During the Fall 2011 semester, Robert has taken classes in soil chemistry, pedology, and numerical soil water flow and transport modeling. During the Spring 2012 semester, Robert is taking soil physics, soil physics laboratory, soil microbiology, and soil professional exam. The course and research work should result in a MS soil/water resources degree by mid 2013. It is anticipated that Robert will attend the Soil Science Society of America Annual meeting in Cincinnati, OH in October 2012 to present results from the study to a wide audience.

### **5. Awards and achievements**

MS student Robert Drapeau has been awarded an energy assistantship by the Office of Academic Affairs of the University of Wyoming.

# Instrumentation for Improved Precipitation Measurement in Wintertime Snowstorms

## Basic Information

<b>Title:</b>	Instrumentation for Improved Precipitation Measurement in Wintertime Snowstorms
<b>Project Number:</b>	2011WY75B
<b>Start Date:</b>	1/1/2010
<b>End Date:</b>	2/28/2013
<b>Funding Source:</b>	104B
<b>Congressional District:</b>	1
<b>Research Category:</b>	Climate and Hydrologic Processes
<b>Focus Category:</b>	Water Quantity, Climatological Processes, Hydrology
<b>Descriptors:</b>	Snow Process Research
<b>Principal Investigators:</b>	Jefferson Snider

## Publications

There are no publications.

# **Instrumentation for Improved Precipitation Measurement in Wintertime Snowstorms**

## **Annual Report, Year 1 of 2**

Principal Investigator - Jefferson Snider, Professor, jsnider@uwyo.edu (307 766 2637)

Affiliation - Dept. of Atmospheric Science, University of Wyoming

Date – April 30, 2012

### **Abstract -**

It is widely recognized that precipitation measurements can be biased by wind-induced errors. Measurement of snowfall is especially confounded by wind occurring at forested measurement sites. Negative bias occurs if a precipitation gauge is shadowed by trees, and positive bias occurs if a secondary flux occurs due to wind resuspension of antecedent snowfall. In addition, a negative wind-induced bias occurs because the downward vertical speed of a snow particle is decreased by the airflow distortion near a precipitation gauge. Because the fall speed of a rain drop is much larger than that of a snow particle, the flow distortion bias is largest for the snow particle. Fall speeds for these two particle types are about 10 m/s (drop) and 1 m/s (snow) assuming a 4 milligram particle mass (liquid equivalent particle diameter = 2 mm).

These complications are evident in many studies of snowfall, even when using a wind shield to diminish the horizontal air velocity, and thus the vertical velocity, near a gauge orifice. With support from this grant, we are operating a new type of precipitation sensor (the “Hotplate”) in an intercomparison with conventional gauges. Both the Hotplate and the conventional gauges are being deployed at a wintertime cloud seeding target site. The primary objective of the work is the development of a correction for the Hotplate’s report of the precipitation rate. One MS student is supported by the project and a Hotplate snow sensor is being upgraded with visible and infrared radiometers reporting measurements necessary for the correction. It is anticipated that the research will advance the Hotplate as a device superior to conventional gauges for measurement of snowfall.

## **Progress –**

With Year-1 support from the USGS-WWDC we made significant progress toward our specific objective of reducing the Hotplate's radiation bias and our overall objective of advancing the Hotplate as a reliable gauge for the measurement of snowfall in Wyoming. Five steps toward that goal were made in Year-1. First, our Hotplate was upgraded and now has radiation sensors for shortwave and longwave irradiances as well as for pressure and relative humidity. That work was performed by the Hotplate manufacture, Yankee Environmental Systems (YES). Second, we designed and built a device which controls the Hotplate's radiation environment. The device is described below. Third, using a protocol developed with previous support from the USGS-WWDC we calibrated the upgraded Hotplate. Fourth, we also calibrated a Hotplate owned by the National Center for Atmospheric Research. Fifth, during early 2012, the UWYO and NCAR Hotplates were deployed at the Glacier Lakes Environmental Experiment Site (Medicine Bow Mountains) and at the Battle Pass (Sierra Madre Mountains). Precipitation measurements were recorded with the intent of making comparisons with measurements made with conventional precipitation gauges.

## **Methodology -**

The MS-level graduate student working on this project, Adam Wettlaufer, arrived in Laramie about the same time our upgraded Hotplate was returned from YES (July 2011). Adam worked with both the project PI (Jeff Snider) and the engineer (Matt Burkhardt) to get the Hotplate setup in the lab, to modify the data acquisition software, and to update the data analysis software. Each of these tasks was complicated by the substantial modifications made to the Hotplate and the data stream it outputs.

Our calibration of the upgraded Hotplate is shown in Figure 1. Plotted on the ordinate is the reference precipitation rate we generate using a volumetric pump and on the abscissa is the precipitation rate based on the YES algorithm. The calibration experiments were conducted when the Hotplate was either ventilated at ~10 m/s or unventilated. Overall there is a consistent trend but the YES algorithm produces values ~20% larger than the reference. The source of this discrepancy has not been identified. Further, the lowest calibration points are seen to significantly deviate from the best-fit line. Ongoing work is aimed at understanding these discrepancies.

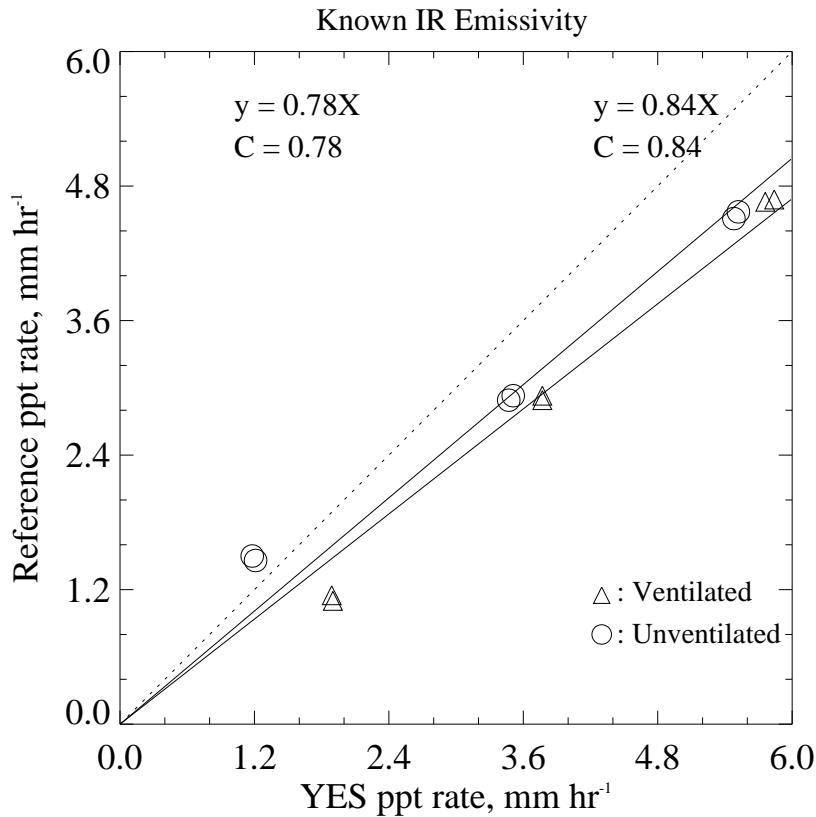


**Figure 1 – Calibration of the precipitation rate subsequent to receiving the upgraded Hotplate from the manufacturer. See text for details.**

The work summarized in Figure 1 was conducted while operating the Hotplate between surfaces with a known infrared emissivity. The experimental setup is shown in Figure 2. To the right of Adam Wettlaufer is the Hotplate with the emissivity surfaces suspended 1 m above and below. The device consists of three vertical support legs and two 4'x4' horizontal pieces of steel roofing coated with a finish which has an infrared emissivity equal to 0.84. The emissivity surfaces are designed to establish a known boundary condition for longwave radiation reaching the upper and lower surfaces of the Hotplate.



**Figure 2 – The Hotplate operated between the 4’x4’ emissivity surfaces in the penthouse of the UW Engineering building, November 2011. Graduate student Adam Wettlaufer is shown in the left picture.**

As we discussed in our USGS-WWDC proposal, the precipitation rate reported by the Hotplate is sensitive to measurement error associated with calibration coefficients, particularly those that describe the heat load due to ventilation, and the manner they applied in the precipitation algorithm. Because of this sensitivity we are developing a method which we think is superior to the manufacturer’s. Figure 3 illustrates our approach. Seen in these two panels are calibration points corresponding to heat load (ordinate) versus wind speed (abscissa) and the fitted relationship. Consistent with common practice in heat transfer analysis the values presented here are nondimensionalized; i.e., plotted on the ordinate is the Nusselt number, a dimensionless representation of the measured heat load, and on the abscissa is the Reynolds number, a dimensionless representation of the measured air speed. In the left-hand plot are data from our laboratory, before we built the device shown in Figure 2; in the right-plot are data from the penthouse after the device was constructed. Subtle differences between the fitted Nu-Re relationship are evident. This difference is significant when the Nu-Re relation is applied in our processing algorithm to infer precipitation rate. It is premature to conclude that the difference is a consequence of the emissivity surfaces, but it may be. Analysis of these results is ongoing.

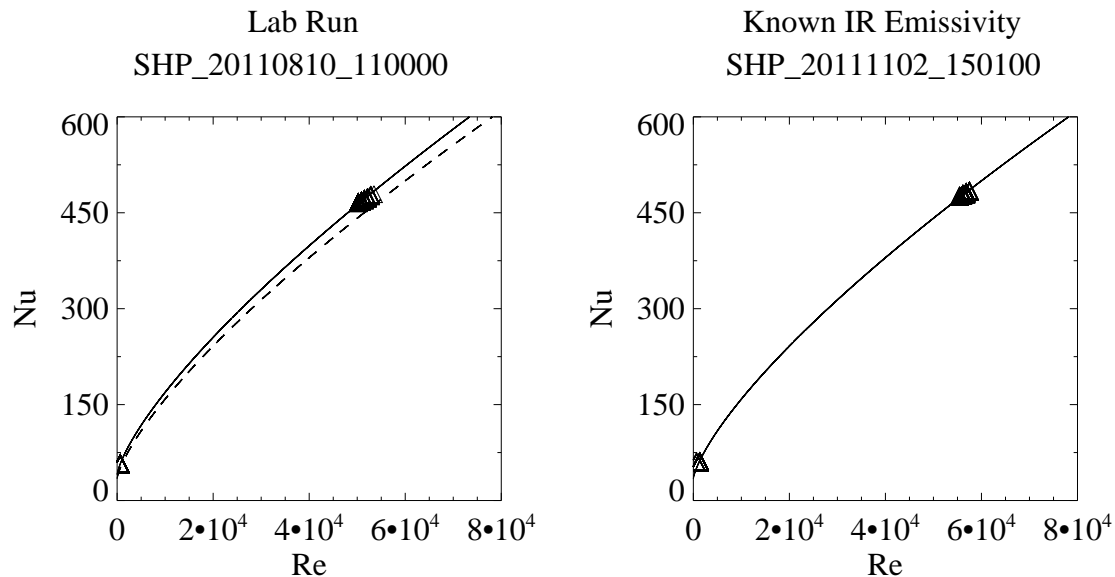


**Figure 3 – Nondimensionalized heat load and air speed data and curve fits. In the left panel are results from our laboratory (without the emissivity surfaces) and in the right results from UW Engineering building’s penthouse (with the emissivity surfaces).**

### Work in Progress –

1) We implemented the Hotplate calibration procedure described in our USGS-WWDC proposal. The technique involves calibrating the Hotplate within a controlled radiation environment. Improved understanding of the factors that can confound precipitation measurements made with the Hotplate is expected to evolve from our research.

2) Field measurements were made early in 2012 using two Hotplates. These are the instrument we had upgraded with USGS-WWDC funding, and an instrument that was loaned to us by the National Center for Atmospheric Research (NCAR). The two instruments are referred to as the UWYO Hotplate and NCAR Hotplate, respectively.

3) The UWYO Hotplate and NCAR Hotplate field measurements were coordinated with measurements made with a co-located precipitation gauge (ETI Instrument Systems, Inc.). One Hotplate-ETI comparison was made at the Battle Pass site and another was made at the Glacier Lakes Environmental Experiment Site. Both data sets were collected concurrent with the Wyoming Weather Modification Pilot Program. These Hotplate-ETI data sets are being analyzed.

### Student Support Information –

During the 2011-2012 academic year Adam Wettlaufer successfully completed two semesters of course work. One of the classes he took was a graduate-level convective heat transfer course, taught in the Department of Mechanical Engineering. During the 2011-2012 academic year, Adam was in class 13 hours a week, but in spite of his course load he made substantial progress with his research. During the 2011-2012 field season he took a leading role in the field work and in the Hotplate calibration work.

## Information Transfer Program Introduction

Information dissemination efforts included reports and presentations by the Director to State and Federal entities and the Private sector. The Director reports annually to the Wyoming Water Development Commission and to the Select Water Committee (of the Wyoming Legislature). Presentations were given throughout the state concerning the research program and project results. The Director serves as the University of Wyoming Advisor to the Wyoming Water Development Commission and attends their monthly meetings. This provides a means for coordinating between University researchers and Agency personnel. The Director also serves as an advisor to the Wyoming Water Association ([www.wyomingwater.org](http://www.wyomingwater.org)) and regularly attends meetings of the Wyoming State Water Forum.

Publications and other information dissemination efforts were reported by the PIs of the projects funded under this program. The project PIs report to the Institute Advisory Committee on an annual basis. Presentations discussing final results are made by PIs of projects which were completed during the year at the July committee meeting. Presentations discussing interim results are made by PIs of continuing projects at the fall/winter committee meeting. PIs are encouraged to publish in peer reviewed journals as well as participate in state-wide water related meetings and conferences. Publications are listed in the individual research reports.

Director 2011 information dissemination activities are listed in the following paragraph:

DIRECTOR SERVICE AND PRESENTATIONS: (1) Wyoming Water Forum, Presentation on Water Research Program update, Cheyenne, WY., March, 2011; (2) Wyoming Water Forum, Presentation on Water Research Program update, Cheyenne, WY., April 4, 2011; (3) Sponsor, UW Water Instructors for the ninth Annual Conference on Wyoming Water Law, with CLE International, Cheyenne, WY., April 7 thru 8, 2011; (4) Weather Modification Association (WMA) annual meetings, Park City, UT., April 12 thru 15, 2011; (5) Wyoming Water Forum, Presentation on Water Research Program final project reports, Cheyenne, WY., May 3, 2011; (6) Wyoming Water Development Commission (Advisor), Cheyenne, WY., May 6, 2011; (7) Wyoming Basin Advisory Group meeting, Presentation on Wind River Range and Teton Range Glacier melt water supplies, Rock Springs, WY., May 9, 2011; (8) Wyoming Climate Issues meeting, Department of Agriculture, Cheyenne, WY., May 19, 2011; (9) Wyoming Water Development Commission/Select Water Committee joint workshop, Cheyenne, WY., June 1, 2011; (10) Wyoming Water Development Commission/Select Water Committee Meeting, Cheyenne, WY., June 2, 2011; (11) Wyoming Weather Modification Technical Advisory Team Meeting, Lander, WY., July 12 thru 13, 2011; (12) Wyoming Water Association Board Meeting/Summer Tour, (Advisor), Jackson Hole, WY., July 14 thru 15, 2011; (13) Mountain West Water Institute Conference, Presentation on UW Office of Water Programs/Wyoming Water Research Program, Salt Lake City, UT., July 18 thru 19, 2011; (14) UW Water Research Program, WRP Priority and Selection Committee meeting to select research priorities and review final project reports, Cheyenne, WY., July 28, 2011; (15) Wyoming Water Association Committee meeting (Advisor), Cheyenne, WY., August 11, 2011; (16) Wyoming Water Development Commission/Select Water Committee joint workshop, Cheyenne, WY., August 17, 2011; (17) Wyoming Water Development Commission/Select Water Committee joint meeting/summer tour, Cody, WY., August 18 thru 19, 2011; (18) Wyoming Water Association Committee meeting (Advisor), Cheyenne, WY., August 25, 2011; (19) Wyoming Legislative Joint Agriculture Committee meeting, presentation on the Office of Water Programs/Wyoming Water Research Program research projects and presentation by Brent Ewers on Beetle Kill and Forest Water Yield, Afton, WY., September 27, 2011; (20) Wyoming Water Forum, Presentation on Water Research Program Project Selection, Cheyenne, WY., October 4, 2011; (21) Wyoming Water Association Committee meeting (Advisor), Cheyenne, WY., October 18, 2011; (22) Wyoming Water Association Board meeting (Advisor), Casper, WY., October 25, 2011; (23) Co-Sponsor Wyoming Water Association Annual Meeting & Educational Seminar, University of Wyoming Water Initiatives, Casper, WY., October 26 thru 28, 2011; (24) Wyoming Water Forum, Presentation on Water Research Program RFP and Project Selection, Cheyenne,

## Information Transfer Program Introduction

WY., November 1, 2011; (25) Wyoming Water Development Commission/Select Water Committee joint workshop, Presentation on the UW Office of Water Programs and Water Research Program, Casper, WY., November 2 thru 4, 2010; (26) Wyoming Weather Modification 2011:2012 Pre-project Ground School, Laramie, WY., November 9 thru 10, 2011; (27) Wyoming Association of Conservation Districts (WACD) Annual Conference, Lander, WY., November 16 thru 17, 2011; (28) UW Water Research Program Meeting, WRP Priority and Selection Committee to select research projects, Cheyenne, WY., November 29, 2011; (29) AGU Fall Meeting, Poster Presentation Paleo Streamflow Variability in Glaciated and Non-Glaciated Watersheds: Wind River Range (Wyoming, USA), San Francisco, CA., December 5 thru 9, 2011; (30) Mountain West Water Institute Waters of the West Workshop, Presentation on UW Office of Water Programs/Wyoming Water Research Program, Salt Lake City, UT., July 18 thru 19, 2011; (31) Sponsored UW Faculty research presentations at Mountain West Water Institute Waters of the West Workshop, Salt Lake City, UT., July 18 thru 19, 2011; (32) Wyoming Water Forum, Presentation on Water Research Program update, Cheyenne, WY., January 3, 2012; (33) Wyoming Water Development Commission Meeting, Presentation on recommendation for FY2012 WRP Annual funding and OWP Biennium funding, Cheyenne, WY., January 11, 2012; (34) Wyoming Legislative Select Water Committee, Presentation on WRP projects and recommendation for FY2012 WRP Annual funding and OWP Biennium funding, State Capital, Cheyenne, WY., January 12, 2012; (35) Wyoming Water Association Board Meeting, Legislative Review, (Advisor), Cheyenne, WY., January 12, 2012; (36) Wyoming Water Forum, Presentation on Water Research Program update, Cheyenne, WY., February 7, 2012; (37) The National Institutes for Water Resources (NIWR) annual meetings, Washington, DC., February 13-15, 2012; (38) Wyoming State Legislature House Agriculture Committee, Wyoming Water Development Commission (Advisor), Omnibus Water Plan, State Capital Bld., Cheyenne, WY., January 16, 2012; (39) AGU Chapman Conference Remote Sensing of the Terrestrial Water Cycle, Kona, HI., February 20 thru 23, 2012; (40) Project Coordination meeting with University of Tennessee and University of Wyoming, Hydrology modeling from Weather Modification, Laramie, WY., February 29, 2012; (41) Wyoming State Legislature Senate Agriculture Committee, Wyoming Water Development Commission (Advisor), Omnibus Water Plan, State Capital Bld., Cheyenne, WY., January 28, 2012.

FY11 Information dissemination activities reported by research project PIs are listed, by project, in the following paragraphs:

Project 2009WY46B, DETECTING THE SIGNATURE OF GLACIOGENIC CLOUD SEEDING IN OROGRAPHIC SNOWSTORMS IN WYOMING II: FURTHER AIRBORNE CLOUD RADAR AND LIDAR MEASUREMENTS, information transfer activities: (1) Greets, B., Presentation at 2012 Annual Meeting of the Weather Modification Association, Las Vegas, 25 thru 27 April 2012; (2) Research updates at the Wyoming Weather Modification Pilot Program Technical Advisory Team meetings, in Lander, July, and in Cheyenne, January; (3) Research update at the WWMPP Ground School in November; (4) Research update at the WWMPP seasonal debriefing meeting in mid April; (5) Dr. Miao presented updated work at the orographic precipitation workshop hosted by Dr. Roy Rasmussen in Boulder 17 thru 19 March 2012.

Project 2010WY54B, IS THE MUDDY CREEK FOOD WEB AFFECTED BY COALBED NATURAL GAS INPUTS?, information transfer activities: (1) Tronstad, L.M. and W. Estes-Zumpf, Trace elements in the muddy creek food web prior to most coalbed natural gas development, Wyoming Landscape Conservation Initiative, Rock Springs, Wyoming, May 14 thru 17, 2012; (2) Tronstad, L.M. and W. Estes-Zumpf, Trace elements in the muddy creek food web prior to coalbed natural gas development, The Wildlife Society Wyoming Chapter, Jackson, Wyoming, Dec. 6 thru 9, 2011; (3) Tronstad, L.M. and W. Estes-Zumpf, Are trace elements bioaccumulating in the Muddy Creek food web?, Wyoming Water Association, Casper, Wyoming, Oct 26 thru 28, 2011; (4) Tronstad, L.M. and W. Estes-Zumpf, Is the Muddy Creek food web affected by coalbed natural gas inputs?, Priority and Selection Committee for the Wyoming Water Research Program, Cheyenne, Wyoming, July 28, 2011.

## Information Transfer Program Introduction

Project 2010WY56B, ENHANCING STREAM FLOWS IN WYOMING, information transfer activity: (1) MacDonnell, Lawrence J. and Curran Trick, Using Voluntary Arrangement to Reduce Diversions and Improve Stream Flows for In-channel Benefits in Wyoming, Presentation at Wyoming Water Association Annual Meeting, Casper, WY., Oct. 28, 2011.

Project 2010WY58B, DEVELOPMENT OF GIS-BASED TOOLS AND HIGH-RESOLUTION MAPPING FOR CONSUMPTIVE WATER USE FOR THE STATE OF WYOMING, information transfer activities: (1) Ryan Rasmussen and Gi-Hyeon Park, Estimation of Growing Season ET using Wyoming ET Calculator, AGU meeting December 5 thru 9, 2011, San Francisco, California; (2) Nancy Thoman and Gi-Hyeon Park, Satellite Based Growing Season ET Estimation using a Statistical Transformation, AGU meeting December 5 thru 9, 2011, San Francisco, California; (3) Gi-Hyeon Park, Nancy Thoman, and Ryan Rasmussen, Application of a Statistical Transformation to enhance Satellite Based ET Estimation, 44th AWRA Annual Water Resources Conference, November 7 thru 10, 2011, Albuquerque, New Mexico.

Project 2010WY59B, TREATMENT OF HIGH-SULFATE WATER USED FOR LIVESTOCK PRODUCTION SYSTEMS, information transfer activities: (1) Jons, A.M, K.L. Kessler, K.J. Austin, C. Wright, and K.M. Cammack, Iron carbonate supplementation of lambs administered high sulfur water, Presented at American Society of Animal Science Summer Meeting, July 10 thru 14, 2011, New Orleans, Louisiana; (2) Jons, A.M., K.J. Austin, K.L. Kessler and K.M. Cammack, 2011, Effects of FeCO<sub>3</sub> supplementation on hepatic gene expression of wethers administered high S water, Colorado Nutrition Roundtable, Fort Collins, CO.

Project 2010WY60B, MULTI-CENTURY DROUGHTS IN WYOMING'S HEADWATERS: EVIDENCE FROM LAKE SEDIMENTS, information transfer activities: (1) Shinker, J. J., Spatial Heterogeneity of Western U.S. Climate Variability, Association of American Geographers, Seattle, Washington, 2011; (2) Heyer, J. and Shinker, J.J., An Investigation of Climatic Controls in the Upper Laramie River Watershed During Low Stream Flow Years, at UW Undergraduate Research Day, April, 2011; (3) Serravezza, M., Ground-penetrating radar as a tools for reconstructing past droughts in Wyoming, UW Roy J. Shlemon Center for Quaternary Studies, Quaternary Research Symposium, Fall 2011; (4) Heyer, J., Fredrickson, J. and Shinker, J.J., Climate, drought and low stream flow in the headwaters of the North Platte River, Annual meeting of the Association of American Geographers, New York City, Feb 23 thru 28, 2012; (5) Fredrickson, J. and Shinker, J.J., Hydroclimatic variability and drought in Wyoming headwater regions, Annual meeting of the Association of American Geographers, New York City, Feb 23 thru 28, 2012.

Project 2010WY61B, IMPACT OF BARK BEETLE OUTBREAKS ON FOREST WATER YIELD IN SOUTHERN WYOMING, information transfer activities: (1) Ewers BE, Impact of Bark Beetle Outbreaks on Precipitation Processing by Forests, Wyoming Weather Modification Technical Advisory Team, Meeting, Cheyenne, WY, Jan. 18, 2012; (2) Frank, J, B Massman, B Ewers, Errors in measured sensible heat flux due to vertical velocity measurements in non orthogonal sonic anemometers, Front Range Student Ecology Symposium, CSU, Ft. Collins, CO, Feb. 22, 2012; (3) Frank, J, B Massman, BE Ewers, Net ecosystem exchange of carbon dioxide and evapotranspiration response of a high elevation Rocky Mountain (Wyoming, USA) forest to a bark beetle epidemic, UW Program in Ecology Symposium, Feb. 17, 2012; (4) DE Reed, BE Ewers, E Pendall, RD Kelly, Mountain Pine Beetle epidemic effects on the carbon, water, and energy fluxes of lodgepole pine ecosystems, UW Program in Ecology Symposium, Feb. 17, 2012; (5) Mackay, DS, BE Ewers, DE Roberts, NG McDowell, E Pendall, JM Frank, DE Reed, WJ Massman, B Mitra, A coupled carbon and plant hydraulic model to predict ecosystem carbon and water flux responses to disturbance and environmental change, American Geophysical Union Meeting, San Francisco, CA, Dec. 2011; (6) Brooks, PD, HR Barnards, JA Biederman, B Borkhuu, SL Edburg, BE Ewers, DJ Gochis, ED Gutmann, AA Harpold, JA Hicke, E Pendall, DE Reed, AJ Somor, PA Troch, Water, Carbon, and Nutrient Cycling Following Insect-Induced Tree Mortality: How well do plot scale observations predict ecosystem scale response. American Geophysical Union Meeting, San Francisco, CA, Dec. 2011; (7) Invited, Ewers, BE, E Pendall, D

## Information Transfer Program Introduction

Reed, H Barnard, F Whitehouse, J Frank, W Massman, P Brooks, J Biederman, K Nathan, B Mitra, DS Mackay, Use of plant hydraulic theory to predict ecosystem fluxes across mountainous gradients in environmental controls and insect disturbance, American Geophysical Union Meeting, San Francisco, CA, Dec. 2011; (8) Frank, JM, WJ Massman, BE Ewers, Net ecosystem exchange of carbon dioxide and evapotranspiration response of a high elevation Rocky Mountain (Wyoming, USA) forest to a bark beetle epidemic, American Geophysical Union Meeting, San Francisco, CA, Dec. 2011; (9) Norton, U, E Pendall, BE Ewers, B Borkhuu, Trace gas emissions from a chronosequence of bark beetle-infested lodgepole pine (*Pinus contorta*) forest stands, American Geophysical Union Meeting, San Francisco, CA, Dec. 2011; (10) DE Reed, BE Ewers, E Pendall, RD Kelly, Mountain Pine Beetle epidemic effects on the carbon, water, and energy fluxes of lodgepole pine ecosystems, American Geophysical Union Meeting, San Francisco, CA, Dec. 2011; (11) Gochis, DJ, ED Gutmann, PD Brooks, DE Reed, BE Ewers, E Pendall, JA Biedermann, AA Harpold, HR Barnard, J Hu, Diagnosing the influence of model structure on the simulation of water, energy and carbon fluxes on bark beetle infested forests, American Geophysical Union Meeting, San Francisco, CA, Dec. 2011; (12) Invited, Ewers, BE. Plant Hydraulic Theory and Mountains, Mountain Research Institute, Berkeley, CA, Dec. 2011; (13) Invited, Ewers, BE, E Pendall, H Barnard, D Williams, U Norton, D Reed, P Brooks, D Gochis, A Harpold, J Frank, W Massman, F Whitehouse, B Borkhuu, J Angstmann, Impact of Bark Beetle Outbreaks on Forest Ecosystem Processes, Wyoming Environment and Natural Resources Speaker Series, Jackson, WY, Dec. 2011; (14) Invited, Ewers, BE, E Pendall, H Barnard, D Williams, U Norton, D Reed, P Brooks, D Gochis, A Harpold, J Frank, W Massman, F Whitehouse, B Borkhuu, J Angstmann, Impact of Bark Beetle Outbreaks on Forest Water Yield, Wyoming Water Development Commission, Cheyenne, WY, Nov. 2011; (15) Invited, Ewers, BE, E Pendall, H Barnard, D Williams, U Norton, D Reed, P Brooks, D Gochis, A Harpold, J Frank, W Massman, F Whitehouse, B Borkhuu, J Angstmann, Impact of Bark Beetle Outbreaks on Forest Water Yield, Joint Agriculture Committee of the Wyoming Legislature, Afton, WY, Oct. 2011; (16) Ewers, BE, E Pendall, U Norton, D Reed, J Frank, B Borkhuu, F Whitehouse, N Brown, H Barnard, P Brooks, T Aston, J Angstmann, W Massman, D Williams, A Harpold, J Biederman, S Edburg, A Meddens, D Gochis, J Hicke, Cascading effects of bark beetles and blue stain fungi on coupled water, C and N cycles, UW Dept. Botany, Sept. 2011; (17) Invited, Ewers, BE, E Pendall, H Barnard, D Williams, U Norton, D King, D Reed, P Brooks, D Gochis, A Harpold, J Frank, W Massman, F Whitehouse, B Borkhuu, J Angstmann, The challenge of predicting the interacting effects of weather modification and bark beetles on forest water yield, Wyoming Weather Modification Technical Advertisory Team Meeting, Lander, WY, July 2011; (18) Borkhuu, B, E Pendall, U Norton, BE Ewers, Effects of mountain pine bark beetle infestation on soil CO<sub>2</sub> efflux in lodgepole forests in Southeastern Wyoming, Soil Science Society Western Meeting, Laramie, WY, June 2011; (19) Invited, Ewers, BE, Testimony on bark beetle impacts on forest hydrology, Joint meeting of the Select Water Committee of the Wyoming Legislature and the Wyoming Water Development Commission, Cheyenne, WY, June 2011; (20) Ewers, BE, E Pendall, H Barnard, F Whitehouse, D Reed, J Frank, P Fornwalt, T Aston, J Angstmann, U Norton, A Harpold, P Brooks, Sap flux measurements quantify the timing of transpiration loss due to fungal xylem occlusion following bark beetle attack and subsequent ecosystem consequences, VIII International Sap Flow Meeting, Volterra, IT, May, 2011; (21) Invited, Ewers, BE, E Pendall, H Barnard, D Williams, U Norton, D Reed, P Brooks, D Gochis, A Harpold, J Frank, W Massman, F Whitehouse, B Borkhuu, J Angstmann, Impact of Bark Beetle Outbreaks on Forest Water Yield, Wyoming Water and Environmental Law Conference, Cheyenne, WY, Apr. 2011; (22) Frank, J, WJ Massman, BE Ewers, Evapotranspiration response of a high elevation Rocky Mountain (Wyoming, USA) forest to a bark beetle epidemic, Bark Beetle Water Symposium, Boulder, CO, 2011; (23) Harpold, AA, PD Brooks, JA Biederman, A Somor, P Troch, D Gochis, E Gutmann, H Barnard, D Reed, E Pendall, BE Ewers, Quantifying the effects of tree dieoff from mountain pine beetles on hydrologic partitioning at the catchment-scale, Bark Beetle-Water Symposium, Boulder, CO, 2011 (24) Gochis, D, E Gutmann, AA Harpold, PD Brooks, JA Biederman, H Barnard, D Reed, E Pendall, BE Ewers, Multi-model assessment and verification of bark beetle impacts on land surface atmosphere energy and water exchanges, Bark Beetle-Water Symposium, Boulder, CO, 2011.

## Information Transfer Program Introduction

Project 2011WY74B, FATE OF COALBED METHANE PRODUCED WATER IN DISPOSAL PONDS IN THE POWDER RIVER BASIN, information transfer activity: (1) Kelleners, T.J., The effects of coal bed natural gas produced water on infiltration, Oral presentation at the UCOWR/NIWR annual conference, July 11 thru 14, 2011, Boulder, CO.

# USGS Summer Intern Program

None.

<b>Student Support</b>					
<b>Category</b>	<b>Section 104 Base Grant</b>	<b>Section 104 NCGP Award</b>	<b>NIWR-USGS Internship</b>	<b>Supplemental Awards</b>	<b>Total</b>
<b>Undergraduate</b>	7	0	0	0	7
<b>Masters</b>	11	0	0	0	11
<b>Ph.D.</b>	8	0	0	0	8
<b>Post-Doc.</b>	0	0	0	0	0
<b>Total</b>	26	0	0	0	26

## Notable Awards and Achievements

UW Institute project Detecting the Signature of Glaciogenic Cloud Seeding in Orographic Snowstorms in Wyoming Using the Wyoming Cloud Radar received the FY11 NIWR IMPACT Award. Bart Geerts, Department of Atmospheric Science, University of Wyoming, is the PI for the award winning project. The study sought to define the signature of glaciogenic seeding of orographic clouds using cloud radar and lidar measurements with the UW King Air research aircraft and examined whether glaciogenic seeding of clouds enhances snowfall in winter storms over the mountains of southeast Wyoming. This study dealt with the cloud-microphysical response to the seeding of AgI and aimed to put the snow generation processes within the seeding plume under the microscope. Prior to this study, most cloud seeding efficacy validation work had focused on the outcome, i.e. the snowfall enhancement, and not directly on the cloud microphysical processes associated with glaciogenic seeding.

## Publications from Prior Years

1. 2006WY33B ("Precipitation Measurement and Growth Mechanisms in Orographic Wyoming Snowstorms") - Articles in Refereed Scientific Journals - December 2011 Jonathan Wolfe's manuscript titled "A Relationship between Reflectivity and Snow Rate for a High-Altitude S-band Radar" was accepted for publication at the Journal of Applied Meteorology and Climatology. A preview of the manuscript is available at:  
<http://journals.ametsoc.org/doi/pdf/10.1175/JAMC-D-11-0112.1>